DIVERSITY AND STABILITY IN FOOD WEBS

Impacts of Non-Equilibrium Dynamics, Topology and Variation

INAUGURAL-DISSERTATION

zur

Erlangung des Doktorgrades

der Mathematisch-Naturwissenschaftlichen Fakultät

der Universität zu Köln

vorgelegt von

FANNY GROLL

aus Köln

Köln, 2016

Berichterstatter:	Prof. Dr. Alexander Altland
(Gutachter)	Prof. Dr. Joachim Krug

Tag der mündlichen Prüfung: 11.07.2016

KURZZUSAMMENFASSUNG

Mit fortschreitendem Klimawandel wird der Erhalt des Artenreichtums immer wichtiger. Nur bei genügend großem Genpool und breitgestreuten Bedürfnissen der Arten an ihre Umgebung werden sich Spezies finden, die sich veränderten Umständen anpassen können. Um Biodiversität zu erhalten, muss aber zunächst einmal verstanden werden, welches Vorgehen welche Folgen nach sich zieht. Mathematische Modelle der Populationsdynamiken könnten entsprechende Prognosen liefern. Es fehlt aber noch ein Modell, das dazu in der Lage wäre, die Mechanismen, der alltäglich und experimentell beobachteten Artenvielfalt wiederzugeben und zu erklären. Eine Kombination theoretischer Modelle mit detaillierten Experimenten ist notwendig, um biologische Prozesse in Modellen zu testen und die Vorhersagen mit den Auswirkungen in der Wirklichkeit zu vergleichen.

In der vorliegenden Arbeit werden verschiedene Nahrungsnetze modelliert und untersucht. Unter anderem werden Modelle zu Experimenten des zoologischen Instituts der Universität zu Köln entwickelt und analysiert. Hier weisen Simulationen der Laborsystemen eine gute Übereinstimmung der numerischen Daten mit den experimentellen Ergebnissen auf. Mit Hilfe der Simulationen kann gezeigt werden, dass wenige Modellannahmen nötig sind um langanhaltende Oszillationen der Populationsgrößen zu reproduzieren. Allerdings zeichnet sich ebenfalls ab, dass ein Zusammenleben „zufällig zusammen gewürfelter“ Arten über lange Zeiträume nicht sehr wahrscheinlich ist. Auch größere Nahrungsnetzmodelle zeigen keine signifikante Abweichung von diesen Beobachtungen und belegen wie außergewöhnlich und kompliziert die natürliche Vielfalt ist. Um eine solche Koexistenz zufällig ausgewählter Arten wie im Experiment regelmäßig zu erzeugen, müssten andere Prozesse oder weitere Einschränkungen in die Modellannahmen eingehen. Eine andere Erklärung für die beobachtete Koexistenz ist ein langsames Aussterben. In numerischen Simulationen überleben Arten vergleichbare Zeitspannen wie im Experiment bevor sie dann letzten Endes aussterben.

Interessanterweise kann festgestellt werden, dass dieselben mathematischen Modelle auch ein Überleben mehrerer Arten im Gleichgewicht erlauben und somit nicht dem sogenannten Konkurrenzausschlussprinzip folgen. Dieser Gleichgewichtszustand ist allerdings fragiler gegenüber Änderungen der Nahrungszufuhr als die oszillierende Artenvielfalt. Insgesamt belegen die Untersuchungen, dass Koexistenz eher oszillierende Populationsgrößen aufweist und dass andererseits oszillierende Populationsgrößen ein Nahrungsnetz

sowohl gegen demographisches Rauschen wie auch gegen Änderungen des Lebensraums stabilisieren.

Diese Modellvorhersagen sind sicher nicht eins zu eins auf reale Ökosysteme übertragbar, aber bei der Regulierung von Tierbeständen sollte der stabilisierende Charakter von Fluktuationen bedacht werden.

ABSTRACT

With progressive climate change, the preservation of biodiversity is becoming increasingly important. Only if the gene pool is large enough and requirements of species are diverse, there will be species that can adapt to the changing circumstances. To maintain biodiversity, we must understand the consequences of the various strategies. Mathematical models of population dynamics could provide prognoses. However, a model that would reproduce and explain the mechanisms behind the diversity of species that we observe experimentally and in nature is still needed. A combination of theoretical models with detailed experiments is needed to test biological processes in models and compare predictions with outcomes in reality.

In this thesis, several food webs are modeled and analyzed. Among others, models are formulated of laboratory experiments performed in the Zoological Institute of the University of Cologne. Numerical data of the simulations is in good agreement with the real experimental results. Via numerical simulations it can be demonstrated that few assumptions are necessary to reproduce in a model the sustained oscillations of the population size that experiments show. However, analysis indicates that species "thrown together by chance" are not very likely to survive together over long periods. Even larger food nets do not show significantly different outcomes and prove how extraordinary and complicated natural diversity is. In order to produce such a coexistence of randomly selected species—as the experiment does—models require additional information about biological processes or restrictions on the assumptions. Another explanation for the observed coexistence is a slow extinction that takes longer than the observation time. Simulated species survive a comparable period of time before they die out eventually.

Interestingly, it can be stated that the same models allow the survival of several species in equilibrium and thus do not follow the so-called competitive exclusion principle. This state of equilibrium is more fragile, however, to changes in nutrient supply than the oscillating coexistence.

Overall, the studies show, that having a diverse system means that population numbers are probably oscillating, and on the other hand oscillating population numbers stabilize a food web both against demographic noise as well as against changes of the habitat.

Model predictions can certainly not be converted at their face value into policies for real ecosystems. But the stabilizing character of fluctuations should be considered in the regulations of animal populations.

CONTENTS

1 INTRODUCTION

'The highest function of ecology is understanding consequences.'

— Frank Herbert, *Dune*

Earth's biosphere is a complicated worldwide interaction network of all species. With growing human population and an increasing impact due to fishing, managing livestock and fisheries management is an ever-growing task [93]. Ecosystems suffer from the cumulative transformation of natural habitats due to direct human influence but also from climate change, droughts, temperature shifts, et cetera. These environmental variations change the composition of species in an ecosystem, influence the population numbers but more importantly, puts several species at imminent threat of extinction and whole ecosystems to collapse. Understanding population dynamics and predicting the evolution of food webs becomes more and more important.

What limits the number of species—the diversity—in a system? What is the influence of a species on the biological diversity in its habitat? How stable is the balance between the species? How severely does an ecological system react to different external influences? Questions of this type are highly relevant both from a fundamental and a social and economical point of view.

We depend on (and are part of) this system's dynamics and development. Exploitation of the oceans for fish, life stock management, extinction of crop pollinators et cetera have direct impact on human life. The tolerance to overfishing of fish stocks, for instance, can have major social and economical consequences. Even more so with growing population pressure and climate change. Understanding the mechanisms leading to a collapse of systems is crucial for food security. If we want to preserve biodiversity we have to know on which ground to make decisions. The question whether chaotic fluctuations occur under realistic conditions and how this will affect the stability and diversity of ecosystems is of obvious relevance.

Once the interactions between species and predator-prey-relations in a food-net are understood, theoretical models predicting its behavior can be developed. Since the classical works of Lotka [69] and Volterra [118] in the 1920s, theoretical modeling has led to important and often surprising contributions to the understanding of ecosystems. For example studies by

Leibold [61] promoted the concept of keystone predators [83]. They predict that predators play an important role in maintaining species diversity: only in the presence of a common predator more than one species can survive in a shared habitat on one trophic level. In the absence of predatory pressure one species will suppress all others.

Various theoretical works indicate deterministic chaos in food webs [42, 74, 75, 102, 103]. On the one hand chaos leads to population fluctuations which are unpredictable, even the smallest uncertainties in the initial situation cause great effects in population levels. On the other hand, and somewhat contrary to intuition, it might contribute to the stabilization of food webs. If population numbers are confined to a **chaotic attractor**, they are bound from above as well as from below and are thereby prevented from extinction: chaotic fluctuations notwithstanding, the ecosystem is stable in the sense that it retains its original form as a whole. This is also true for systems in which a coexistence of all species in a stable stationary state is not possible.

We cannot hope to model and simulate all species in a natural habitat in the minutest detail along with the complex web of their interactions, specific parameters and movement. To tackle this complex system there are two approaches, both with their own weaknesses and advantages. One way to go is to concentrate on a few "most important" species or to "coarse grain" and combine species into functional groups by their hunting behavior or role in the ecosystem. The latter approach is taken for example by global models of the oceanic ecosystem [16, 120] but has also been applied successfully on smaller scale in niche models reproducing food web structures of lake systems via Monte Carlo simulations [122].

The other route to take is first to study small food webs or motifs in the interaction network [79]. This is a reasonable strategy, as we can assume, that such communities exist in isolation for some timespan till interacting with the environment. Moreover, the global development in a system certainly depends on the underlying subsets. The collective behavior of coupled dynamical systems in more complex systems is not always predictable, but some rough generalizations are known [100]. Characteristics of and results for small food webs generalize to larger webs [123] and can be interpreted as webs for functional groups. The values characterizing the behavior and growth of species are not easily all determined and vary inside natural populations. By numerically simulating hundreds of food webs with slightly different parameters we can get an idea of how likely particular configurations will develop by chance under fixed assumptions and formulate general rules regarding dynamics in communities of species.

In an analogous manner whole-ecosystem experiments will control and observe a selection of parameters but not all. The problem with these approaches is that species that are small in numbers can still have an important

influence on the rest of the habitat and thus might incorrectly be overlooked as insignificant. Certain mechanisms might not be observed this way.

Our paradigm are small microbial food webs. Well controlled laboratory experiments in chemostats can provide a basis for such models. **Chemostats** are closed containers with microbial species in water with constant food inflow and overflow, controlled temperature and light. Such a food web in chemostat offers maximal control of the species introduced as well as the environmental parameters. Accordingly such a microbial aquatic food web is our minimal model. It makes use of well-studied growth laws and established models [14, 63], offers comparable hypothesis for experiments and is still variable enough to deal with diverse questions. To address more general aspects of the problem we increase the degree of complexity in our models: The structure of a food web can be more or less complex, species might entertain stronger or weaker interactions. The number of interdependent species in the web could alter the stability of diversity as well as the number of levels.

The aim of this study is to look for robust mechanisms that guarantee coexistence of several species and to identify classes of food webs with regard to their stability and species diversity. Those classes can for example be characterized by the topology of their inter-species relations, e.g. feeding on products of metabolism of another species or competition on nutrients or via a common predator.

1.1 OUTLINE OF THIS THESIS

Natural food webs manifest a complexity that fascinates and poses challenges at the same time. With few ingredients, a relatively simple and small food web of three species can exhibit various dynamical patterns from equilibrium over limit cycles to chaotic attractors (as we will see in chapter 2). Chaotic and non linear dynamical systems have been studied extensively in theoretical physics, in the realm of laser physics, mechanical vibrations or socio-economic problems. In the field of ecological models, the role of non-equilibrium dynamics is not fully understood and still in development.

The present work results from a close cooperation with experimental biologists that aimed at an understanding of maintained diversity and sustained oscillations in real world systems. This offered unique and exciting opportunities but on the other hand such a collaboration involves uncertainties: The availability of new data and the execution of new experiments cannot be controlled and novel challenges arise. Theoretical models of practical laboratory experiments were simulated numerically to compare to empirical data and the

influences of species interactions[1]. With the many unknown parameters in ecology and the natural variation, random sampling of parameters and numerical simulations offer one way to explore dynamics and diversity of food webs without restricting the analysis to explicit parameter values.

This dissertation mainly addresses three questions:

1. Which factors affect the stability of a food web or an ecosystem?

2. How does the composition of a food web or an ecosystem affect its stability?

3. Are some species more important than others concerning food web stability?

Stability in this contexts refers to the **persistence** of species diversity in a system, i.e. to the stability of the number of distinct species and to the **resistance** to changes in the system's parameters. A potential loss of species corresponds to an unstable system, in a stable system the number of species stays constant. The aim is to infer system properties that indicate strong or weak stability against external perturbation. This would help deciding which species in a food web are most important to protect and which habitat could be especially prone to breakdown.

After reviewing the fundamentals of ecological models and diversity and defining the required terms in section 1.2 and 1.3, chapter 2 investigates a predator-prey model that simulates the life chemostat system of Becks et al. [10]. In the experiment as well as in the model, chaotic population dynamics occur over broad parameter ranges. The model reproduces experimental data qualitatively with population abundances of apt orders of magnitude. The system features a chaotic attractor that arises from the interplay of two distinct limit cycles. Demographic numerical simulations demonstrate that the attractor in turn causes the mean extinction times of the food web to increase exponentially with system size. In other words chaos stabilizes the populations against demographic noise.

Chapter 3 reviews a theoretical model [47] and modifies it to describe the processes in the chemostat experiment realized by Schieffer [94] and Arns [7] in Cologne. The chapter addresses the feasibility of coexistence in non-equilibrium as well as fixed population numbers. Although both types are possible in numerical simulations, chaotic coexistence proves much more stable under changes of dilution rates. Not only does chaos (or fluctuations)

1 The numerical calculations here and in the following chapters were either performed with C++ or with Mathematica Version 10 (Wolfram Research, Inc., Mathematica, Version 10.0, Champaign, IL (2014)).

support multi-species coexistence but it also stabilizes diversity better against perturbations than stationary setups. On the other hand, numerical calculations show that high species richness is not a likely outcome under the general assumptions of the model. Natural diversity needs additional explanations and mechanisms.

Chapter 4 examines the impact of specialization and the excretion of metabolic products on competitive microbial communities. A numerical study of systems of 20 competitors was performed. The model features a common good, excreted by producers, that can be utilized by generalists. Varying the food web structure (the number of producers and generalists) and sampling random species with fixed species interactions we draw the conclusions that first, producers enable higher species richness and second, that specialists promote diversity.

Chapter 5 explores in a third model the consequences of the food web structure on stability and diversity in systems. Starting with a substantially larger number of species and multiple trophic levels, diversity still declines over ecological time scales. On average, systems end up with three to four species and four trophic levels above the resources. An investigation of dynamical properties indicates the importance of non-equilibrium dynamics for the maintenance of species richness in ecosystems.

Code for the simulations of each chapter can be found in the respective appendices.

1.2 FUNDAMENTALS OF ECOLOGICAL MODELS

"We remembered the relationship between a food animal called a snowshoe rabbit and a predatory cat called a lynx. The cat population always grew to follow the population of the rabbits, and then overfeeding dumped the predators into famine times and severe die-back."

— Frank Herbert, *Chapterhouse Dune*

Historically, the field of population dynamics developed not so much from mathematical biology but from considerations mostly concerned with human population in particular. Malthusian growth models—named after Robert Malthus [72] and his influential essay "on the principle of population"—assume exponential growth with a constant rate r

$$\frac{dP}{dt} = rt \quad \Leftrightarrow \quad P(t) = P_0 e^{rt} \tag{1.1}$$

where t is the time and P_0 the initial population size. With positive growth rate r the population grows indefinitely, if r is negative, population numbers approach zero. Malthus assumed linear growth in food production and accordingly predicted a future of famine and starvation for British society when, in 50 years from then (1798) on, population numbers would have overtaken food supply. Luckily for Great Britain, farming became more efficient and society did not follow this simple growth model.

In 1838 Verhulst [115] published an equation incorporating the limited **carrying capacity** κ of an environment to support a population.

$$\frac{dP}{dt} = rP \cdot \left(1 - \frac{P}{\kappa}\right) \quad \Leftrightarrow \quad P(t) = \frac{\kappa P_0 e^{rt}}{\kappa + P_0 (e^{rt} - 1)} \tag{1.2}$$

This model predicts more realistic logistic growth where populations saturate at the maximum value $\lim_{t\to\infty} P(t) = \kappa$ when resources like food or space get scarce.

During this period, theoretical ecological sciences started to evolve. Sprengel [97] and von Liebig [119] developed and promoted, respectively, an agricultural theory about plant growth and the optimal use of mineral fertilizer. They formulated a principle stating that the growth of crops is controlled by the scarcest resource.

In 1926 Volterra [117, 118] published the famous Lotka-Volterra equations to explain fluctuations in the statistics of fish catches. He also discussed potential application to plant parasites. Independently, Lotka [69] derived the same type of predator-prey equations in 1925 after proposing them for the description of autocatalytic chemical reactions in 1910. Volterra discussed basic interactions of two or three species competing for food or feeding on one another. These models predict stationary population numbers, damped oscillations or ongoing oscillations in the case of the popular predator-prey system.

Still nowadays population models are a measure to predict development of food supply and to ensure it by managing livestocks, fisheries and ecosystems in general.

1.2.1 Food Web Models

In the life sciences, population dynamics study the size of populations of species or groups of species in a mutual environment.

The definition of a biological **species** via genetic differences or reproduction is not always well-defined. In the theoretical framework, we will define a species in terms of its traits. Members of one species are distinguished from

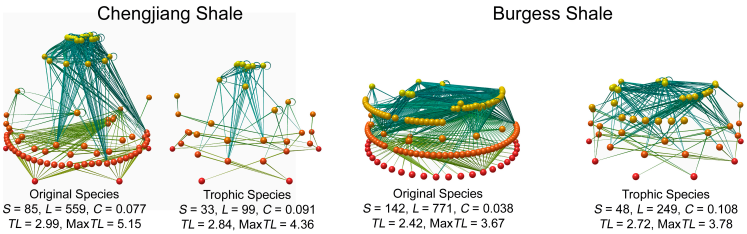

Figure 1: Reconstructions of fossil food webs and trophic levels from the Chengjiang and Burgess Shale produced by Dunne et al. [22]. Species or taxa are represented by spheres, connected by feeding links. The lowest level is composed of primary producers (red), the top level contains predators (yellow). Food webs can be simplified by gathering species by common feeding behavior into "trophic species".
S: number of species (nodes). L: number of trophic links. C: connectance; L/S2. MaxTL: maximum trophic level of a species in the web.
`http://dx.doi.org/10.1371/journal.pbio.0060102.g001`

other species by properties like growth rate, the way they interact with other individuals and the environment et cetera.

In natural ecological systems, several species live together, interacting with each other. A **food web** represents the combined **trophic** (feeding) interactions graphically. Arrows indicate directed feeding links or rather who eats whom. Sometimes this is also referred to as the flow of energy or nutrients through the web. Starting at the lowest level with producers (autotrophs) like phytoplankton, algae and plants that convert light, mineral nutrients and gas into organic matter. The next higher level would be consumers grazing on the producers. These will be fed on by the next higher rank of predators and so on. In a simple case, species with mutual predators and prey or resources can be ordered into **trophic levels**. Inside each level several species compete against each other for food but also in defense against predation pressure. If we consider only one species per level (A eats B eats C) one might also call this a **food chain**. In general natural ecosystems can be much more complex and interconnected (see Figure 1).

To describe population numbers in ecological systems mathematically, we treat the number of individuals of each species as a continuous quantity. By neglecting the discrete nature of birth and death processes we implicitly assume sufficiently large system sizes and numbers. This assumption breaks of course down for small systems. Consequences from the discreteness in small systems are discussed in chapter 2. Another approximation in this study is that the aquatic communities are well mixed and that this process destroys spatial

information. Seasonal environmental fluctuations will not be considered, just as age structure of the populations.

All changes in population numbers can then be incorporated into rate equations. Growth and death rates determine the evolution and might depend explicitly on the numbers of predators or the availability of nutrients or implicitly on the abundance of competitors . In these systems—homogeneous in time and space—this will result in coupled differential equations of first order that do not depend on time explicitly.

One Species

To define the main ingredients we consider the Malthusian model of a single population without external restrictions. With N we refer to the number of individuals and with t to the time. (In other contexts we might as well refer to a population density of, say, cells per liter. It can have advantages to define equations independent of the total volume.) Characterizing mortality and reproductivity by mortality rate m and birth rate μ, respectively, the rate equations are

$$\frac{dN}{dt} = bN - mN = (b - m)N = \alpha N. \tag{1.3}$$

Here the mortality rate specifies the ratio of the population dying in each unit time, and the birth rate the ratio of reproducing or new individuals per time. The net per capita change per time is then the combined rate $\alpha = b - m$. The differential equation of first order for N is solved by an exponential

$$N(t) = N_0 e^{\alpha t} \tag{1.4}$$

Population numbers will either grow indefinitely if α is positive or decline when α takes values below zero.

CONSUMER WITH EXPLICIT RESOURCE The next step is to take into account nutrient dependence. A basic interaction of one consumer population growing on a single resource can be described by the following equations.

$$\begin{aligned} \frac{dR}{dt} &= g - \epsilon \mu(R) N \\ \frac{dN}{dt} &= (\mu(R) - m)\, N \end{aligned} \tag{1.5}$$

The concentration of resource R affects the concentration of consumers N and vice versa. With g we denote the net growth of resource in a system without consumers (for example production minus degradation). A mortality rate

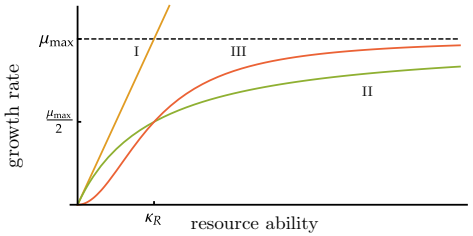

Figure 2: Types of functional response according to Holling [46]

of consumers m counteracts their growth or reproduction rate $\mu(R)$. Both, mortality and growth, are described as rates per capita and time. Growth should obviously depend on the availability of food. The resource intake and consumer growth are related by the factor ϵ that describes the amount of resource needed to yield one new consumer.

TYPES OF FUNCTIONAL RESPONSE Obviously the system's population dynamics depend on how effective species process nutrients or handle prey. Holling [46] characterized three major types of predation by their functional response (or growth rate function) $\mu(R)$. The simplest assumption (Holling's type I) is a linear dependence on food density. Holling's type II and III assume a limited ability to process resources and to reproduce and are thereby saturating to a maximal growth rate for high resource concentrations. Type II grows linearly with low resource concentration, type III (sigmoidal functional response) follows a more than linearly increasing function (see Fig. 2). Monod [80] set up an equation similar to Holling's type II to model growth kinetics that were found in empirical studies on microbes in aquatic environment. Monod's equation or Holling's type II is the typical choice for $\mu(R)$ in the context of bacterial and microbial growth [14, 63].

$$\mu = \mu_{max} \frac{R}{\kappa_R + R} \tag{1.6}$$

The specific growth rate μ is bounded by a maximal growth rate μ_{max}. When resource concentration amounts to κ_R, organisms grow at half the maximal rate (**half saturation constant**).

Two Species: Predator Prey Systems

By introducing predators feeding on prey we can expand the model to multiple trophic levels and describe more complex food webs. Simple predator prey

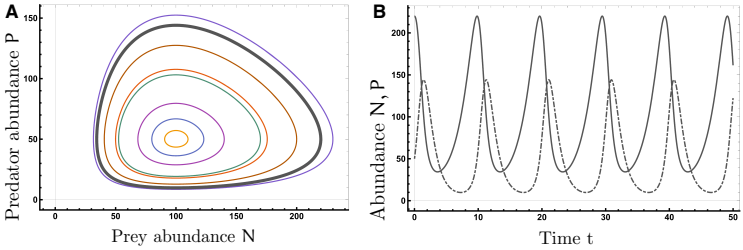

Figure 3: Simulations of a Lotka-Volterra system (1.7) with $\alpha_1 = 0.5, \alpha_2 = 1, \gamma_1 = \gamma_2 = 0.01$
left: Trajectories in phase space for several initial configurations, the gray cycle corresponds to the trajectories in the right panel
right: Numbers of predator and prey evolving over time for initial conditions $(N, P) = (220, 50)$

models have been discussed by Volterra [118] and similar equations were independently studied by Lotka [69]. A population of predators is modeled to feed on a prey population and to multiply correspondingly. For the well-known Lotka-Volterra equations the Malthusian system is extended.

$$\begin{aligned} \frac{dN}{dt} &= \alpha_1 N - \gamma_1 PN \quad &= (\alpha_1 - \gamma_1 P)\, N \\ \frac{dP}{dt} &= \gamma_2 PN - \alpha_2 P \quad &= (\gamma_2 N - \alpha_2)\, P \end{aligned} \tag{1.7}$$

The reproduction rate of the prey species is still assumed to be linear and without predators, prey would obey the exponential growth of a single-species system (1.4). The number of predators in the system P grows with the number of prey N which in turn decreases. The rate equations feature linear functional response and predators are subject to a constant death process. In this system, there are two equilibrium states. Trivially, if both species are extinct ($N = P = 0$) the situation will remain this way. The other solution is a coexistence fixed point in phase space ($N = \frac{\alpha_2}{\gamma_2}$, $P = \frac{\alpha_1}{\gamma_1}$). If initial conditions differ from these configurations we see trajectories evolving along a closed orbit (**limit cycle**) in phase space around the second fixed point (see Fig. 3) and initial population numbers determine the cycle the system will follow. Population numbers oscillate with a fixed frequency around the fixed point. Inspite of the simple equations, some biological observations agree with this prediction, e.g. the famous field observations of lynx and snow shoe hares

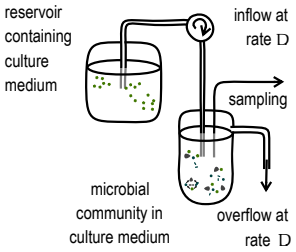

Figure 4: A schematic illustration of a chemostat experiment. Nutrient medium is pumped into a vessel containing a community of microbial organisms. This leads to an overflow from the vessel at the same rate and causes dilution in the mixture.

[24] and laboratory *Paramecium-Didinium* data [70]. Interestingly this particular system features a constant of motion

$$G = \gamma_2 N - \alpha_2 \ln N + \gamma_1 P - \alpha_1 \ln P \tag{1.8}$$

accounting for properties allowing analytical treatment. Due to its neutral population cycles, such systems can easily be pushed to extinction by decreasing the system size and increasing stochastic noise (see e.g. Dobrinevski and Frey [21], McKane and Newman [78], Parker and Kamenev [85]). In other predator-prey systems noise can produce complex spatio-temporal structures and with long-lived population oscillations [20].

A more realistic model is the popular Rosenzweig Mac Arthur model [91] incorporating a carrying capacity similar to Verhulst's equation (1.2)

$$\begin{aligned} \frac{dN}{dt} &= rN \cdot \left(1 - \frac{N}{K}\right) - \frac{NP}{N+K} \\ \frac{dP}{dt} &= \gamma \frac{NP}{N+K} - \beta P \end{aligned} \tag{1.9}$$

1.2.2 Chemostat Experiments

Microbial food webs are a convenient system to study population growth. High reproduction rates allow observations of several generations during a span of days. The system can be modified so as to model other kinds of food webs. Communities of bacteria or phytoplankton and bacterivorous ciliates can act as models for food webs of higher animals and vertebrates. At the

same time the experimental setup is transparent enough to be understood qualitatively and quantitatively. Well controlled experiments on microbial growth can be performed in a **chemostat** Such an installation is shown in schematic form in Figure 4. Here, an aquatic community of microorganisms—bacteria, ciliates, algae—is cultured in a vessel in dissolved nutrients. Constant inflow from a reservoir provides nutrient medium and at the same time dilutes the system.

One Species: Consumer with Resource

As an example let us first assume a single bacterial strain and a resource and adapt equation (1.5). An important parameter characterizing this setup is the dilution rate per time, D, at which fresh medium of concentration R_0 is pumped into the vessel. This results in an effective mortality rate $m = D + d$ where d represents the loss rate per capita from any other process as death or predation. Let us assume death rates are negligibly small in comparison to dilution. This yields the following system of equations.

$$\begin{aligned} \frac{dR}{dt} &= (R_0 - R) \cdot D - \epsilon \mu(R) \cdot N \\ \frac{dN}{dt} &= (\mu(R) - D) \cdot N \end{aligned} \tag{1.10}$$

With this in our simple case of one bacterial consumer feeding on a resource the population of bacteria would typically grow until an equilibrium is met. Assuming a Holling's type II growth rate (1.6) yields the fixed point values.

$$\left.\begin{aligned} \frac{dR}{dt} &= 0 \\ \frac{dN}{dt} &= 0 \end{aligned}\right\} \quad \Rightarrow \quad \begin{aligned} D &= \mu(R^*) \\ N^* &= \frac{R_0 - R^*}{\epsilon} \end{aligned} \quad \overset{(1.6)}{\Rightarrow} \quad \begin{aligned} R^* &= \frac{kD}{\mu_{max} - D} \\ N^* &= \frac{R_0 - R^*}{\epsilon} \end{aligned} \tag{1.11}$$

Obviously this result is only reasonable if nutrient concentration R^* is positive, i.e. if $\mu_{max} > D$. This statement simply corresponds to the requirement of the maximal growth rate being greater than dilution.

This basic building block can be employed to describe competing species. Dependance on several resources has to be included by choosing the appropriate growth rates.

Two Species: Predator Prey

Of course this experimental model can also be used to study predator prey systems by selecting appropriate microorganisms.The corresponding version in chemostat with Holling's type II functional response reads

$$\begin{aligned}\frac{dR}{dt} &= (R_0 - R)\cdot D - \epsilon\mu(R)\cdot N \\ \frac{dN}{dt} &= N\cdot(\mu(R) - D) - \phi(N)\cdot P \\ \frac{dP}{dt} &= (\beta\phi(N) - D)\cdot P\end{aligned} \tag{1.12}$$

with a newly introduced functional response of predator growth depending on the prey concentration. A loss in prey numbers accompanies the growth of predator population P. Again a conversion β accounts for the number of predator organisms resulting from the loss of one prey individual.

More Species and More Resources: Competition

These models can easily be expanded to food webs of higher complexity. Consider, for example a community of n planktonic species grazing on k resources. Population abundances N_i grow depending on the availability of the resources. The availability of a resource j on the other hand, R_j, depends on the consumption of resources by the plankton.

$$\begin{aligned}\frac{dN_i}{dt} &= N_i\,(\mu_i(R_1,\dots R_k) - m_i) && i = 1,\dots n \\ \frac{dR_j}{dt} &= D(S_j - R_j) - \sum_{i=1}^{n} c_{ij} N_i \mu_i(R_1,\dots R_k) && j = 1,\dots k\end{aligned} \tag{1.13}$$

Specific mortality and growth rates are denoted by m_i and $\mu_i(R_1,\dots R_k)$ respectively. A constant turnover rate D supplies fresh resources from a reservoir with concentration S_j of resource j. The content of resource j in species i amounts to c_{ji}.

Now we are faced with a new concept: The growth rates $\mu_i(R_1,\dots R_k)$ are determined by several nutrients and further considerations are necessary to decide on the functional response. Assume that we know how a species will respond to a single nutrient R_j (provided all else is sufficiently supplied). For microorganisms we will describe this by a function $\mu_i(R_j)$ of the Holling's type II . Is there a way to combine the nutrient-specific growth-rates $\mu_i(R_j)$ into a general growth-rate-function dependent on all nutrients $\mu_i(R_1,\dots R_k)$?

This will depend on the way how the nutrients are utilized by the organisms. Nutrients can act as **heterologous** (=**essential**) in an organism. **Perfectly essential** means that for the species considered no resource can be replaced by any one or more of the other resources. Other chemicals might be replaceable (**homologous**) because they fulfill similar functions or can be converted into one another [62, 126].

For example; Huisman and Weissing [47–49] simulate a system of an aquatic phytoplankton with **perfectly essential** resources. We will discuss this particular case in more detail later.

1.3 DIVERSITY IN DYNAMIC POPULATIONS

For the conservation of biodiversity, we have to identify mechanisms maintaining and promoting species richness in natural habitats. Mathematical models can predict consequences of management strategies. The term **diversity** can refer to different quantities depending on context and author. Sometimes **species abundances**—the number of individuals per species— and their evenness are included and scientists calculate a weighted average. In this thesis, **species richness** and **species diversity** both, will be synonymous to the number of species in a system independent of the individual population numbers.

1.3.1 Competitive Exclusion and Chaotic Coexistence

Several resources limit the growth of organisms in nature: Mineral nutrients, gas, light and water are essential for survival and production. In the 19th century Sprengel [97] developed the nowadays so called **Liebig's law of the minimum**. The idea was promoted lateron by Justus von Liebig[119].

> "(...) denn fest steht der Satz: eine Pflanze, die 9 oder 10 Stoffe zur Nahrung bedarf, kann niemals ihre höchste Ausbildung erreichen, sobald von einem einzigen dieser Stoffe nicht die erforderliche Menge vorhanden ist." — *Sprengel [97]*

This concept was based on the knowledge from agricultural science, that plants depend on a number of nutrients to grow. It states, that plants will grow not according to the total amount of resources, but that they are limited by the nutrient shortest in supply—the **limiting factor**. In other words some nutrients cannot be replaced and oversupply of one nutrient can not make up for the shortage of another.

Now consider several species limited by a number of resource. The **Competitive Exclusion Principle** was formulated in 1904 by Grinnell [36] for such systems relying on field observations.

> "Two species of approximately the same food habits are not likely to remain long evenly balanced in numbers in the same region. One will crowd out the other" — *Grinnell [36]*

Gause [29] elaborated this idea based on laboratory experiments with two *Paramecium* species. He let the two species evolve in a constant environment providing a constant flow of food and fresh water. His claim was, that with constant ecological and environmental factors two species cannot compete for the same resource and coexist. He could show however, that the two species could coexist when he varied the supply of food and water. A more general formulation is that two species cannot inhabit an identical ecological niche at the same time: In a constant environment one will always outgrow the other.

This principle entails discussions about the **Paradox of the Plankton**:

> "The problem that is presented by the phytoplankton is essentially how it is possible for a number of species to coexist in a relatively isotropic or unstructured environment all competing for the same sorts of materials." — Hutchinson [50]

While Gause could demonstrate the principle to hold true in laboratory with two species of *Paramecium* or yeast, everyday experience as well as data from microcosm and mesocosm experiments show different results. Soil bacterial communities competing for a few easily digestible nutrients exhibit a high diversity [25]. Although phytoplankton growth is assumed to be limited only by nitrate, phosphate, light and carbon (because all other elements are abundant in natural waters), several thousand species can be observed in the surface layers of the world's oceans in a relatively constant environment and little spatial structure [18, 101]. In the group of Benincà et al. [12] containers with 90 liters of water, along with sediment, detritus and the microscopic life therein were isolated from the Baltic sea. The interactions of bacteria, phytoplankton, herbivorous and predatory zooplankton and detritivores were studied over eight years in their complex aquatic habitat. Contrary to the predictions of the Competitive Exclusion Principle, the number of surviving species exceeded the number of assumedly essential nutrients (phosphor, nitrogen, carbon, light) by far.

Candidates to resolve the Paradox include chaotic advection in hydrodynamical flows, external perturbation as an ever-changing environment, spatial variation and migration. But those hypothesis cannot provide explanations for the observed coexistence in well-controlled laboratory conditions and well mixed chemostats [7, 94].

At first, theoreticians supported the Competitive Exclusion Principle by mathematical proofs. These proofs, however, relied on linear growth rates

functions and searched for coexistence at stationary densities [64, 66, 71, 89, 118]. Later it has been demonstrated under more general assumptions that at fixed densities a coexistence of n species on $k < n$ resources is impossible [77]. Nevertheless if one considers models with nonlinear growth rates and *non equilibrium dynamics*, coexistence of n species on $k < n$ resources actually becomes feasible [3, 4, 54, 58, 77, 125]. Koch [58] gave numerical indication via simulations of 2-species coexistence on one resource on a periodic orbit. Analytically this coexistence was proven for two species by McGehee and Armstrong [77]. A proof for n species coexisting on one resource was provided by Zicarelli [125] and expanded by Kaplan and Yorke [54] to more limiting factors. Gross et al. [38] proved the existence of chaotic parameter regions generically in food chains of length greater than three.

Altogether this suggests **one way out of the Paradox**. Namely, that a constant environment is not a sufficient condition for competitive exclusion, but that non-stationary population numbers make coexistence possible. The principle cannot be generalized to dynamical systems and one should consider non equilibrium dynamics to account for diversity. Theoretically, non equilibrium systems may allow communities with more species than limiting resources to coexist. These dynamics are bounded and can either evolve towards a periodic **limit cycle** or they can be chaotic and follow a **chaotic attractor**, i.e. a lower dimensional complex structure embedded in the phase space of population numbers. To feature bounded chaotic solutions, autonomous differential equations of first order of continuous functions have to be at least three dimensional according to the Poincare-Bendixson theorem [98]. So when the system's dimension exceeds three, population dynamics can become more complex and even chaotic.

This leaves the question whether biological systems commonly undergo chaotic dynamics. Or whether this explanation for biodiversity and the Paradox of Plankton is merely academic.

Experiments have shown hints of sustained oscillations in short time series of small laboratory food webs [23, 27, 53, 110]. In cultures of cannibalizing developmental stages of the flour beetle *Tribolium*, the mortality was changed artificially to observe crossovers from stable fixed points to chaos that had been predicted theoretically[17, 19, 44, 56]. Graham et al. [35] cultivated a community of nitrifying bacteria and protozoa in wastewater bioreactors for 207 days reporting strongly fluctuating population numbers.

Too short observation times and slow transient behavior could be a reason that exclusion does not take place during the experiments. But in the before mentioned long term experiment by Benincà et al. [12] species abundances of ten aquatic functional groups and the detritus pool were counted twice a week and the nutrient concentration was measured. This resulted in a total of

690 data points per functional group, demonstrating strong erratic fluctuations in the population numbers. The duration of this experiment and sustained species richness and oscillations are a clear sign that no 'slow exclusion' is taking place. The study by Benincà et al. [12] reported that the forecast period was limited to 15 to 30 days which might indicate deterministic chaos. However, this impressive study is not without shortcomings. By gathering species into functional groups single-species information are lost. Measuring twice a week might disguise important dynamics and a lack of an external control parameter prevents a clear decision.

A combination of experimental results and model calculations can provide more confidence and an understanding of underlying mechanisms. Bifurcation analyses numerically confirmed chaotic dynamics for biologically relevant parameter values in models of two-prey-one-predator food webs in microbial chemostat systems [59, 114]. An actual microbial food web of this structure was examined by Becks and Arndt [8, 9], Becks et al. [10]. Bacterial strains – *Pedobacter* and *Brevundimonas* – have been placed in diluted nutrient medium together with a ciliate preying upon both. An externally controlled dilution rate determines the nutrient supply for the bacteria and at the same time acts as an effective mortality rate via overflow. And indeed by altering this parameter the population dynamics could clearly be tuned from equilibrium to periodic orbits to chaos and back in time series of 30 - 60 days duration.

Numerical simulations of plankton systems demonstrate longterm coexistence for particular parameter configurations as well.

Huisman and Weissing [47] demonstrated via numerical simulations of equations (1.13), that for perfectly essential resources, non-equilibrium dynamics with more species than resources are possible. In the model multiple phytoplankton species survive on a few abiotic resources in a constant environment. Population numbers of all species can show strong sustained oscillations dependent on the parameter values. Huisman and Weissing provide specific parameter configurations that enabled oscillating coexistence of six species on three resources and chaotic resilience of twelve species on five nutrients. Deterministic chaos was indicated by bifurcation analyses.

It is still not clear, however, whether this specific numerical model should be treated as an exception and oddity or whether it reflects processes in real biological systems. An experiment testing this prediction was performed at the Institute for General Ecology at the University of Cologne by Schieffer [94] and Arns [7] that will be presented and modeled theoretically in this thesis. In the experiment up to six bacterial strains were cultivated in a common nutrient medium containing three essential resources. The choice of bacteria was just influenced by their ability to feed on a certain nutrient medium. Over the

period of the experiment (30 - 50 days) all strains survived with fluctuating population numbers supporting the thesis of chaotic coexistence.

1.3.2 Stochastic Fluctuations and Demographic Noise

Ecological systems are subject to 'intrinsic' and 'extrinsic' noise sources. Extrinsic noise could for instance be changes in temperature, fluctuations in nutrient supply and migration from external habitats. Intrinsic noise – also called demographic noise – is caused by the discrete unit steps at which population sizes change and take place even in perfectly isolated systems. Even if differential equations predict infinite survival, with demographic noise a population might die out. In the simplest case the discrete system population numbers have to take values of zero or one when the continuous system takes real number in between. Another case where discreteness can induce significant differences is a stationary coexistence in the deterministic equations. If the continuous approximation abundances evolve towards a non-integer stable fixed point, discontinuity forces the numbers to jump "too far". The fixed point cannot be realized. Now the numbers have again to evolve back towards the fixed point. For this reason the discrete system is forced to fluctuate around the stable point. Those fluctuations may transfigure otherwise regular dynamics to behave randomly or induce periodicity [30, 109]. Such a type of effective randomness is particularly important for systems with small population sizes. Nevertheless, even in very large systems demographic noise can cause qualitative and strong effects [78]. For the food webs under consideration, the main question is how demographic noise will interfere with deterministic chaotic fluctuations present and influence stability. The discrete nature of the food-web's dynamics is captured in the master equations of the system. These can be simulated and analyzed numerically in terms of the so-called Gillespie algorithm [31, 32]. From these simulations one can extract extinction rates in different dynamic regimes as will be done in chapter 2.

1.3.3 Verification of Chaos

There are numerous ways to demonstrate chaos in dynamical systems. Principal approaches include bifurcation diagrams, the identification of Lyapunov exponents, or the analysis of Poincaré sections. Detecting deterministic chaos in experiments is more difficult. Populations are always subject to intrinsic demographic fluctuations, at levels which depend on the size of the population and the underlying deterministic dynamics. One needs to exclude these mechanisms, rather than deterministic chaos, as a primary cause of fluctuations in the system. In the majority of cases the series of data are too short to

construct bifurcation diagrams or to reliably estimate Lyapunov exponents. A better approach is to search for parameter-dependent controllable crossovers from stationary to chaotic behavior. In this way, chaotic and stochastic fluctuations, respectively can be discriminated from each other. Model calculations can give confirmation if experimental data demonstrates qualitative changes in time-series.

2 CHAOS STABILIZING A PREDATOR-PREY SYSTEM

Surprise? Who's talking about surprise? Chaos is no surprise. It has predictable characteristics. For one thing, it carries away order and strengthens the forces at the extremes.

— Frank Herbert, *Dune*

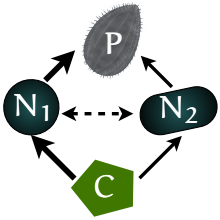

Figure 5: A predator P feeds on two prey species $N_{1,2}$ competing for a mutual food source C. Bold arrows represent stronger energy flow, indirect influence via competition is depicted by a dashed link.

We examine a mathematical model of a simple food web consisting of two prey populations competing for nutrients and one predator population. In this model a control parameter triggers a bifurcation that initiates a transition to chaos. Chaos might alter the evolution of a system unpredictable during little time and induce wild fluctuations. Still, with the evolution of a chaotic attractor it can stabilize the system by bounding the population numbers in a region in phase space.

The experimental analogue is an aquatic system in a chemostat where similar dynamics where shown by Becks et al. [10] in Cologne. In nature such an ecosystem is exposed to different perturbations like seasonal fluctuations and stochasticity - meaning demographic noise. Interactions of the Lotka-Volterra type can easily be pushed to extinction by demographic noise [84].

In our cooperation with the group of Hartmut Arndt[1], we aimed at finding a general catalogue of techniques to approach such a system and to analyze

1 Zoological Institute, University of Cologne

its features. We address the question, how stable an attractor is when encountering perturbations, we characterize the stability of a chaotic attractor and we ask whether a food web will persist if ruled by deterministic chaos rather than by regular limit cycles or Lotka-Volterra-like dynamics.

Parts of the following chapter are borrowed from [37][2]. For a first characterization of the dynamics in this model I fall back upon parts of my diploma thesis. Starting from there, I expose the implications for generic ecological food webs, identify the deterministic chaos via the largest Lyapunov exponent and I calculate the mean extinction times of the food web numerically for the subsequent interpretation[3].

2.1 INTRODUCTION

Ecological networks can show various different dynamics. As experiments confirmed they can also be ruled by deterministic chaos [10, 12, 17]. In that case the abundances of the species are restricted to a chaotic attractor undergoing large fluctuations but secure from extinction. To understand the effect of chaotic dynamics in ecological systems one can resort to a model of a small predator-prey-system. Our paradigm is an aquatic microbial community comprising two prey and a predator species. The three microscopic species are cultivated in a solution of nutrients in water in a chemostat (Fig. 7). They are constantly provided with fresh water and food.

Two bacterial strains (in experiments *Brevundimonas*, *Pedobacter*) compete for food. A ciliate (*Tetrahymena pyriformis*) acts as common predator. A more (less) efficient usage of food and being more (less) preferred by the predator can balance each other out and lead to a coexistence of the two strains (Fig. 6). Starting at the upmost position with many predators we can imagine the following cycle: First the less preferred species can take advantage of that fact and will grow. At the same time the number of predators decreases when the preferential food is getting sparse. With the now reduced feeding pressure the fast growing competitor will flourish. And finally the predator can reproduce again and we end up at our initial condition.

Experiments on this community have shown equilibrium, periodic and chaotic oscillations of population numbers [10]. The type of dynamics depends on the inflow of dissolved nutrients into the chemostat. This inflow—or dilution—drives the systems dynamics and acts as control parameter.

A minimal model was formulated considering the grazing of bacteria and the predation of the ciliate. The rate equations are assumed to follow ordinary

2 I have performed the numerical simulations and the analysis, created the graphics and composed the manuscript.

3 For numerical implementation see Appendix A

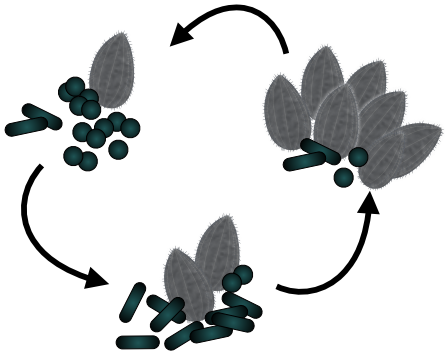

Figure 6: A predator feeds on two prey species. It prefers the prey that is faster growing. This compensation enables the depicted cycle. In the experiment this is realized by the bacterivorous ciliate *Tetrahymena pyriformis* (gray) and two strains of bacteria - preferred fast growing *Pedobacter* (depicted by spheres) and slow growing *Brevundimonas* (rod like).

Holling's type II growth. With inserting the experimentally determined specific parameters the model outcome is indeed qualitatively consistent with the experimental results.

Numerical simulations of the different species concentrations undergo periodic oscillations or stay constant in an equilibrium, a regime of chaotic population dynamics is formed over a wide range of intermediate dilution strengths. This parameter window is bounded by two regimes of periodic coexistence (**stable limit cycles**). Chaotic trajectories stick to a structure (**chaotic attractor**) in phase space that seems to interpolate between the two distinct periodic dynamics. With this attractor stable coexistence of all three species is possible. An additional stability against perturbations is provided in the sense, that species abundances might react with huge fluctuations but settle quickly back onto the attractor manifold. The food web in its structure and composition remains unchanged. The same mechanism helps to stabilize against the destabilizing effects of migration and supports persistence.

In small systems finite numbers and discrete birth and death processes produce fluctuations (**demographic noise**) and can push species towards extinction that would persist in larger systems. In Lotka-Volterra systems the mean time to extinction grows polynomially with population size[84, 85]. In this chaotic system we can confirm the attractor's protective properties: The mean time to extinction in this case scales exponentially with system size.

This study discusses and quantitatively models the conceptual mechanisms promoting chaotic multi-species coexistence in a two-prey one-predator model system motivated by the experiment of Becks et al. [10]. As previous studies suggest [28, 60, 103, 114] the system shows periodic and chaotic coexistence. An attractor evolves that topologically bears resemblance to Gilpin's classification of Vance's model [34, 57, 113]. The principles behind the formation of the attractor manifold may be summarized as follows: our system is governed by an important control parameter—the external dilution rate which acts as a paradigm for the availability of resources that the species consume. Both in the regime of low and high resource availability, the system builds up limit cycles controlling the population size. The two cycles at high and low dilution rate are topologically distinct, in a manner to be discussed below. The wide range of intermediate parameter strength is governed by a 'competition' between the two cycle regimes, and this will be shown to lead to the formation of a chaotic attractor interpolating between the limiting dynamics.

The suggestion that chaotic attractors may emerge from the competition between parametrically separated limit cycles is one main result of the present chapter. Fixed points and limit cycles for different parameter regimes are a generic feature of predator-prey systems and their interplay might suggest a generic mechanism promoting the transition to chaos. Below, the predictions derived for our current specific model will be shown to be in good agreement with the experiment Becks et al. [10] where population numbers in chemostat experiments could be tuned from stationary to periodic or chaotic and back depending on the applied dilution rate.

Another outcome is the confirmation of the protecting properties of chaos. Although fluctuations strongly suppress population numbers the chaotic attractor actually protects them exponentially against extinction.

2.2 METHODS

The system we consider models an aquatic well-mixed microbial community established in a chemostat. Prey populations compete with each other for nutrients but also via a common predator.

In the experiments under consideration two bacterial strains live on soluble organic matter, while a bacterivorous ciliate feeds upon the two different bacterial strains. The competition is characterized by a trade-off: one bacterial strain is preferred by the predator but grows faster. The other strain is less-preferred but slow-growing. At a rate D fresh nutrient solution flows into the chemostat vessel of constant volume. Via the overflow, a mixture of microbes and nutrients leaves the system and thereby dilutes the community inside the

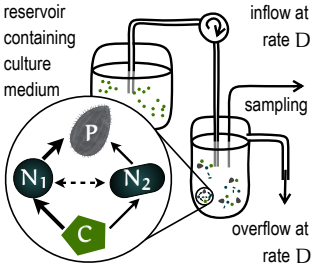

Figure 7: Outline of the experimental setup. Inset the schematic structure of interactions in the the predator prey system. Bold (thin) arrows mark strong (weak) energy/biomass flow, indirect competition is shown as dashed arrow. P=predator, C=carbon source, N_1=prey 1, N_2=prey 2

chemostat. By tuning this dilution or turnover rate we will test the behavioral range of the system (Fig. 7). The following differential equations describe the temporal behavior of the concentrations in the system in the way proposed in Bohannan and Lenski [14] and Levin [64].

$$\begin{aligned}
\frac{dC}{dt} &= (C_0 - C)D - \epsilon_1 N_1 \mu_1(C) - \epsilon_2 N_2 \mu_2(C) \\
\frac{dN_i}{dt} &= N_i \mu_i(C) - P\phi_i(N_i) - DN_i \quad , i = 1,2 \\
\frac{dP}{dt} &= \beta_1 P \phi_1(N_1) + \beta_2 P \phi_2(N_2) - DP
\end{aligned} \tag{2.1}$$

The concentration P of predators per unit volume grows at a per capita rate that depends on the prey populations; the concentration of prey N_i declines accordingly. The grazing rate of a predator on the bacteria i is denoted by $\phi_i(N_i)$. The ratio of new predators per ingested prey i is β_i (yield). In almost the same manner the bacteria of type i multiply by a rate $\mu_i(C)$ while feeding with a rate $\epsilon_i \mu_i(C)$, where ϵ_i is the reciprocal yield of ingested biomass per new prey. The growth rate $\mu_i(C)$ of prey i saturates at $\hat{\mu}_i$ following Holling's type II or Monod's equation (1.6) with half saturation rate K_{si} just as the grazing rates $\phi_i(N_i)$:

$$\begin{aligned}
\mu_i(C) &= \frac{\hat{\mu}_i C}{K_{si} + C} \\
\phi_i(N_i) &= \frac{\hat{\phi}_i N_i}{K_{Ni} + N_i}
\end{aligned} \tag{2.2}$$

For one specific microbial community and nutrient solution the dilution rate is the only variable left. All other parameters define biological properties of the species. The parameter values are chosen to model the specific experiments determined by Becks et al. [10] and Nomdedeu et al. [82] (see Table 1).

2.3 THEORETICAL RESULTS

Numerical integration of Eq. 2.1 shows that the population numbers perform dynamical patterns depending on the strength of dilution. They can be organized into a few general groups: stationary, periodic and chaotic dynamics. Without predator only one prey species will survive, the other will quickly go extinct while in the presence of a predator two species coexist. More interestingly, all three species can coexist. The dilution values corresponding to qualitative changes in the dynamics are summarized in Table 1.

Table 1: Model parameters measured in experiments by Becks et al. [10] and Nomdedeu et al. [82] and critical dilution values (numerical results up to 4 digits)

SYMBOL	DEFINITION	VALUE
C_0	concentration in nutrient medium $[\frac{\mu g\ Gluc}{ml}]$	3
ϵ_i	reciprocal yields $[\frac{\mu g\ Gluc}{ind_i}]$	$2 \cdot 10^{-6}$
β	predator yields $[\frac{ind_p}{ind_i}]$	$2.5 \cdot 10^{-4}$
μ_1	maximal growth rates $[h^{-1}]$	0.15
μ_2		0.172
ϕ_1	maximal feeding rates $[\frac{ind_i}{ind_p \cdot h}]$	150
ϕ_2		450
K_{s1}	half saturation concentrations $[\frac{\mu g\ Gluc}{ml}]$	0.0274
K_{s2}		0.002
K_{N1}	half saturation concentrations $[10^3 \frac{ind_i}{ml}]$	422
K_{N2}		400
a	critical dilution rate $[h^{-1}]$	0.0267
b		0.0309
c		0.0544
d		0.0790

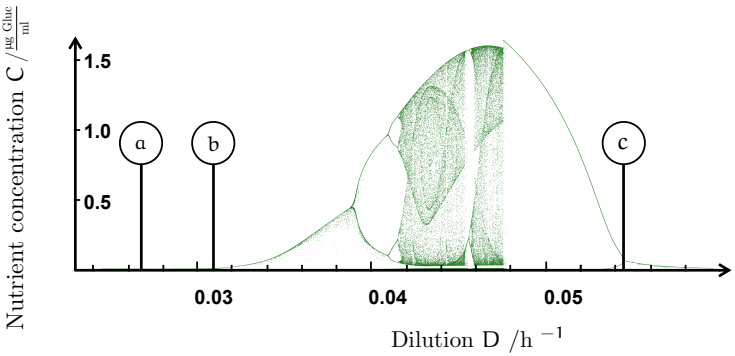

Figure 8: Bifurcation diagram for the nutrient concentration with varying dilution rate. Critical values a – c refer to Table 1

The regimes of different dynamics can be described in several ways. Figure 8 encodes the relevant structures in terms of a **bifurcation diagram**. In the bifurcation diagram all extremal values of the long-term dynamics of one quantity (presently nutrient concentration C) are plotted with respect to the bifurcation parameter (here the dilution rate D); a line represents a shifting fixed point; two lines mean that the population number is oscillating between those two extrema; four indicate periodic dynamics with two maxima and two minima et cetera. The diagram clearly shows different regimes, and transitions between them.

A chaotic dynamical system can be characterized by its **Lyapunov exponents** [111]. They measure wether small perturbations of initial conditions will grow exponentially over time into major deviations between trajectories or wether they will shrink. If the maximal exponent is strictly positive and the system folds back and is bounded (as is here the case) this is considered to be a definition of deterministic chaos. Mathematically stable—i.e. convergent—systems show negative Lyapunov exponents. Plot 9 demonstrates that the system features negative largest Lyapunov exponents except for a clearly positive range between dilutions of about $D = 0.04$ per day and $D = 0.05$. This is the regime where trajectories show irregular dynamics and fill up an attractor manifold (cp. Fig. 12).

However, before discussing these patterns, we note that an alternative way to encode system information is in terms of its **fixed point structure**: fixed points of the differential equations 2.1, i.e. configurations (C, N_1, N_2, P) where $d_t C = d_t N_i = d_t P = 0$, can be found numerically. Depending

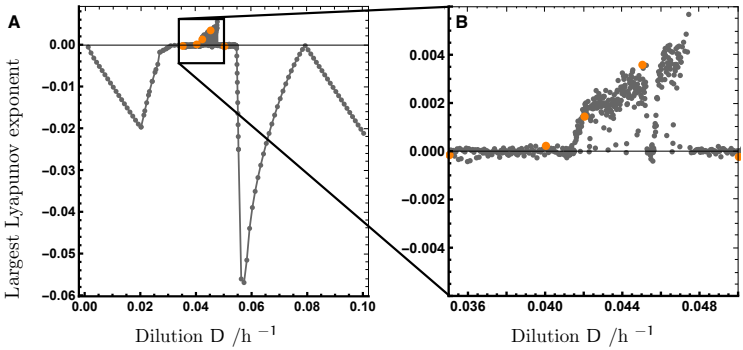

Figure 9: The largest Lyapunov exponent of the system as a function of the dilution rate indicates chaos for $0.04 < D < 0.05$.
A: The whole range of dilution rates $0.0 < D < 0.1$.
B: A zoom into the region of positive Lyapunov exponents $0.035 < D < 0.050$.

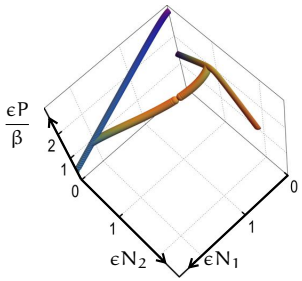

Figure 10: Fixed points migrating through phase space with growing dilution. Dilution rate D is colour-coded from weak (purple, $D = 0.001h^{-1}$) to strong dilution (orange, $D = 0.07h^{-1}$)

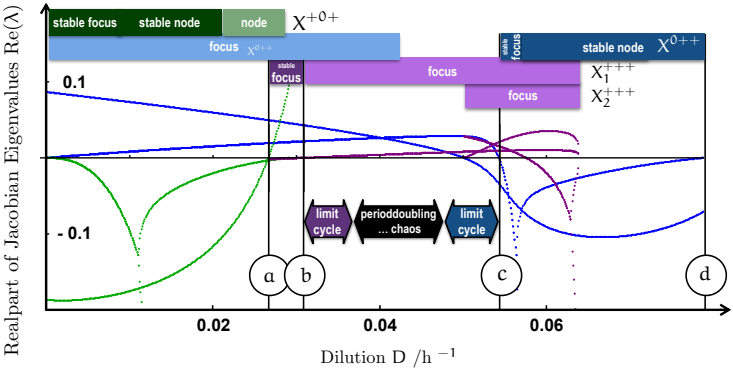

Figure 11: Real parts of the eigenvalues of the Jacobian of the linearized system for all fixed points of coexistence with varying dilution. Negative real parts correspond to stable directions, dark bars indicate regimes of stable fixed points. green: X^{+0+}, blue: X^{0++}, purple: the two 3-species fixed points $X^{+++}_{1,2}$. Critical values a – d refer to Table 1

on the parameter values of the system different fixed points are realized and shown in Figure 10. We denote the different multiple-species fixed points as

- X^{+0+}: predator feeds only on prey 1
- X^{0++}: predator feeds only on prey 2
- $X^{+++}_{1,2}$: the two different 3-species equilibria

To investigate the stability properties of these stationary configurations we determine the eigenvalues of the Jacobian of the linearized system. Eigenvalues with non-zero imaginary parts correspond to a spiral point (or focus), three real eigenvalues imply nodes. If all three eigenvalues possess negative real parts the focus or node, respectively, is stable while positive real parts correspond to unstable directions.

Here, we restrict ourselves to a discussion of the fixed points relevant to the attractor formation (Fig. 11):

- $D < a$: stable 2-species coexistence X^{+0+}
- $D = a$: stable 3-species equilibrium X_1^{+++} emerges from X^{+0+} (Fig. 10) and X^{+0+} looses stability.
- $D = b$: the 3-species equilibrium X_1^{+++} becomes a saddle, i.e. looses stability
- $c \leqslant D \leqslant d$: stable 2-species coexistence X^{0++}
- $D > d$: no stable fixed point

In the parameter window without stable fixed points, $b < D < c$, the population numbers oscillate periodically or chaotically. Two foci are of particular interest to the formation of the chaotic attractor: at the lower end of the window ($D = b$) a 3-species focus X_1^{+++} looses stability; at the other end ($D = c$) a 2-species focus X^{0++} becomes stable.

Simulating the dynamics numerically, we learn that the foci evolve into limit cycles (of 3 or 2 species respectively) when entering the window of fixed-point-instability from the respective ends. In-between, the influences overlap and enable dynamical 3-species coexistence (Fig. 12 **A-C**). A trajectory starting near the central saddle focus X_1^{+++} circles outwards in the corresponding unstable plane. In the proximity of X^{0++} the trajectory leaves that plane to orbit around X^{0++} until it enters again the region of influence of X_1^{+++}. Starting at $D = b$ with increasing dilution cycles of higher order develop via period-doubling until no periodicity occurs anymore and a chaotic attractor determines the dynamics.

The bifurcation diagram in Figure 8 substantiates this range of dynamical behavior. For weak and strong dilution the system is in equilibrium (one point). At $D = b$ the Hopf-bifurcation leads to chaotic dynamics via consecutive period-doublings: a stable cycle (two points) and cycles of higher order (more points) arise. This oscillating or chaotic regime ends with the 2-species focus turning stable for $D > c$. When dilution exceeds $D = d$ this node grows unstable as well and all species are washed out.

Figure 12 **A-C** shows a plot of the ensuing **dynamical patterns in phase space**: for small dilution rates a limit cycle around an unstable fixed point governs the dynamics. For strong dilution rates the trajectories follow a 2-species limit cycle. In the intermediate regime a chaotic attractor appears interpolating between those dynamics. Visual inspection suggests the attractor to have the topology of the well known Rössler attractor [92]. However, we have not been able to identify the Rössler differential equations as a limiting case of our model equations and therefore cannot say with certainty that the identification holds. Attractors of this topology have been shown to exist in other mathematical three dimensional predator-prey models by Gilpin [34].

In finite systems, fluctuations due to the discreteness of population numbers—demographic noise—drive populations into extinction that deterministically would survive. These events will occur at random at a certain rate or probability. In the well-known Lotka-Volterra system the mean time to extinction scales polynomially with population size. Stochasticity was taken into account in numerical Monte-Carlo simulations of the model following the established Gillespie Algorithm [31, 32]. In each iteration step the rates or probabilities of the birth and death processes $\mu = 1, \ldots 6$ of all three species a_μ and the total rate for "any event" $a_0 = \sum a_\mu$ were calculated. The time τ until the next occurrence of an event was calculated from the Poisson-distribution

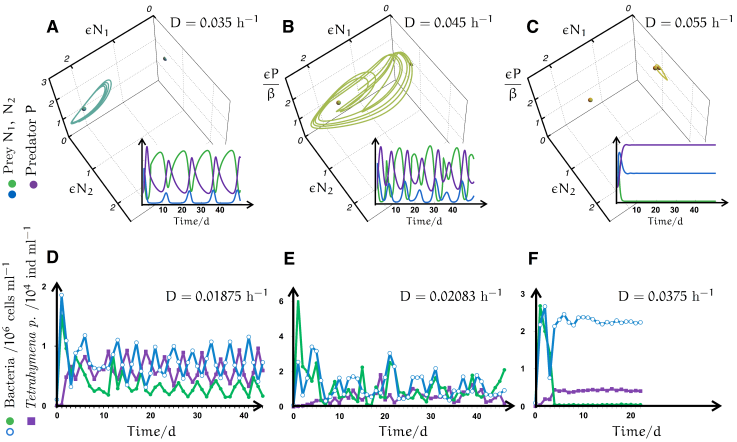

Figure 12: **A**-**C**: Phase space diagrams of days 50 to 100, demonstrating the changes in population dynamics by increasing dilution rate. Inset the corresponding time series of days 0 to 50. **A**: stable limit cycles at D = 0.031 h^{-1}; **B**: chaotic attractor at intermediate dilution rates, as an example D = 0.047 h^{-1}; **C**: stable limit cycles at D = 0.05 h^{-1};
D-**F**: Time-series data from Becks et al. [10]. Open circles, abundances of *Pedobacter* (preferred prey); filled circles, abundances of *Brevundimonas* (less-preferred prey); filled box, numbers of *Tetrahymena pyriformis* (predator); **D**: D = 0.01875 h^{-1}, **E**: D = 0.02083 h^{-1}, **F**: D = 0.0375 h^{-1}

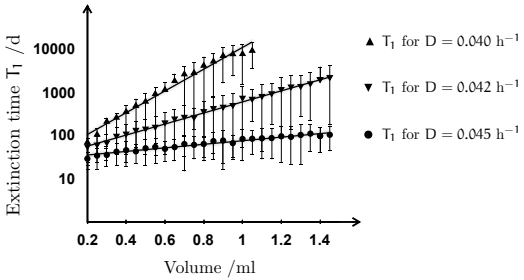

Figure 13: Logarithmic plot of the mean time to first extinction for dilution rates D = 0.04, 0.042 and 0.045. Error bars denote the standard deviation of the monitored runs.

$P_1(\tau) = a_0 \exp(-a_0\tau)$. A birth or death processes μ was generated according to the probability densities a_μ/a_0 such that events follow the probability density

$$P(\tau, \mu) = a_\mu \exp(-a_0\tau). \tag{2.3}$$

This was done for a set of dilution rates and system sizes starting at 0.2 ml to exclude extreme finite size effects and ranging up to 1.45 ml. For each dilution rate the system started from an initial state on the deterministic attractor with concentrations of the order 100 predatory organisms, and 10^6 and 10^5 bacteria respectively. Population numbers evolved several times until one of the species went extinct or a maximum time was reached and the mean time to extinction was calculated. As Figure 13 shows, the mean time to extinction scale exponentially with population size. Similar structures were observed for other dilution rates. The remaining points show exponential behavior with coefficients of determination above 95%. As expected the attractor indeed protects populations exponentially as opposed to the marginally stable generalized Lotka-Volterra model analyzed by Parker and Kamenev [84].

The differential equations above have been modeled to describe the chemostat experiments of Becks et al. [10]. Without any parameter fitting the data indeed shows qualitative agreement with the dynamical patterns of Figure 12 D-F: at weak dilution the three species show periodic behavior as with a limit cycle, increasing the dilution leads to strongly fluctuating aperiodic dynamics in all three species and at even stronger dilution the fast-growing preferred prey and the predator coexist in stable equilibrium. In the model, the slow-growing strain goes extinct for strong dilution. In the experiment, population abundances do not vanish completely but drop by a factor of 50. A reason for

this deviation might be that small areas in the chemostat do not mix well — thereby protecting some bacteria from being washed out by dilution.

2.4 DISCUSSION

Population sizes in small ecological networks can show strong fluctuations even if stochastic effects and/or exterior causes are ruled out by high population numbers and constant environmental conditions, respectively [10, 12]. Under such conditions, chaotic dynamics remain as the dominant source of fluctuations. On general grounds one expects chaos to act as a source of fluctuations and of stability against extinction at the same time. Large fluctuations are a hallmark of chaotic dynamics, and stability follows if a chaotic attractor manifold sitting in the bulk of the phase space of population numbers prevents those population numbers from escaping to the boundaries of extinction.

We here studied a predator-prey system that is minimal in the sense that a chaotic attractor manifold is generated out of the interplay of only three species. Via a mechanism that is arguably universal chaos arises due to the parameter-controlled competition of two limit cycles governing the regime of extremely high and low net resource availability. The system addressed has been realized in experiments [10], and in our numerical analysis parameters were chosen to describe the bacterial species *Pedobacter*, *Brevundimonas* and the ciliate *Tetrahymena pyriformis* involved in that work. Our results are in qualitative agreement with experimental observation.

The beneficial character of chaos was demonstrated in the sense, that the chaotic attractor makes the system less prone to extinction by demographic noise. The mean time to extinction scales exponentially with system size rather than polynomially as in non-chaotic systems.

The perhaps most important observation of the present study is that chaos appears to present itself as an emergent feature when distinct limit cycles get 'tuned' into each other upon variation of a parameter. Limit cycles are an abundant motif in dynamical equations or at least in few-variable sub-sectors of these equations. For example, in the solution of a complex equation, a limit cycle may be transiently realized in the behavior of few of its variables. Upon changing parametric conditions, the patterns of such cycles change, and the present work demonstrates how this may be accompanied by the onset of chaos. Perhaps, then, chaos is a transient phenomenon more frequently realized than one may naively think, and this would entail consequences for both the strength of fluctuations and the stability of food web dynamics. Further work will be required to address these questions in generality.

3 SENSITIVITY OF COMPETITIVE CHAOS AND EQUILIBRIUM

'Growth is limited by that necessity which is present in the least amount. And, naturally, the least favorable condition controls the growth rate.'

— Frank Herbert, *Dune*

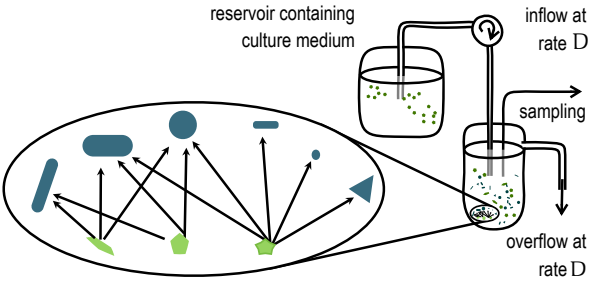

Figure 14: Model set-up: Six competing bacterial strains (blue) with three nutrients (green) in chemostat.

Mechanisms maintaining biodiversity in defiance of competition are not yet fully understood but crucial for the preservation of wildlife and flora. Numerical simulations of theoretical models including nonlinear species interactions can feature species oscillations and chaos. In principle these models allow non-equilibrium coexistence of more species than the number of available resources with indications for chaos [47–49]. The occurence of chaos has been demonstrated in laboratory experiments on microorganisms and beetles [10, 17]. Questions I want to discuss here are

1. How likely is such a chaotic coexistence?
2. Does this happen in a biological context?
3. If so, what is the sensitivity of that multi-species-coexistence?

An experiment by Schieffer [94] and Arns [7] aimed to verify the potential of oscillations supporting diversity in a well-controlled chemostat setup. Without any external disturbances an oscillating long term coexistence of up to six bacterial strains was recorded.

In this chapter, the conceptual framework of Huisman and Weissing [47] is adapted to the experiment to substantiate the data theoretically. The new model predicts indeed potentially high diversity over broad parameter regimes for substantial time spans of thousands of generations in a setup with oscillations. A stationary coexistence can be implemented as well but is highly sensitiv to parameter variation. This highlights the importance of oscillations for conserving diversity and the danger of guidelines considering mainly stationary situations.

Parts of the results discussed in this chapter can be found in Arndt et al. [6]. The adaptation of the model, its description, numerical implementation and analysis were created by me as well as the corresponding graphics if not stated otherwise[1]. The experiments were composed and analyzed by the collaborators.

3.1 INTRODUCTION

The search for a generic trigger of biodiversity and for ways to preserve it is a long standing topic of research [50, 68, 105]. In natural ecosystems a species richness is observed that is at odds with the original competition theory [18, 68]. Classically it is assumed that in equilibrium the number of coexisting competitors is limited by the number of resources [40, 41]. And although various mechanisms are suggested to promote multi species coexistence (e.g. global diversity with locally relatively uniform patches, interspecific competition and scattering, alternative resources in spatially structured habitats) a definite confirmation of the actual processes does not exist [65, 106]. Other interpretations of observed diversity rely on micro-evolution and eco-evolutionary dynamics [52, 95]. Occurrences of chaotic and non equilibrium dynamics have been observed in competition models (e.g. Armstrong and McGehee [5], Gilpin [33], May and Leonard [76], Smale [96]). And those intrinsically nonlinear dynamics habe been suspected by theoreticians to be a cause for diversity [4, 5, 47–49, 125].

Numerical simulations suggest that nonlinear interactions of competitive species can result in oscillating and chaotic dynamics which in turn would allow longterm coexistence of more species than limiting resources [47]. Continuing chaotic or dampened oscillations of population numbers without

1 For numerical implementation see Appendix B

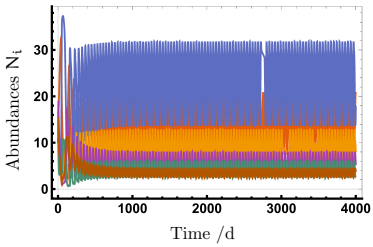

Figure 15: Numerical simulations show oscillating coexistence of six species on three essential resources. Exemplary time series simulated for parameters taken from Huisman and Weissing [47].

external perturbation have indeed been observed in such diverse real world systems as developmental stages in insects[17], rotifers grazing on algae[27], two bacteria and one ciliate predator [10] and mixed communities [12, 35]. First evidence of nonlinear dynamics as a driver of multi species coexistence is provided by the experimental study Schieffer [94]. We modified the model of Huisman and Weissing [47] with reasonable parameter values to portray the microbial food web. Our model analysis accompanies this notion and demonstrates that the theoretical predictions can actually apply to this particular system. It shows that such non equilibrium coexistence can be expected to develop and to be much more resilient than stationary coexistence.

3.2 THE MODEL BY HUISMAN & WEISSING

Let us first review the original model by Huisman and Weissing [47–49]. They simulate a system of an aquatic phytoplankton with perfectly essential resources. A community of n planktonic species feeds on k resources that cannot be replaced with one another. Population abundances N_i grow depending on the availability of the resources. The availability of a resource j on the other hand, R_j, depends on the consumption of resources by the plankton. Specific mortality and growth rates are denoted by m_i and $\mu_i(R_1, \ldots R_k)$ respectively. A constant turnover rate D supplies fresh

resources from a reservoir with concentrations S_j of each resource. The content of resource j in species i amounts to c_{ji}.

$$\begin{aligned} \frac{dN_i}{dt} &= N_i\,(\mu_i(R_1,\dots R_k) - m_i) && i = 1,\dots n \\ \frac{dR_j}{dt} &= D(S_j - R_j) - \sum_{i=1}^{n} c_{ij} N_i \mu_i(R_1,\dots R_k) && j = 1,\dots k \end{aligned} \tag{3.1}$$

The growth rates μ_i were assumed to follow Holling's type II functional response (1.6) and to be limited by the scarcest resource obeying the **Law of the Minimum**. Under optimal conditions species i could grow with maximal growth rate r_i. The response to the concentration of nutrient k is determined by the half saturation constant K_{ki}.

$$\mu_i(R_1,\dots R_k) = r_i \min\left(\frac{R_1}{K_{1i}+R_1},\dots \frac{R_k}{K_{ki}+R_k}\right) \tag{3.2}$$

Huisman and Weissing [47] demonstrated via numerical simulations, that for perfectly essential resources non-equilibrium dynamics with more species than resources are possible. They provide specific parameter configurations that enabled oscillating coexistence of up to twelve species on three resources (see Fig. 15 for six species).

3.3 CHAOTIC COEXISTENCE

3.3.1 The Experiment

An experimental realization of the Huisman-Weissing model was investigated in chemostat by Arns [7], Schieffer [94]. Up to six different heterotrophic bacterial species were growing with three nutrients (carbon, nitrogen and phosphor). Combinations of *Bacillus subtilis*, *Pedobacter sp.*, *Corynebacterium glutamicum*, *Azotobacter vinelandii*, *Escherichia coli*, and an undetermined eubacterium were inoculated into replicated one-stage chemostats (for more detail see Becks and Arndt [8, 9], Becks et al. [10]). The rate of dilution and nutrient supply was in all experiments set to $D = 0.75 d^{-1}$. The nutrient medium contained glucose, supplying 20 mg carbon per liter, moreover 7 mg nitrogen l^{-1} and 0.77 mg phosphor l^{-1}.

Regardless of the initial number of species, this diversity was conserved in the chemostat from the beginning of the experiment till its finish (Fig. 16, **B**). Although a chemostat approach provides well controlled conditions and prevents external stimulus the population numbers were still highly fluctuat-

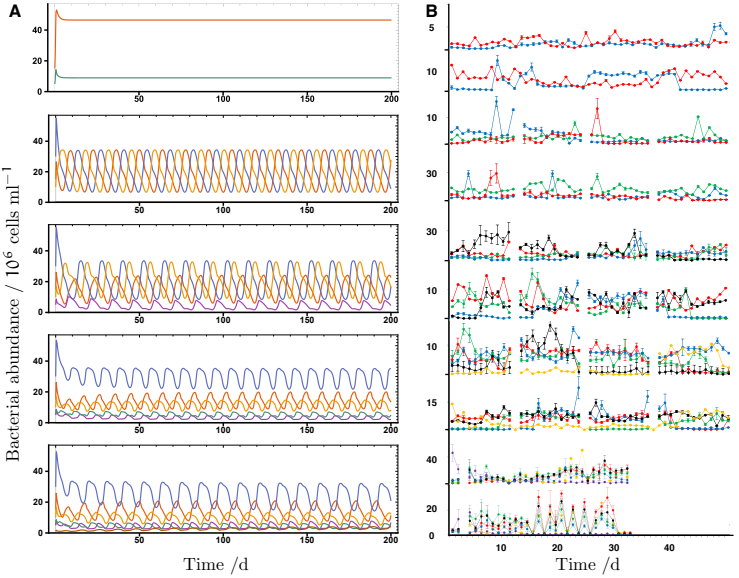

Figure 16: Comparison of population dynamics in systems with up to six bacteria.
A: Time series from simulations of the competition model with two to six coexisting bacteria.
B: Time series from the laboratory experiment, adapted from Schieffer [94] andArns [7].

ing. Positive Lyapunov exponents of all microbial dynamics indicate chaos [111]. Time delay reconstructions do not show point attractors (corresponding to damped oscillations into a stationary point) but do suggest chaotic attractors. There is no visible pattern in the time series in Figure 16 and trajectories of initially very similar replicate experiments diverged quickly and substantially. Altogether, deterministic chaos would explain for all of these findings granted that the size of the data sets does not permit an unambiguous statement.

3.3.2 The Model

For a mathematical description of the experiment, we referred to Huisman and Weissing [47] (see equations (3.1), (3.2)). Our model depicts an aquatic community of six bacterial strains competing for three essential solute nutrients (here:

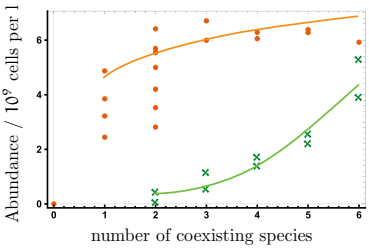

Figure 17: Total biomass (population numbers of all bacteria combined) with increasing of coexisting species.
Orange disks mark total abundances in all possible sets of coexisting numerical species (orange line: logarithmic fit),
green crosses indicate data from replicated experiments (green line: exponential fit).

glucose, nitrate, phosphate) in a chemostat of constant volume. At a constant rate D fresh nutrient solution flows into the system diluting the chemostat and acting as a death process. Additional mortality was neglected, so all mortality rates are $m_i = D$. With population concentrations N_i and resource concentrations R_X the following differential equations describe the change in the system during a time step dt:

$$\begin{aligned} \frac{dN_i}{dt} &= N_i\,(\mu_i(R_C, R_N, R_P) - D) \\ i &= 1, \ldots n \\ \frac{dR_X}{dt} &= D(S_X - R_X) - \sum_{i=1}^{n} c_{Xi} N_i \mu_i(R_C, R_N, R_P) \\ X &= C, N, P \end{aligned} \tag{3.3}$$

In our model R_C , R_N , R_P correspond to R_1 , R_2 , R_3 in the model of Huisman and Weissing [47]. By S_X we denote the concentrations of the corresponding resource (carbon, phosphor and nitrogen) in the nutrient medium.

Yield y_{Xi} (the part of resource uptake converted into biomass) and ϵ_{Xi} (content of resource X per bacterium of type i) result in a conversion of

$$c_{Xi} = \frac{\epsilon_{Xi}}{y_{Xi}}.$$

HETEROLOGOUS GROWTH ON MULTIPLE RESOURCES The nutrients in this set up are assumed to act **heterologous**. Here, carbon cannot substitute for nitrogen or phosphor in the biological processes and vice versa.

$$\mu_i(R_C, R_N, R_P) = \mu_{i,max} min\left(\frac{R_C}{K_{Ci} + R_C}, \frac{R_N}{K_{Ni} + R_N}, \frac{R_P}{K_{Pi} + R_P}\right)$$

In this framework growth is limited by the scarcest nutrient. The individual specific growth rates for each nutrient follow Holling's typ II eq. (1.6). They saturate at a maximal rate $\mu_{i,max}$ for optimal conditions and reach half maximum value at half saturation concentration K_{Xi}.

ADAPTATIONS TO THE EXPERIMENT To study chaotic coexistence we rescale a model system of Huisman and Weissing [47]. The minimal necessary changes to match the experimental set-up were adjustments of the resource concentrations, maximal growth rates and the carbon content per cell. The original simulations for chaotic dynamics assumed a dilution of $0.25d^{-1}$ and maximal growth rates of $\mu_{i,max} = 1d^{-1}$. A rescaling of time $t \to \frac{t}{3}$ and thereby $D = 0.75d^{-1}$ adjusts the rates to the experiment. The resulting growth rates $\mu_{i,max} = 3d^{-1}$ agree with the measured rates (see Table 3). Moreover, the experiments demand concentrations of the nutrient medium of

$$S_C = 20\,\frac{mg\ C}{l},\ S_N = 7\,\frac{mg\ N}{l},\ S_P = 0.77\,\frac{mg\ P}{l}$$

instead of the values of the Huisman-Weissing model $S_1 = S_2 = S_3 = 10$. Therefore we rescale

$$\begin{aligned} c_{Xi} &= S_X \frac{c_{ji}}{S_j} \\ K_{Xi} &= S_X \frac{K_{ji}}{S_j} \end{aligned} \qquad X = C, N, P \qquad j = 1, 2, 3 \tag{3.4}$$

and obtain new values for our half saturation constants

$$\Rightarrow K = \begin{pmatrix} 2 & 1.5 & 0.5 & 1.4 & 0.4 & 1.3 \\ 0.175 & 0.7 & 0.525 & 0.14 & 0.707 & 0.385 \\ 0.05775 & 0.01925 & 0.077 & 0.0847 & 0.0539 & 0.07315 \end{pmatrix}. \tag{3.5}$$

With cell diameters in the experiment ranging from 0.25 µm to 2.5 µm and assumed spherical cell shape, the individual cell volume ranged between 0.001 μm^3

and $1\,\mu m^3$. Average carbon content was assumed to be $0.35\,pg\,C/\mu m^3$ [13], thus the average carbon content per cell should be of the order

$$\epsilon_C = Vol \cdot 0.35\,pg\,C\,\mu m^{-3} \approx 10^{-13} - 10^{-10}\,\frac{mg\,C}{ind}. \tag{3.6}$$

In compliance with the **C:N:P ratio**, ϵ_N and ϵ_N take corresponding values.[2]

$$\begin{aligned} \epsilon_N &\approx \frac{9\,g\,N}{77\,g\,C}\,\epsilon_C \\ \epsilon_P &\approx \frac{1\,g\,P}{77\,g\,C}\,\epsilon_C \end{aligned} \tag{3.7}$$

After additionally rescaling by a factor of 10^9, the conversion and the resulting population abundances take values of realistic magnitude and the new conversion reads

$$c = 10^{-9}\begin{pmatrix} 0.2 & 0.4 & 0.3 & 0.1 & 0.02 & 0.8 \\ 0.105 & 0.07 & 0.14 & 0.105 & 0.21 & 0.245 \\ 0.0154 & 0.01155 & 0.0077 & 0.01925 & 0.00385 & 0.0154 \end{pmatrix} \tag{3.8}$$

For the contour plot, dilution rates were varied between 0 per day and 3 per day. Time series of 400 days (Fig. 18) and 4000 days (Fig. 19) were simulated with this set of parameters. At each moment in time the number of surviving species (at least one cell per liter) was monitored and color coded. For the dynamics (Fig. 16, **A**) exemplary time series starting with subsets of the six species were simulated. To compare the overall abundance (Fig. 17) all possible combinations of coexisting species (at least 1000 days) are tested at a dilution rate of $0.75\,d^{-1}$. For each case the total abundance and production are averaged for 100 days and plotted against the number of species. We are not aware of analytical solutions. Instead, we employ numerical integration.

2 The so-called Redfield Ratio originally describes the ratio of carbon and nitrogen to phosphor in marine plankton. Redfield [86] analyzed this ratio empirically for samples from all oceanic regions and found molar ratios of C_{106} to N_{16} to P_1. Recent findings vary between $C_{163} : N_{22} : P_{6.6}$ in the global oceans [73] and $C_{192} : N_{20} : P_1$ in small freshwater lakes [99] (translating to approximate ratios in mass of 10 : 1.5 : 1 to 77 : 9 : 1, respectively).

Table 2: Definitions of quantities and parameters of the model.

SYMBOL	DEFINITION	UNIT
X=C,N P	Resource (carbon, nitrogen, phosphor)	
R_X	Resource concentration	$mgX\ l^{-1}$
S_X	Resource concentration in nutrient medium	$mgX\ l^{-1}$
N_i	No of cells of species i per liter	$ind_i\ l^{-1}$
D	Dilution rate	d^{-1}
y_{Xi}	Yield (converted X per uptake of X)	$mgX\ mgX^{-1}$
ϵ_{Xi}	Content of X per cell of species i	$mgX\ ind_i^{-1}$
c_{Xi}	Uptake of X per cell of species i	$mgX\ ind_i^{-1}$
$\mu_{i,max}$	Maximal growthrate	d^{-1}
K_{Xi}	Half saturation	$mgX\ l^{-1}$

Table 3: Maximal growth rates per day in chemostats in the experiments Arns [7] and Schieffer [94] (rounded to two digital places)

Pedobacter sp.	2.13
Bacillus subtilis	2.96
Corynebacterium glutamicum	3.27
Escherichia coli	3.42
Azotobacter vinelandii	3.51
undetermined eubacterium	3.27

3.3.3 Results

The Huisman-Weissing model [47] was designed to capture the dynamics of a set of competing planktonic algae. The experimental setup we consider here, on the other hand, consists of up to six bacteria species competing for three resources (glucose, nitrate and phosphate). A required rescaling of parameters values yields a chemostat model relevant to the experimentally monitored species and circumstances. The abundances and properties of the model species fixed by this rescaling are surprisingly well within the ranges of the bacterial strains used in the experiments (see Fig. 16 and Fig. 17). Note,

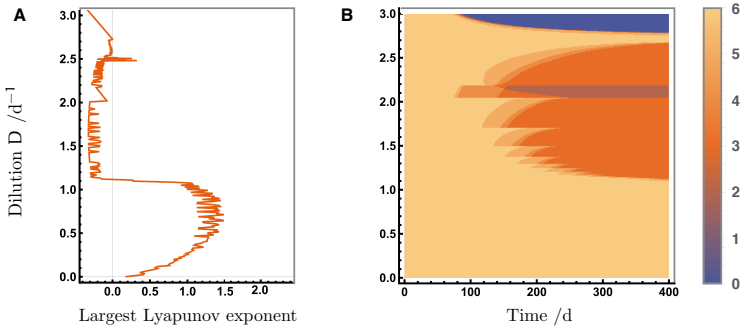

Figure 18: **A**: Largest Lyapunov exponents of the competitive coexistence of six species depending on the dilution rate.
B: Analysis of the sensitivity of the number of survivors on the dilution rate. For strong dilution ($D > 2.75 d^{-1}$) all species go extinct after a transition time of about 100 days, for dilution rates smaller than $1.08 d^{-1}$ coexistence of all six species is possible. For $D < 1.08 d^{-1}$ Lyapunov exponents are positive and indicate chaotic dynamics.

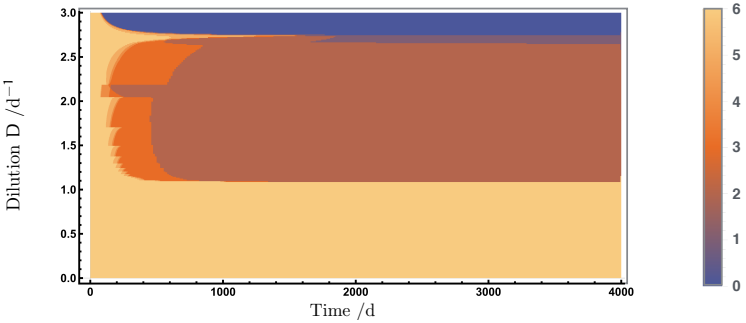

Figure 19: Analysis of the sensitivity of the number of survivors on the dilution rate for 4000 days.

Table 4: Parameter values for model outputs in figures 18, 16, 17 and 19.

PARAMETER	VALUE	UNIT
D	0.75	d^{-1}
S_C	20	mgC l^{-1}
S_N	7	mgN l^{-1}
S_P	0.77	mgP l^{-1}
$N_1(t=0)$	15	10^9 cells l^{-1}
$N_2(t=0)$	30	10^9 cells l^{-1}
$N_3(t=0)$	10	10^9 cells l^{-1}
$N_4(t=0)$	5	10^9 cells l^{-1}
$N_5(t=0)$	5	10^9 cells l^{-1}
$N_6(t=0)$	1	10^9 cells l^{-1}
$\mu_{i,max}$	3	d^{-1}

however, that while for the laboratory set up consecutive species were added to the initial community and coexisted, such a succession of coexistence was not found in the model. For instance, from the pool of six model species that coexist in the final community, only two 4-species combinations persist in a system without the others. Neither of those two groups contain a subset of three that can coexist on their own. Moreover, the two-species coexistence will not show oscillations in the theoretical model, while experimental results show at least some variation.

The ability of the six-bacteria coexistence to withstand perturbations was tested in the theoretical framework. Time series data of the simulations point to a resilience to changes in dilution rates but to a sensitivity to changes in the initial concentrations. Contourplot 18 depicts the diversity in the system and shows extinction of all species for strong dilution ($D > 2.75 d^{-1}$) after a transition period. On the other hand a coexistence of all species for more than a year is possible at dilution rates $D < 1.08 d^{-1}$. Actually, in these model species would even survive at least ten years (Fig. 19). An examination of the largest Lyapunov exponents in Figure 18 displays positive values and indicates deterministic chaos for the same range of dilution rates. Astonishingly, this model exhibits a coexistence of all six bacterial strains for at least 75 to 100 days for reasonable dilution. Ecologically, such a transitional coexistence for three months is a significant phenomenon that has been neglected in diversity theories. This implies, that not only do theoretical models permit chaotic coexistence in biologically realistic models but that it is a generic substantial

mean for diversity. It provides stability against perturbations of the nutrient supply and against fluctuations in environmental influences. Thereby an explanation is found for ecological diversity in much broader parameter ranges and more variable systems and communities than previously thought [47].

3.4 EQUILIBRIUM COEXISTENCE

Actually, there is another theoretical configuration for potential 6-species coexistence. We can artificially construct a system of six species coexisting on three resources even in equilibrium. This should astonish, as we established in the introduction, that exactly this should not be possible. The reason for this discrepancy appears to be in the restrictions of the mathematical models in McGehee and Armstrong [77].

First we can reduce the number of parameters by rescaling time and resource concentration.

$$\begin{aligned} \tau &= D\,t, \qquad & \nu_{i,max} &= \frac{\mu_{i,max}}{D} \\ r_j &= \frac{R_j}{S_j}, \qquad & \kappa_{ij} &= \frac{K_{ij}}{S_j}, \qquad & \tilde{c}_{ij} &= \frac{c_{ij}}{S_j} \end{aligned} \tag{3.9}$$

With this the differential equations become

$$\begin{aligned} \frac{dN_i}{dt} &= (\nu_i(\mathbf{r}) - 1)\, N_i && i = 1,\dots 6 \\ \frac{dr_j}{dt} &= 1 - r_j - \sum_{i=1}^{n} \tilde{c}_{ij} N_i \nu_i(\mathbf{r}) && j = 1,\dots 3 \\ \nu_i(\mathbf{r}) &= \nu_{i,max} \min_j \left\{ \frac{r_j}{\kappa_{ij} + r_j} \right\} \end{aligned} \tag{3.10}$$

Now consider a fixed point. Derivatives must vanish and the first equation determines the resource concentrations in equilibrium:

$$\begin{aligned} 0 &= (\nu_i(\mathbf{r}) - 1)\, N_i && i = 1,\dots 6 \\ \overset{N_i \neq 0}{\Rightarrow}\ 1 &= \nu_i(\mathbf{r}) = \nu_{i,max} \min_j \left\{ \frac{r_j}{\kappa_{ij} + r_j} \right\} && j = 1,\dots 3 \end{aligned} \tag{3.11}$$

Via these six equations the three resource concentrations are overdetermined. There have to be at least two species i_1, i_2 limited by the same resource r_{j_1}.

In other words, there have to be $i_1 \neq i_2$ and one j_1 that minimizes both of the following expressions at the same time.

$$\begin{aligned} \min_j \left\{ \frac{r_j}{\kappa_{i_1,j} + r_j} \right\} &= \frac{r_{j_1}}{\kappa_{i_1,j_1} + r_{j_1}} \\ \min_j \left\{ \frac{r_j}{\kappa_{i_2,j} + r_j} \right\} &= \frac{r_{j_1}}{\kappa_{i_2,j_1} + r_{j_1}} \end{aligned} \tag{3.12}$$

This can be established by a community of the following configuration

$$\kappa = \begin{pmatrix} \alpha_K & \gamma_K & \beta_K & \gamma_K & \beta_K & \alpha_K \\ \beta_K & \alpha_K & \gamma_K & \beta_K & \alpha_K & \gamma_K \\ \gamma_K & \beta_K & \alpha_K & \alpha_K & \gamma_K & \beta_K \end{pmatrix}. \tag{3.13}$$

By this we construct two groups of three species each, that feature cyclic competition advantages in the distinct groups. If one species is best at utilizing the first resource the second is best in handling the second resource and so on. Set maximal growth rates $\nu_i = 4$, $\alpha_K = 0.1, \beta_K = 0.075, \gamma_K = 0.025$, initial inoculations $N_i(t = 0) = 1$ and efficiencies given by

$$\tilde{c} = \begin{pmatrix} 0.01 & 0.02 & 0.03 & 0.02 & 0.01 & 0.03 \\ 0.03 & 0.01 & 0.02 & 0.01 & 0.03 & 0.02 \\ 0.02 & 0.03 & 0.01 & 0.03 & 0.02 & 0.01 \end{pmatrix}. \tag{3.13 a}$$

And indeed in this configuration all six species evolve towards a stable fixed point. In fact they behave identical, although defined by distinct sets of parameters (see Fig 20 A).

Let us examine this fixed point and its stability a bit further. By adjusting the initial densities to $N_i(t = 0) = 0.1 + 0.01i$, $(i = 1..6)$ the different species spread and approach different fixed densities (Fig 20 B). If one species differs even more from the others — for example change $N_1(t = 0) = 0.3$ — population densities fluctuate (Fig 20 C). Rescaling back to different nutrient concentrations in the supply will separate the species with respect to their limiting resource (Fig 20 D). The coexistence of this setup is quite robust against small changes of $\tilde{c}$ and $N_i(t = 0)$. The exact dynamical properties (fixed point, limit cycle, etc.) may change but it is easy to preserve six surviving species.

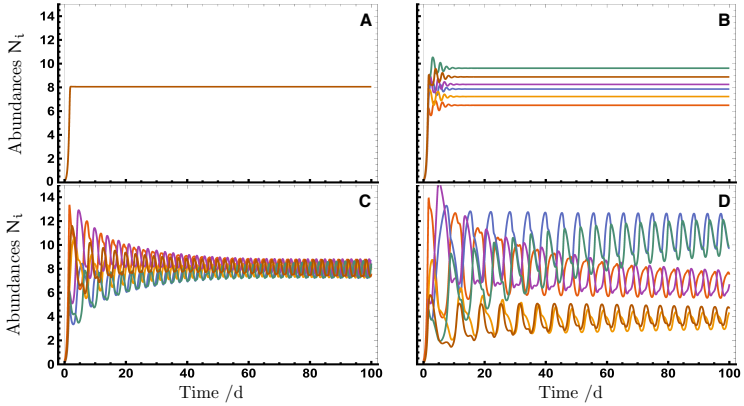

Figure 20: Population dynamics for certain realizations of the Huisman-Weissing model with parameters (3.13)

Now we want to modify the model to a biologically more realistic setup. Rescale population densities to cells per liter and assume dilution rate and nutrient concentration according to the experiment. Species parameters should describe bacterial strains that would live in this environment. Consider species characterized by the same $\tilde{c}$ as in the chaotic model community (3.8) but with new values for the half-concentration

$$\kappa = \begin{pmatrix} 5 & 7 & 9 & 10 & 13 & 15 \\ .5 & .5 & 1.5 & 2 & 3 & .25 \\ 0.01 & 0.02 & 0.03 & 0.04 & 0.05 & 0.06 \end{pmatrix} \tag{3.14}$$

These are biologically reasonable and all species of this community coexist at fixed densities at a dilution of 0.75 per day in the simulated experimental setup . In contrast to chaotic existence, the equilibrium coexistence is much less sensitive regarding a change in the initial conditions over orders of magnitude. Again we analyze sensitivity by counting the survivors over a period of 4000 days for dilution rates ranging from $D = 0$ to 3. A species is accepted as 'alive' if at least one cell per liter is present. (Admittedly, a chemostat contains rarely more than 200 ml, so this is maybe a bit optimistic.) Results are portrayed in Figure 21.

3.4.1 Results

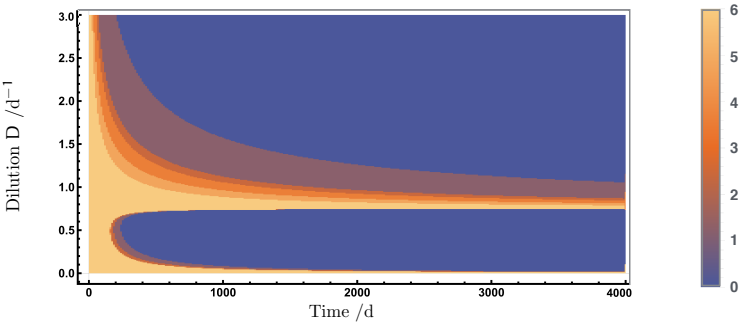

Figure 21: Analysis of the sensitivity of the diversity in community (3.13) on the dilution rate. If dilution is $D = 0.75$, all species survive. Otherwise population numbers decrease and after a transient time of 200 days all are extinct.

The abundances in the equilibrium model community are comparable to the population numbers in chaotic coexistence (Fig. 16 and 21).

As the sensitivity analysis shows, a strip of dilution rates permits 6-species coexistence, but if dilution is tuned beyond that range extinction sets in around day 200. In comparison to the analysis of the chaotic coexistence in Fig. 19, the main difference is that longterm coexistence is only possible for one specific dilution rate $D = 0.75 d^{-1}$. The chaotic setup could survive for any dilution less than $D = 1.08\ d^{-1}$.

3.5 STATISTICAL ANALYSIS

As we have seen, the system can exhibit various diverse dynamics depending on the specific system and the species parameters. Two exemplary sets of parameters demonstrate coexistence for significant periods of time for different community setups; either at fixed population numbers or performing chaotic dynamics. At the same time we have seen, that this coexistence can be sensitive to parameters changes.

For a more general statement on wether such species compositions might likely be combined by chance, we need a more rigorous test of the parameter space. We take a statistical viewpoint and simulate random communities.

3.5.1 Methods

Assume a range for parameters that is biologically reasonable. And assume of the thousands of bacterial strains that exist, six were to end up by chance in one small habitat. What is the probability that all survive? How likely is the survival of a subset?

To this end we simulated the six-species three-resources model with random parameter values. Values were sampled from a uniform distribution on a biologically reasonable interval (Table 5, [62, 114]).

Table 5: Parameter ranges for statistical model analysis (Fig. 22)

PARAMETER	RANGE	
conversion c_{Ci}	$10^{-11} - 10^{-9}$	$\frac{mgC}{ind_i}$
conversion c_{Ni}	$10^{-12} - 10^{-10}$	$\frac{mgN}{ind_i}$
conversion c_{Pi}	$10^{-13} - 10^{-11}$	$\frac{mgP}{ind_i}$
maximal growth rate μ_{imax}	$2.7 - 17$	d^{-1}
half saturation constant K_{Ci}	$10^{-4} - 10$	$\frac{mgX}{l}$

3.5.2 Results

For random parameter configurations the number of surviving species is monitored for 1000 days. The average diversity in a system of six species is depicted in Figure 22 in the panel **A**. Averaging over all simulations yields a probability distribution clearly favoring single-species and two-species coexistence. As time evolves, the number of species declines as one would expect. Because a slow dilution corresponds to low mortality rates, the sensitivity analysis indicates a positive dependence. The influence of time and dilution appears to be marginal if one excludes too small dilution and too short times. That means that the parameter ranges are not too restricting and therefore it is sufficient to study the distribution for a specific dilution rate. A probability distribution $\mathcal{P}(n_{fin})$ of the number of surviving species was calculated for a sample of 500 simulations with dilution $D = 0.75\,d^{-1}$ at $t = 400$ days (Fig. 22, **B-C**). The distribution indicates strong preference of

single-species food webs. About three out of ten food webs consist of at least two competitors, only four out of 100 webs contain three competitors. In less than one food web out of 100 four or more species coexist at day 400.

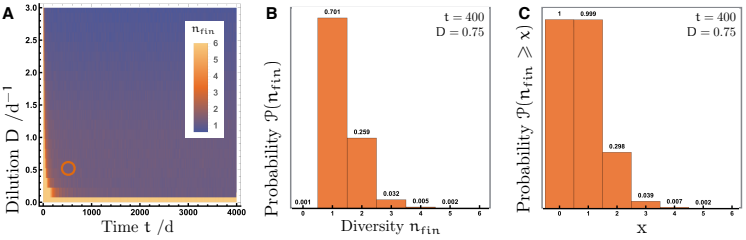

Figure 22: Distribution of species richness in a web of six competitors
A: Mean species richness for different dilution rates and points in time
B: Distribution of species richness at day $t = 400$, dilution $D = 0.75 d^{-1}$
C: Cumulative distribution at day $t = 400$, dilution $D = 0.75 d^{-1}$

3.6 DISCUSSION

Our model compares well to results of the experiment and therefore seems suited to describe the system's processes. The order of magnitude of species concentrations, coexistence and the dynamical characteristics in the numerical population dynamics at $D = 0.75^{d-1}$ are consistent with the experimental time series data (Figure 16).

PRODUCTIVITY In a chemostat, productivity is defined as the total biomass per volume times dilution rate. Simulations show an interdependence of diversity and total biomass (or ecosystem productivity) that can be fitted by a logarithmic curve (Figure 17). Strikingly, this is compatible with theoretical results derived in Tilman et al. [107] in spite of the different approach. The model in Tilman et al. [107] introduces random plants into a habitat, lets one species replace the others and compares the total biomass with the initial diversity. In contrast we observe the total biomass of coexisting species.

In the model in Tilman et al. [107] each species is characterized by a value R^* which refers to the remaining resource concentration a monoculture would spare of the supply S. These values are drawn from a uniform distribution on the interval $[R^*_{min}, R^*_{max}]$. In competition for a single resource the best competitor displaces all the others in the course of time. In this setup the

relation of average total biomass in the final monocultural equilibrium and original species richness n was calculated to follow

$$B(n) \propto S - R^*_{min} - \frac{R^*_{max} - R^*_{min}}{n+1}.$$

Numerical sampling of more complex models (more resources, a spatially heterogeneous habitat) yield similar results and concur with greenhouse and field experiments (for a review see Tilman et al. [108]). Average total biomass increases with the initial diversity but decelerates and might approach a maximum. Upper and lower bounds of the productivity increase as well. Positive relations between diversity and productivity were demonstrated in experiments. Studies on european grasslands suggest a log-linear relationship [43]. The approach of a maximal value was supported by field observations [88] and experiments with bulk bacteria [11]. van Ruijven and Berendse [112] report positive dependence between plant species richness and productivity in field experiments and propose complementary effects of differing species explain the increase.

The study of Schieffer [94] was the first laboratory experiments with well-defined diversity investigating this effect in well-controlled chemostat conditions.

Although Tilman's study relies on a final stationary monoculture the non equilibrium multi-species communities in our model show a comparable logarithmic biomass increase (Figure 17).

DIVERSITY We give evidence that in a laboratory experiment and in the corresponding model simulations six species can compete for as few as three resources and still coexist. We reason that diversity is associated with non equilibrium or chaotic dynamics. Unfortunately, the experiments Schieffer [94] and Arns [7] result in time series that are too short for a clear identification of wether oscillations are inherently chaotic, oscillating in multiple cycles or subject to demographic noise. So further comparison to model output is not possible in that respect.

In the mathematical model we demonstrate chaotic as well as stable coexistence of up to six competitors for biologically reasonable parameter configurations. Rate equations of food web models typically possesses nonlinear properties. Therefore chaotic dynamics are possible and indeed for rare combinations of parameter values we see exactly that. But we could also show equilibrium coexistence in the model and slow extinction over ecological timescales. This means the range of possibilities of coexistence is broader than often assumed.

STABILITY Now let us consider the sensitivity of diversity. For the laboratory experiment, 'random' bacteria were chosen and successively added to the initial set of two. No preferences were imposed, apart from their suitability for the nutrient medium and the process of microscopic identification. All subsets that were tested in experiments coexisted as well. It is highly unlikely that only one perfect species combination enables coexistence and exactly that one was chosen by mere chance for the experiment. We have to assume that in nature this a generic feature.

In the model, the number of distinct species stays constant over broad parameter ranges if we insert our set of six 'chaotic coexistors'. This is an indication and confirmation of the stabilizing properties of chaos we established in the previous chapter for a predator-prey food web. In the chaotic community, a modification of dilution rates does not easily disturb coexistence. Diversity appears to be almost dilution-independent for about 100 days. After a very short timespan the dynamical pattern is quickly established and then sustained.

For our 'equilibrium coexistors' diversity things look different. Their situation depends much stronger on the optimal dilution. A perturbation of the dilution rate or the food supply would kick the system out of its delicate coexistence.

All things considered, it can be inferred that non linear interactions and dynamics are robust mechanisms promoting diversity intrinsically, notwithstanding a stationary environment. Coexistence at fixed population densities does provide additional possibilities for species richness. But for *stable* diversity, chaotic coexistence is much more favorable and beneficial

HOW LIKELY IS SUCH A DIVERSE SYSTEM? Apparently, a habitat can support more species than it provides resources. Mathematical models confirm non-equilibrium as well as equilibrium coexistence. Although more often than not, only one or two species survive a reasonable time span.

Multi-species coexistence is in principle possible but is not the typical result in our proposed scenario. This will only happen for rare combinations of parameters that have to be finely tuned. To end up in a system of (oscillating) multi-species coexistence by introducing random species into a habitat is not very likely.

In most cases we do not see oscillating dynamics at all. Multiple species only coexist during a transitional phase that can be shorter or longer. In fact when we simulate and calculate probabilities of one, two or three species coexisting after a certain time span, we find that mostly only one or two species coexist. The probability of survival of more than three species is almost vanishingly

small. This suggests that there have to be additional mechanisms ensuring diversity in natural food webs.

Then again, we have to consider the long transient times our model features. With survivals up to 200 days a community of bacteria in nature would have survived a season and environmental factors would change anyways. A setup of six random species coexist in the experiment by Schieffer [94]. This rules out coevolutionary effects and might be a sign for fluctuating transient survival.

In general, on the other hand, during long transient times, the species might be able to adapt and evolve [104]. Thus the model might not be applicable to predict long term behavior for natural microbial food webs as such. But the statement should still hold, that diversity is less exotic than expected by the competitive exclusion principle and that fluctuations will stabilize populations.

Ecosystem functioning is typically dependent on small organisms [18, 101]. If we desire to conserve natural resources and habitats in an age of extinction we need to understand functions and sources of species richness [81]. The mathematical model does not only agree qualitatively with experimental results, but even hints that intrinsic sustained oscillations could be more ubiquitous than expected and could stabilize species richness. In addition to spatial heterogeneity and niche diversity, non equilibrium dynamics are an important driver of biological diversity as well and have to be accounted for.

4 INTERPLAY OF COMPETITION, COOPERATION AND SPECIALISATION

"You can't just boss bacteria around like that," said the younger Mrs. Hempstock. "They don't like it."

— Neil Gaiman, *The Ocean at the End of the Lane*

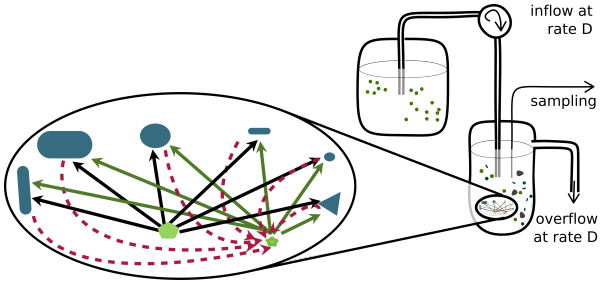

Figure 23: Model set-up: Six competing bacterial strains (blue) with two nutrients (green) in chemostat. Bold arrows indicate possible consumption, dashed arrows represent the production of the second nutrient as byproduct of digestion/consumption

According to the **competitive exclusion principle** the number of species in a system at long term cannot exceed the number of provided resources in a constant environment [64, 66, 71, 77, 89, 118]. In nature, on the other hand, thousands of different plankton species coexist feeding on essentially a handful of resources [18, 25, 101]. Moreover, experiments show somewhat ambiguous results, but there are hints, that species coexist with wildly fluctuating numbers [10, 17, 19, 27]. This seeming contradiction is resolved by the mathematical proofs, that the **Competitive Exclusion Principle** in general holds only true in equilibrium [3, 4, 54, 58, 77, 125]. Numerical simulations demonstrate, that biodiversity can actually persist when population abundances fluctuate [47]. The question remains, which mechanisms might in fact promote diversity.

4.1 INTRODUCTION

In previous chapters we considered simple predator-prey interaction and competition for mutual resources. But natural interaction webs of microorganisms can be complex. In a natural habitat, typically a consortium of bacteria grows on a mixture of substrates. Those substrates can be substitutable (**homologous**) or serve different physiological functions (**heterologous**). Species might even produce a secondary substrate that can be utilized by other species. This secondary production creates a cooperative or commensalistic character in the competition. The influence of excretion on the coexistence of mixed cultures in mixed substrates is of practical biological interest for cultivation set ups. The same mechanisms might apply for food webs of higher cooperating species. In a stationary system the possibility of coexistence is significantly enhanced, if a substitutable substrate is excreted [45, 87].

The goal of this study is to analyze requirements on such competing consortia that help promote multi species coexistence and diversity. Our paradigm is a model of several competing species that are introduced into a chemostat and grow on a mixed substrate. Some species excrete a resource that serves as a common good for other members of the community. An analysis of numerical simulations allows predictions for non equilibrium situations.

We set up small isolated model systems without external disturbances. Our models represent aquatic microbial communities. They are supposed to be well mixed and population numbers typically amount to at least 10^2 (ciliates) or 10^5 (bacteria) individuals per milliliter [10, 94]. We can therefore describe the populations by differential equations of continuous functions.

It is not feasible to measure each and every property. We probably do not even know all mechanisms taking place in the real world. Furthermore natural individuals of one species are not exactly identical. Organisms will all differ slightly from each other in traits as for example size, fitness and their ability to prey or to process food. There is always a certain variation in a population [1, 15, 116, 121, 124].

As many model-parameters are not easily determined in experiments (or not at all) we try to tackle the task with statistical analysis. That means parameter values are generated according to a random uniform distribution in biological bounds. For each structure of interactions we run simulations with random parameter configurations and look for structure- and time-dependent properties.

4.2 METHODS

4.2.1 Statistical Approach

We analyze a model of small aquatic food webs with nutrients, bacteria and other microbes in small tanks. To gain insight into these structures we pursue a statistical approach: The starting point is the numerical implementation of food webs with a given web of species interaction, growth functions et cetera. We consider different aquatic microbial communities where each species is defined by parameters determining its attributes. A whole distribution of parameter combinations is then randomly generated (within biological bounds) and tested according to its temporal evolution. Individual systems evolve numerically for some time in simulations and the outcome is monitored. Specifically, we deduce probabilities for the survival of a given number of species over distributions of network parameters at fixed network topology.

4.2.2 Model

In the setup for this chapter, a community of microorganisms competes for two nutrient sources. An example could be bacterial strains feeding on two carbon sources or sugars. (For examples see Zinn et al. [126].) We assume bacteria could specialize on the use of one of the sources (**specialist**) or they use both (**generalist**). In the latter case the two nutrients act **homologous**: Bacteria can survive on each of them if the other is not present. In the chemostat setup simulated in this chapter, one of the carbon sources is continually introduced into the system; the other resource is excreted as a metabolic product by particular species (**producers**)[26, 87]. Some species (not necessarily the same) can profit from this common good.

HOMOLOGOUS GROWTH ON TWO RESOURCES With just one nutrient j, species i should grow according to a well-established Holling's type II function (1.6). In optimal conditions, the function approaches the maximal specific growth $\mu_{ji,max}$, for a nutrient concentration of κ_{ji}, it grows at half the optimal rate. This sets first constraints.

$$\mu_i(0, C_2) = \frac{\mu_{2i,max} C_2}{\kappa_{2i} + C_2}, \qquad \mu_i(C_1, 0) = \frac{\mu_{1i,max} C_1}{\kappa_{1i} + C_1}$$

A combined growth rate of species i on two homologous nutrients should approach but not exceed the solitary maximal growth rates in a surplus

situation. With the $\mu_{1i,max}$ maximal growth on nutrient j this requirement reads

$$\mu_i(C_1, C_2) \leqslant \max(\mu_{1i,max}, \mu_{2i,max}) \tag{4.1}$$

A functional response that obeys those necessary boundary conditions is provided in the analysis of functional response for homologous nutrients by Lendenmann et al. [62]. With $\mu_{i,max} = \max(\mu_{ji,max}, \mu_{ji,max})$ labeling the maximal growth rate of species i, the specific growth according to the respective uptake of nutrients j by species i should amount to

$$\mu_{ji}(C_1, C_2) = \frac{\mu_{i,max} \cdot \frac{\mu_{ji,max} C_j}{\kappa_{ji}}}{\mu_{i,max} + \sum_j \frac{\mu_{ji,max} C_j}{\kappa_{ji}}}. \tag{4.2}$$

And the total growth of species i feeding on both resources is given by the sum

$$\mu_i(C_1, C_2) = \mu_{1i}(C_1, C_2) + \mu_{2i}(C_1, C_2). \tag{4.3}$$

CHEMOSTAT MODEL The interactions of the chemostat system are now incorporated in the following rate equations.

$$\begin{aligned}
\frac{dN_i(t)}{dt} &= (\mu_i(C_1, C_2) - D)\, N_i \qquad (i = 1, \ldots n) \\
\frac{dC_1(t)}{dt} &= D \cdot (S_1 - C_1) - \sum_i \epsilon_{ji} \cdot \mu_{1i}(C_1, C_2) N_i \\
\frac{dC_2(t)}{dt} &= -DC_2 - \sum_i \epsilon_{ji} \cdot \mu_{2i}(C_1, C_2) N_i + \sum_i \rho_i \cdot \mu_{1i}(C_1, C_2) N_i
\end{aligned} \tag{4.4}$$

Nutrients are processed with a specific efficiency ϵ_{ji} (which is equivalent to the inverse of the bacteria yield per nutrient uptake). And the carbon release of species i during metabolism in form of C_2 is determined by ρ_i. For fixed initial community size or diversity n, we can study systems where one, two, up to n generalists are introduced. Generalists can grow not only on C_1 but also on C_2. This property is taken into account by positive entries in the second row of the maximal growth rates matrix μ_{max}. The remaining species are implemented as specialists. The number of producers p can also range from 0 up to n. The ability to excrete C_2 is reflected by non zero entries in ρ.

Table 6: Quantities and (ranges of) parameter values for the simulations to match the experiments in Arns [7], Schieffer [94].

SYMBOL	DEFINITION	VALUES
n	total number of species introduced	
g	number of generalists	
p	total number of producing species	
p_g	number of producing generalists	
N_i	population abundance of species i per liter	
C_j	concentration of resource j in $\frac{\mu g\ C}{l}$	
D	turnover rate	$0.75\ l^{-1}$
$\mu_{ji,max}$	specific mortality rate of species i on nutrient j	$1 - 6$
S_1	supply concentration of resource C_1	$18.75\ \frac{\mu g\ C}{l}$
ϵ_{ji}	efficiency, i.e. uptake of resource j per growth of species i	$\frac{1}{0.1} - \frac{1}{0.49}\ \frac{\mu g\ C}{ind_i}$
κ_{ji}	half-saturation constant for resource j of species i	$0.002 - 0.02\ \mu g\ C$
ρ_i	productivity, i.e. excretion of C_2 per uptake of C_1 for species i	$0.2 - 0.5\ \frac{\mu g\ C}{\mu g\ C}$

RANDOM SAMPLING A food web or interaction set up is characterized by the total number of species n, the number of producers p, the number of generalists g and the number of producing generalists p_g. And with

$$\begin{aligned} 0 \leqslant g \leqslant n \\ 0 \leqslant p \leqslant n \\ \min(g, p) \leqslant p_g \leqslant \max(0, p - n + g) \end{aligned} \tag{4.5}$$

this results in a catalogue of more than $\mathcal{O}(n^2)$ different communities to compare.

Numerical simulations of the system are executed to perform a statistical analysis. For maximal growth rates, saturation constants and efficiencies biological bounds were established [82, 114] (see Table 6). Random values are generated according to this variance for interaction setups with varied number

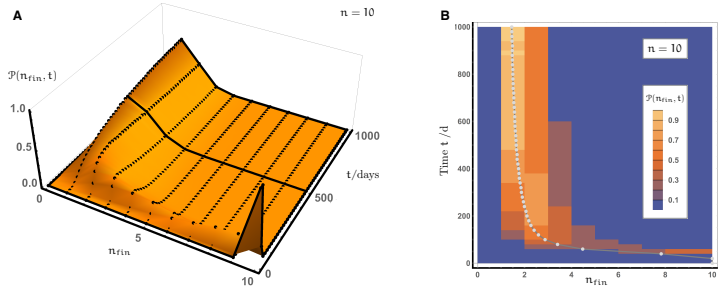

Figure 24: Probability distribution of the diversity for $t = 0$ to $t = 1000$ days in systems with initially 10 species.
B: Density plot of the same data with mean diversity inset as gray disks.

of specialists[1]. The number of surviving species, or final diversity $n_{fin}(t)$, is monitored over 100 random parameter configurations after some time span t. By averaging we obtain the probability distribution $\mathcal{P}(n_{fin})(t)$ and the average number of survivors $\langle n_{fin} \rangle (t)$.

4.3 RESULTS

Numerical simulations generate mean diversity distributions for a huge number of community configurations at different points in time. To gain a first intuition for the time scales in the system we "coarse grain" to the level of initial community size. We can study the number of survivors in a system of 10 competitors over a time of 1000 days in figure 24. A fast decline of diversity over the first 100 days from the initial 10 strains of bacteria is readily identifiable. The distribution quickly broadens and shifts towards smaller numbers. In the course of time it slowly peaks up again around the coexistence of two or the survival of a single species.

To understand the impact of structural community properties in more detail we restrict our analysis to a fixed time span of 500 days. Numerical results show a large variance for different community structures (see figure 25). The average probability peaks at one or two survivors and drops to $\mathcal{P}(4) \approx 2\%$ and $\mathcal{P}(n_{fin} \leqslant 4) \approx 2\%$, respectively, for 4 survivors. The bulk of simulations is well described by the total system average and does not depend crucially

1 For numerical implementation see Appendix C

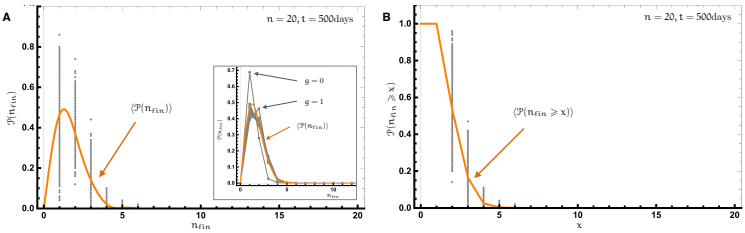

Figure 25: Diversity distributions in systems of 20 species at day $t = 500$. The probability for each set (g, p, p_g) (gray points) and mean probabilities (joined by orange interpolating curves).
A: Distribution of the probability $\mathcal{P}(n_{fin})$ (inset: Probability distribution $\mathcal{P}(n_{fin})$ averaged over p and p_g)
B: Cumulative probability $\mathcal{P}(n_{fin} \geqslant x)$

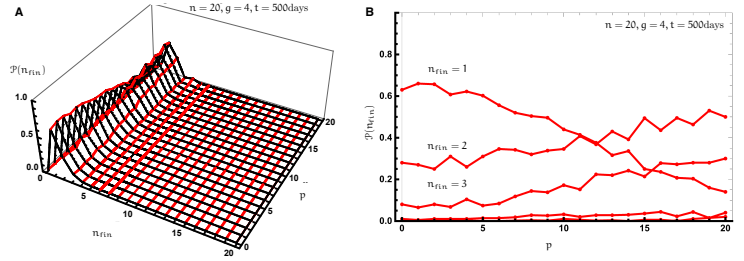

Figure 26: Probability distribution for $g = 4$ in systems of 20 species at day $t = 500$, averaged over the number of producing generalists p_g. The number of producers p is constant along red lines.

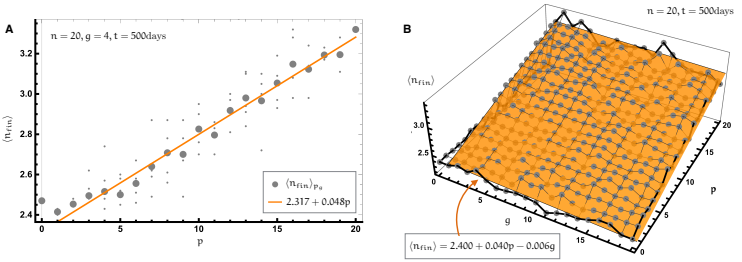

Figure 27: Mean diversity $\langle n_{fin} \rangle$ in systems of 20 species at day $t = 500$.
A: For $g = 4$ generalists large points indicate an average of $\langle n_{fin} \rangle$ over the number of producing generalists p_g. A least square fit is depicted by an orange line.
B: Numerical results of the mean diversity (gray points) and a least square fit to the mean diversity as a function of g and p (orange).

on the number of generalists g. Only if the systems contains no generalists, $\mathcal{P}(n_{fin})$ exhibits a sharp peak for $n_{fin} = 1$ survivors.

We investigate the impact of the community structure and implicit interactions by gathering systems according to the number of producers p. Figure 26 illustrates the diversity distributions at a fixed point in time after $t = 500$ days for systems with p ranging from 0 to $n = 20$. If less than half of the species produce the secondary resource the most probable outcome after 500 days will be a single species. For a higher number of producers the diversity distribution flips and typical systems contain two or more species.

Now consider a particular subset of the data with $g = 4$ generalists and the mean diversity $\langle n_{fin} \rangle = \sum n_{fin} \mathcal{P}(n_{fin})$. As Figure 26 suggests, this quantity shows a strong dependence on the number of producers p and a linear dependence can approximate the behavior satisfactorily (Fig. 27, **A**). If we break down details of the community structure even further another substructure is revealed. If we exclude $g = 0$ and fix the number of producing species p, the mean final diversity n_{fin} increases when the number of producing generalists g is reduced.

4.4 DISCUSSION

We compare probability distributions of species diversity to identify properties that are beneficial for multi species coexistence. Communities of ten and twenty species were simulated and yield consistent conclusions. Typically only

one or two species show sustained longterm survival up to 1000 days. This is in agreement with the **Competitive Exclusion Principle**. We can expect a fast growing specialist consuming the primary carbon source and the fittest generalist surviving by resorting to the excreted secondary source.

Population dynamics feature a transient behavior and extinction takes hundreds of days to progress. The distribution of species diversity is examined after 500 days. This time span is relevant in biological context, because seasonal variations would have perturbed a real world system by that time anyway. With a probability of 16% three or more species persist till that date and in two out of 100 random systems, at least four species coexist longer than one year. Non equilibrium dynamics and transients delay competitive exclusion significantly.

Now, let us focus on the impact of species interactions in the context of diversity: As expected, the more species excrete secondary resource, the less species go extinct. Another dependence that might at first glance appear counter-intuitive can be deduced. Interestingly, a producing specialist is more beneficial for the whole community than a producing generalist.

Apparently, the optimal situation for high diversity in this particular setup is characterized by a large number of specialists, that excrete the secondary nutrient source and few generalists that can profit thereof. In this case the majority of systems supports a community of more than two species until day 500. Excretion of one intermediate metabolic substance permits the coexistence of two species. Long transient periods and non-equilibrium dynamics extend the possible and typical diversity even to three or four species during reasonable time spans. It is likely that in natural habitats bacteria will grow in a more diverse environment with multiple homologous nutrient sources. With more complex nutrients arises the possibility of more intermediate products that can be consumed as common goods. Together with specialization and natural circumstances preventing stationary states, this accounts for more variety than the **Competitive Exclusion Principle** predicts.

5 IMPACT OF NETWORK STRUCTURE AND COMPLEXITY

All you really need to know for the moment is that the universe is a lot more complicated than you might think, even if you start from a position of thinking it's pretty damn complicated in the first place.

— Douglas Adams, *Mostly Harmless*

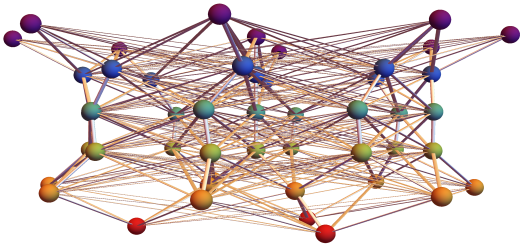

Figure 28: We consider food webs of several distinct trophic levels. The base consists of nutrients (red), followed by consumers (yellow) to top predators (purple).

5.1 INTRODUCTION

In the preceding chapters I established the difficulty of maintaining a diverse system in several simple set ups with at most one predator. The aim of this chapter is to substantiate this notion in conceptual food webs of larger complexity.

Natural food webs can be of arbitrary complexity and typically do not comply to exact **trophic levels**. A predator can hunt smaller predators but can also feed on their prey. To keep the theoretical system manageable we assume distinct **trophic levels**. On each level we introduce a certain number of species. The level in the food web defines the parameter range of properties of all species therein.

We will see, that increasing the number of trophic levels and the initial number of species in a food web does not substantially alter the situation. If random species enter a food web of fixed structure, the typical situation will still be that of a small number of species persisting with the majority of species disappearing.

5.2 METHODS

MODEL FORMULATION A model to realize higher complexity is a microbial food web of multiple trophic levels in chemostat. Let this arrangement consist of ℓ levels with L_1 to L_ℓ different species on level 1 to ℓ, respectively. The lowest level consists of nutrient sources that are utilized by primary consumers (second level) that are grazed upon by species from the next level and so on. These interactions can be simulated by the following differential equations

$$\frac{dN_{i,j}}{dt} = \text{growth}_{i,j}(N_{i,j},\ \mathbf{N}_{i-1}) - \text{loss}_{i,j}(\mathbf{N}_i,\ \mathbf{N}_{i+1}) \tag{5.1}$$

$$i = 1, \dots \ell \tag{5.2}$$

$$j = 1, \dots L_i \tag{5.3}$$

where $N_{i,j}$ is the population density of species j in level i. Resource densities are labeled by $N_{1,j}$, the turnover rate is again D. Each species feeds on the next lower level and thus the growth depends on the species densities of the level below, $\mathbf{N}_{i-1}$. Predation of the next upper level $\mathbf{N}_{i+1}$ will add to the loss term. Species of the same level will affect the loss indirectly via the mutual predators.

HOMOLOGOUS GROWTH ON MULTIPLE RESOURCES Assume organisms do not need one prey in particular but could survive on any one of them. Similarly, the nutrients are presumed to contain mixtures of chemicals and primary consumers can use the nutrients substitutably. To model growth on **homologous** resources we demand simple Holling's type II for growth in a monoculture on a single resource (1.6).

$$\mu(R_i) = \mu_{i,max}\frac{R_i}{k_i + R_i} \tag{5.4}$$

For the combined growth rate on multiple resources (or several prey species) we employ the model established in Lendenmann et al. [62].

$$\mu(\mathbf{R}) = \frac{\mu_{max} \sum \frac{\mu_{i,max}}{k_s} R_s}{\mu_{max} + \sum \frac{\mu_{s,max}}{k_s} R_s}, \qquad \mu_{max} = \max_s \{\mu_{s,max}\} \tag{5.5}$$

This equation meets the boundary conditions

$$\mu(\mathbf{R} = \mathbf{0}) = 0, \qquad \mu(R_s \to \infty) \to \max_s \{\mu_{s,max}\}. \tag{5.6}$$

It was tested for several microbial mixed culture chemostat experiments and proved to describe experimental results well. By rewriting equation (5.5) and defining new growth parameters, the expression can be simplified:

$$\mu(\mathbf{R}) = \mu_{max} \frac{\sum b_s R_s}{1 + \sum b_s R_s}, \qquad b_s = \frac{\mu_{s,max}}{\mu_{max} k_s} \tag{5.7}$$

Now we can formulate our growth terms for species in level i. Let us recall that level $i = 1$ contains the resources, that are pumped into the system at dilution rate D in the same manner as in previous chapters. For all consumer levels $i > 1$ the formula (5.7) applies.

$$\text{growth}_{i,j} = \begin{cases} S_j \; D & i = 1 \text{ (resources)} \\ N_{i,j} \; \mu_{i,j\,max} \dfrac{\sum_{s=1}^{L_{i-1}} b_{i,j,s} N_{i-1,s}}{1 + \sum_{s=1}^{L_{i-1}} b_{i,j,s} N_{i-1,s}} & \text{else} \end{cases} \tag{5.8}$$

With this, the growth rate of species j on level i is determined by all population densities in level $i - 1$. Top predators die at a fixed rate or leave the vessel being washed out by dilution. All other levels suffer predation or grazing from the next higher level. Accordingly, the loss term reads

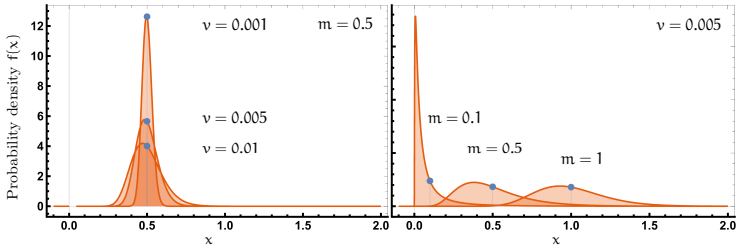

Figure 29: Probability density functions for Lognormal functions with various mean values and different variances.

$$\text{loss}_{i,j} = \begin{cases} N_{i,j}\ D & i = 1 \text{ (resources)} \\ N_{i,j}\ \left(D + \text{death}_{i,j}\right) & i = \ell \text{ (top predators)} \\ N_{i,j}\ \left(D + \text{death}_{i,j}\right) + N_{i,j}\ \dfrac{\sum_{s=1}^{L_{i+1}} \text{growth}_{i+1,s}}{\sum_{l=1}^{L_i} N_{i,l}} & \text{else} \end{cases} \tag{5.9}$$

Now each food web is characterized by the initial configuration $\{L_1, \ldots L_\ell\}$. We will distinguish food webs by the number of initial levels ℓ, the number of nutrients L_1 and the total sum of initial species $n_{in} = \sum_{i=2}^{\ell} L_i$. Food webs are simulated over 230 days and final species richness per level and in total (n_{fin}) is observed.

RANDOM SAMPLING The evolution of natural species is characterized by a number of properties, e.g. their ability to handle versatile food, the handling rate, their protection against predators. Parameters related to those properties are not always easy to determine and sometimes their measurement might not be feasible at all. Moreover, a population might feature an internal variance that we mathematically can treat as individual species modeling microevolution.

For the random sampling of parameters this study makes use of **lognormal distributions.** A lognormal distribution is the probability distribution

of a random variable whose logarithm has a normal distribution. Such distributions are generated as products of a series of independent positive random variables when the Central Limit Theorem applies. With many $X_1, X_2, \dots X_n$ independent positive random variables, their product $T_n = \prod_{i=1}^{n} X_i$ tends to be lognormal, ie. $\ln T_n = \sum_{i=1}^{n} \ln X_i$ approaches a normal distribution for large $n \to \infty$. The corresponding probability density functions are of the form

$$f(x) = \begin{cases} \dfrac{1}{\sqrt{2\pi}\sigma x} \exp\Big(-\dfrac{(\ln(x)-\mu)^2}{2\sigma^2}\Big) & x > 0 \\ 0 & x \leqslant 0 \end{cases} \tag{5.10}$$

where μ and σ^2 refer to the mean and variance, respectively, of the corresponding normal distribution. The distributions are skewed with the median e^{μ} determined by μ and σ changing the skewness (see Figure 29). The mean m and variance v of the lognormal distribution are given by

$$m = e^{\mu + \frac{\sigma^2}{2}} \qquad v = e^{2\mu+\sigma^2}\,(e^{\sigma^2} - 1) \tag{5.11}$$

Often natural effects are multiplicative and variance in biological systems obeys lognormal distributions. They appear, for example, in the size and weight of organs and organisms, in human age distributions, blood pressure and in disease latency periods, in word lengths as well as species abundances, growth of bacteria and fungi and in pollutants in food webs [51, 55, 67]. It is reasonable to assume that growth rates and other properties of our model species are influenced by multiple multiplicative variables. Therefore they can be presumed to be approximated by a lognormal distribution.

Now, random species can be sampled according to Table 7 for a food web layout $\{L_1, \dots L_\ell\}$ ($\ell \in \{4, 6, 8\}$)[1]. The values here are chosen to be more universally applicable than in the previous chapters, generally assuming faster reproduction and feeding in the lower levels. The units of time do not necessarily translate directly into days and population numbers can be scaled to other concentrations. Food web layouts with $\ell \in \{4, 6\}$ are chosen such that the initial number of species is $n_{in} = 45$. For food webs with $\ell = 8$ trophic levels only layouts with $n_{in} = 105$ initial species are sampled (Table 8). Species population numbers $\mathbf{N}$ are observed over 230 days for 500 random food webs per layout.

1 For numerical implementation see Appendix D

Table 7: Parameter ranges for lognormal distribution

PARAMETER	SYMBOL	MEAN	VARIANCE
death rate on level i	$death_{i,j}$	$0.1\ D\ i^{-1}$	$0.01\ D^2\ i^{-2}$
maximal growth rate on level i	$\mu_{i,j\ max}$	$10\ D\ i^{-1}$	$10\ D^2\ i^{-2}$
growth parameter	$b_{i,j,s}$	$5\ i^{-1}$	$10\ i^{-2}$

Table 8: Food web configurations simulated for this analysis with ℓ levels and L_i species introduced in level i. The number of nutrients is $L_1 \in \{3, 4\}$.

	L_2	L_3	L_4	L_5	L_6	L_7	L_8
$\ell = 4$	5	15	25				
	15	15	15				
	25	15	5				
$\ell = 6$	3	6	9	12	15		
	9	9	9	9	9		
	15	12	9	6	3		
$\ell = 8$	15	15	15	15	15	15	15

5.3 RESULTS

Probability distributions were calculated for the final compositions—level-wise and for the whole community with either three or four nutrients (Tables 10,11). The resulting skewed distributions are depicted in Figures 30 **A** - **C** with averages denoted by vertical lines. The average food web in these layouts contains 3.5 species after the observation time.

To untangle different influences, we distinguish systems by the quantity of nutrient sources. There is a slight increase for three nutrient sources which becomes more apparent if we compare the species diversity averaged over the initial system layout (Table 9).

The average number of species in all of the levels takes values between zero and two (Fig. 30 **D**). On average, most species live in the third trophic level, while primary producers (level 2) act as a bottleneck for nutrient flow in the system with relatively low species richness compared to level 3. The number

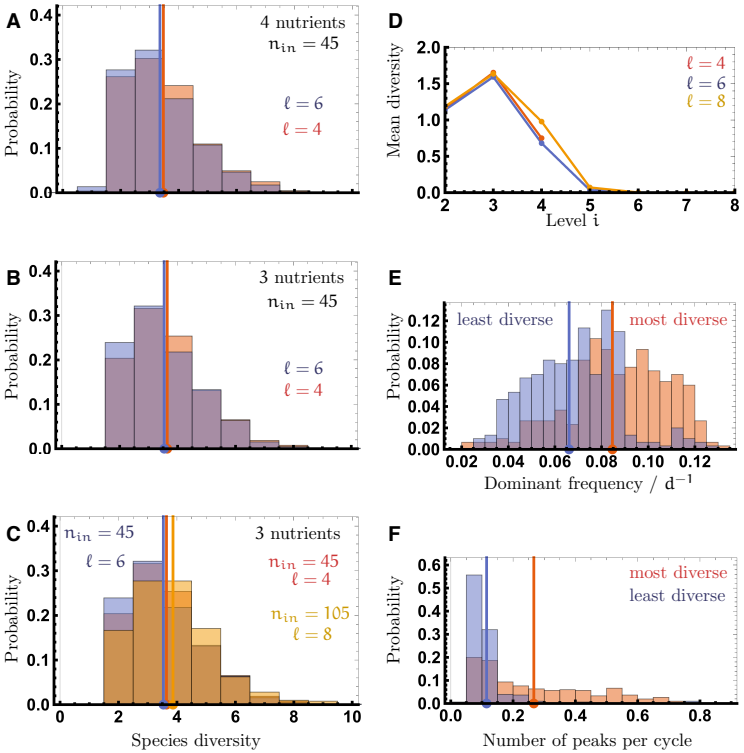

Figure 30: A, B, C: Distributions of the final diversity at day 230 in food web layouts of either three or four nutrients and four, six or eight levels. Lines indicate the mean diversity.
D: Mean diversity per trophic level.
E, F: Dynamical properties of the 300 most and least diverse food web configurations, respectively.

of initial trophic levels does not change the average number of species per level significantly. In extremely rare cases (0.04%) three species survive in level 5 till day 230 but in the majority of simulations (more than 96%) not even one species persists on level 5 (if three nutrients are provided, otherwise extinction of level 5 is even more common).

Additional simulations of 105 initial species on 8 initial trophic levels substantiate these results. On average, the diversity on the final day of observation still does not exceed four species in a food web. Levels 7 and 8 are empty and do not sustain species for the simulation period. The mean diversity per trophic level in appears to be robust under changes of the initial number of trophic levels or the initial number of species in a food web.

Population dynamics for systems of highest and lowest diversity are portrayed in Figure 30 (**E**, **F**). 10% of all 3000 configurations with the highest and lowest diversity, respectively, were examined with respect to their dynamical properties. Dynamics were characterized by the frequency of the time series. The count of distinct local maxima per period gives a measurement of the complexity of the dynamics.

Table 9: Averages of the total species richness over food webs of length ℓ and with L_1 nutrients

FOOD WEB LENGTH	NUMBER OF NUTRIENTS	MEAN DIVERSITY $\langle n_{fin} \rangle$
$\ell = 4, 6$	$L_1 = 3, 4$	3.50396
$\ell = 4, 6$	$L_1 = 3$	3.59032
$\ell = 4, 6$	$L_1 = 4$	3.41581
$\ell = 8$	$L_1 = 3$	3.86373

Table 10: Probabilities to find $n_{i,fin}$ final survivors on level i in food webs of 4 or 6 initial levels if three nutrients are provided.

	$i = 2$	$i = 3$	$i = 4$	$i = 5$	$i = 6$
$\mathcal{P}(n_{i,fin} = 0)$	0.00200401	0.	0.460254	0.951236	0.999332
$\mathcal{P}(n_{i,fin} = 1)$	0.873747	0.611222	0.356045	0.0400802	0.000668
$\mathcal{P}(n_{i,fin} = 2)$	0.110888	0.258517	0.132265	0.0086840	0.
$\mathcal{P}(n_{i,fin} = 3)$	0.0133601	0.0928524	0.0467602	0.	0.
$\mathcal{P}(n_{i,fin} = 4)$	0.	0.0320641	0.00467602	0.	0.
$\mathcal{P}(n_{i,fin} = 5)$	0.	0.0040080	0.	0.	0.
$\mathcal{P}(n_{i,fin} = 6)$	0.	0.0006680	0.	0.	0.
$\mathcal{P}(n_{i,fin} = 7)$	0.	0.0006680	0.	0.	0.
$\mathcal{P}(n_{i,fin} \geqslant 8)$	0.	0.	0.	0.	0.
$\langle n_{i,fin} \rangle$	1.1356	1.56379	0.779559	0.0574482	0.000668

Table 11: Probabilities to find $n_{i,fin}$ final survivors on level i in food webs of 4 or 6 initial levels if four nutrients are provided.

	$i = 2$	$i = 3$	$i = 4$	$i = 5$	$i = 6$
$\mathcal{P}(n_{i,fin} = 0)$	0.0132316	0.00305344	0.589313	0.991349	1.
$\mathcal{P}(n_{i,fin} = 1)$	0.849873	0.539949	0.279898	0.00712468	0.
$\mathcal{P}(n_{i,fin} = 2)$	0.116539	0.300254	0.0951654	0.00101781	0.
$\mathcal{P}(n_{i,fin} = 3)$	0.0193384	0.123155	0.026972	0.00050890	0.
$\mathcal{P}(n_{i,fin} = 4)$	0.00101781	0.0239186	0.00712468	0.	0.
$\mathcal{P}(n_{i,fin} = 5)$	0.	0.00916031	0.00152672	0.	0.
$\mathcal{P}(n_{i,fin} = 6)$	0.	0.00050890	0.	0.	0.
$\mathcal{P}(n_{i,fin} \geqslant 7)$	0.	0.	0.	0.	0.
$\langle n_{i,fin} \rangle$	1.14064	1.62272	0.581474	0.0121704	0.

5.4 DISCUSSION

As we have seen in previous chapters, most randomly induced species die out in the main fraction of systems. This still holds true with the perfectly

homologous resources modeled here. Increasing the complexity does not change the fact, that in the end apart from three to four survivors all introduced species are extinct.

Interestingly, additional alternative nutrient sources do not promote diversity, but quite the contrary, total diversity is higher in systems with three instead of four assumed resources. This supports the view, that over-fertilization can endanger ecosystems rather than help [90].

Even with more than twice as many initial species and 8 initial trophic levels, the diversity does not exceed four species in the average food web. Rarely, systems maintain more than four levels.

Altogether, this model validates the notion, that we cannot explain ever-present long food chains and complex food webs by mere chance encounters of species. To yield longer trophic chains, additional phenomena have to be taken into account. Constant migration and mutation could—via trial and error—lead to more complex systems over generations. Maybe a combination of those phenomena is needed to understand (high) diversity. For instance, Allhoff et al. [2] study eco-evolutionary food webs, where species are characterized by body size, preferred prey body mass and width of the prey body mass spectrum. In that model new species emerge via evolution and die according to ecological interactions giving rise to webs of higher complexity. Theoretically, long-term diversity appears to be unlikely although reality proves the opposite.

One important message from this analysis is the impact of dynamical properties. In exceptional cases, up to 12 species can survive in coexistence for more than half a year. In these systems of higher diversity, the species richness is mostly due to a surplus of species in levels $\geqslant 3$. The dynamics in diverse systems oscillates at higher frequency and harbors more complex dynamics. Species richness in the simulated food webs is typically not characterized by stationary population numbers. High species diversity is maintained by dynamics of high diversity.

6 SUMMARY

Mathematical analysis and computer modelling are revealing to us that the shapes and processes we encounter in nature - the way that plants grow, the way that mountains erode or rivers flow, the way that snowflakes or islands achieve their shapes, the way that light plays on a surface, the way the milk folds and spins into your coffee as you stir it, the way that laughter sweeps through a crowd of people - all these things in their seemingly magical complexity can be described by the interaction of mathematical processes that are, if anything, even more magical in their simplicity. Shapes that we think of as random are in fact the products of complex shifting webs of numbers obeying simple rules. The very word 'natural' that we have often taken to mean 'unstructured' in fact describes shapes and processes that appear so unfathomably complex that we cannot consciously perceive the simple natural laws at work. They can all be described by numbers.

— Douglas Adams, *Dirk Gently's Holistic Detective Agency*

The relevance of biodiversity for the stability of ecosystems is an issue that has been controversial in environmental sciences for decades. Theoretical models indicate that chaotic population dynamics go along with high species richness. Chaos can create diversity or, to be more precisely, maintain it. Numerical simulations and analysis demonstrated chaos in realistic food web models. Experiments have shown chaos in real food webs and natural ecosystems prove biodiversity in real world. This thesis inquires into the relation between chaos and diversity in natural food webs.

We could convince ourselves that in a microbial food web of three species chaotic dynamics are not only observed in experiments but that simple interaction rules can indeed reproduce similar time series. The chaotic attractor in this model emerges from an interplay of distinct periodic cycles. This makes one suspect, that chaos should arise commonly when periodic sub patterns merge. Extinction times in this food web scale exponentially with the system size. This scaling behavior proves the stabilizing role of chaos in ecological context.

A model could be modified to match the processes in another experiment of six bacterial species. We could reproduce the sustained oscillations that the experimentalists measured. Simple competition on three essential resources is enough to account for them. The same model would also allow stationary coexistence at fixed population numbers for different (biologically feasible)

parameters. However, sensitivity analysis indicates that chaotic coexistence is less prone to extinction when the nutrient supply changes. So we must assume, that if we are faced with diversity in a food web, the dynamics are very likely to be intrinsically oscillating. On the other hand, if population dynamics are fluctuating this might mean that the system is more likely to persist than a stationary setup. Statistical analysis of numerical simulations indicate that probabilities are low that a group of species ends up in one habitat by chance and will live happily ever after. The divergence of theoretical predictions from natural observations might be due to assumptions being too general. The model might lack mechanisms that are present in natural interactions. Also, long transitions and slow extinction together with evolution and natural selection in populations could explain biological persistence of species richness.

Cooperation was introduced in the form of a metabolic byproduct into a theoretical model. Excretion is a common mechanism where species are able to profit from byproducts of others. Cooperation can promote and maintain higher species numbers. The model confirms the idea that specialists play an important role in the extinction behavior of competitive systems and that incorporating the niche concept might be a valuable strategy in understanding and maybe even conserving high biodiversity.

To investigate more complex setups a model of multiple trophic levels and a 15-fold increase of species was simulated. The postulated setup generated regularly non-equilibrium dynamics. Nevertheless, the average species richness does not approach particularly high values that would justify to call the system diverse. Modeling natural diversity might require still larger food webs. As Gross et al. [39] demonstrated, food webs can undergo transitions where variability in link strengths induces stability in small webs but acts destabilizing in larger webs.

Overall, this thesis was able to demonstrate that simple models can describe mechanisms in real world food webs in a satisfactory manner and that we can find models that permit coexistence of diverse species on few resources but that those parameter combinations are rare. Equilibrium coexistence of numerous competitive species is not impossible, albeit not as likely to emerge or to persist as chaotic coexistence.

We have yet to answer whether nature "found" the right species combinations by millions of years of trial and error or wether ecosystems have to be considered open with external disturbances keeping the system in transient to equilibrium. The open questions remain of whether coexistence nowadays is the result of a long-term optimization process? Are biological systems open systems? Is a seasonal shake-up inevitable to grant species richness maintained?

To answer those questions one should simulate larger food nets or integrate evolution, adaption, migration or the influence of trade-off functions. (Trade-off functions incorporate disadvantages that species suffer in exchange for favorable properties.) Rigorously modeling populations and their dynamics with explicit variance in the characterizing traits would certainly be interesting and promising. But comparative studies of theory and experiment would require experimental data of population dynamics *and* the change in the population composition and shifts in the distribution of properties with high resolution in time. The interesting aspect of this thesis was the combination of experiments with applied modeling and comparative analysis as a mean to enhance understanding of ecological mechanisms. Experiments with a high resolution in time and species are needed together with theoretical models to explicitly investigate the impact of intrinsic dynamics on diversity in larger food webs.

We should be in awe for nature producing so easily something that needs so much fine tuning in our mathematical models. The theoretical findings suggest not to take biodiversity as much for granted as long as we are not able to reproduce it even in small scale without fiddling with the specific properties of the theoretical organisms. Changing the composition of species in an ecosystem and altering their environment poses a major threat to that community. General results from simulations of simplified interactions and species models might not necessarily translate directly to real life situations and convey practical directions. But at least it seems reasonable to recommend that ecosystem regulations should allow strong fluctuations of population numbers. As we have seen, non-equilibrium oscillations can stabilize the diversity in a habitat and wildlife management should bear in mind that fixed densities can endanger a food net instead of stabilizing it by balancing species out.

Appendices: Code

A CHAOS STABILIZING A PREDATOR-PREY SYSTEM

A.1 LYAPUNOV EXPONENT

```
ClearAll["Global`*"];
C0 = 3;
\[Epsilon] = 2*10^(-6);
\[Beta] = (1/4000);
\[Mu]max1 = 0.15;
\[Mu]max2 = 0.172;
Ks1 = 0.0274;
Ks2 = 0.002;
\[Phi]max1 = 150*\[Beta];
\[Phi]max2 = 400*\[Beta];
KN1 = 422000*\[Epsilon];
KN2 = 400000*\[Epsilon];
n0 = {0, 1, 1, 1};

fc = (C0 - c)*d - \[Mu]max1*c*n1/(Ks1 + c) - \[Mu]max2*c*
    n2/(Ks2 + c);
fn1 = \[Mu]max1*c*n1/(Ks1 + c) - \[Phi]max1*p*n1/(KN1 + n1) - d*n1;
fn2 = \[Mu]max2*c*n2/(Ks2 + c) - \[Phi]max2*p*n2/(KN2 + n2) - d*n2;
fp = \[Phi]max1*p*n1/(KN1 + n1) + \[Phi]max2*p*n2/(KN2 + n2) - d*p;

vars := {c, n1, n2, p}
a = {ca[t], n1a[t], n2a[t], pa[t]};
b = {cb[t], n1b[t], n2b[t], pb[t]};

Put["Attraktor–Lyapunov"]
(*discrete steps*)
steps = 100;
tin = 0; tfin = 10000;
tstep = 1;
(*accuracy*)
acc = 12;

lcedata = {};

Timing[For[j = 0, j <= steps, j++,
  sweep = 0.001 + 0.1*j/steps;
```

```
d = sweep;
(*differential equations for two trajectories*)

da = {fc, fn1, fn2, fp} /. Array[vars[[#]] -> a[[#]] &, 4];
db = {fc, fn1, fn2, fp} /. Array[vars[[#]] -> b[[#]] &, 4];
(*initial conditions*)
a0 = n0;
a0 = Evaluate[(a /.
     NDSolve[{D[a, t] == da, a == a0 /. {t -> 0}}, {a}, {t, 0,
        30000}, MaxSteps -> \[Infinity]][[1]]) /. t -> 30000];
dx0 = 10^-5;
b0 = a0 + Join[Array[0 &, 3], {dx0}];

d0 = Norm[a0 - b0];(*initial distance*)
sum = 0;
Monitor[For[i = 1, i < tfin/tstep, i++,
   sdeq = {D[a, t] == da, D[b, t] == db, a == a0 /. {t -> 0},
     b == b0 /. {t -> 0}};

   sol =
    NDSolve[sdeq, {a, b}, {t, 0, tstep}, MaxSteps -> Infinity,
     Method -> "Adams", PrecisionGoal -> acc, AccuracyGoal -> acc];

   aa[t_] = a /. sol[[1]]; bb[t_] = b /. sol[[1]];

   d1 = Norm[aa[tstep] - bb[tstep]];
   sum += Log[d1/d0];
   dlce = sum/(tstep*i);

   \[Delta] = (aa[tstep] - bb[tstep])*(d0/d1);
   a0 = aa[tstep]; b0 = a0 + \[Delta];
   i = i++]
  AppendTo[lcedata, {sweep, dlce}];
 {sweep, dlce} >>> "Attraktor–Lyapunov"
 , {sweep, i}]]]

ListPlot[{lcedata}, Frame -> True, Axes -> True,
 PlotRange -> {All, .005}, Joined -> True,
 FrameLabel -> {"sweep", "LCE"},
 FrameStyle -> Directive["Helvetica", 17], AxesOrigin -> {0, 0},
 Mesh -> All, PlotTheme -> "Scientific"]

Show[ListPlot[Sort[ReadList["Attraktor–Lyapunov–2"]],
  PlotStyle -> PointSize[Medium],
  PlotRange -> {{0.035, 0.05}, {-0.006, 0.006}}, Mesh -> All],
 ListPlot[ReadList["Attraktor–Lyapunov–1"],
  PlotStyle -> Directive[PointSize[Large], Orange], PlotRange -> All,
  Mesh -> All]]
```

A.2 EXTINCTION TIMES

```
#include <stdio.h>
#include <stdlib.h>
#include <time.h>
#include <string.h>
#include <math.h>
#include <algorithm>
#include <iostream>
#include <fstream>
#include <iomanip>
#include <sstream>
#include <cstring>
#include <sstream>
#include <cstring>
#include "gsl/gsl_rng.h"
#include "gsl/gsl_randist.h"

using namespace std;

int runs=100;
int data1=0,data2=0,datap=0;

double Tmax=20000;
double Vol;

int iter;
int noreac=8;
double mu1, mu2,phi1,phi2;
double r1,r2;
int m;
int P[3];                                   // populations (pred,prey1,prey2)
     in each step of iteration
int dN;
double C,dC;                            // concentration nutrient
double T,step,avT1,avT2,avTp;                       // time T
double d;
//different dilutionrates
double Rate[7];
double start[7][4];

//parameter values
double C0=      3;
double mumax1=0.15;
double mumax2=0.172;
double phimax1=150;
double phimax2=400;
double beta=0.00025;
double eps=0.000002;
```

```
double KN1=422000;
double KN2=400000;
double Ks1=0.0274;
double Ks2=0.002;

// Hollingfunction
double holling(double sat, double x, double h){
    double r=(sat*x)/(x+h);
    return r;
}

//// Random Number Generator a la GSL...
gsl_rng * myRNG = gsl_rng_alloc(gsl_rng_mt19937);

// RN  between 0 and 1
//generate random number r01!=0
double r01 (void) {
    double r=0;
    while (r==0)
    {
        r=gsl_ran_flat(myRNG, 0, 1);
    }
    return r;
}

// filename
string filename (double a, double b, string c){

   stringstream out;
   out<<"Data/average_first_passage_"<<a<<"_"<<b<<"_"<<c<<"_"<<2016<<"_"<<1<<"_"
        <<4<<".dat";
   string name=out.str();
   out.str(std::string());
   return name;
}

// stochastic step
void dynamics (double d) {

    mu1=holling(mumax1, C, Ks1*Vol);
    mu2=holling(mumax2, C, Ks2*Vol);
    phi1=holling(phimax1, P[1], KN1*Vol);
    phi2=holling(phimax2, P[2], KN2*Vol);

    //reaction probabilities
    double A[noreac];
    A[0]=(C0*Vol)*d;                                    //* -> C
    A[1]=C*d+eps*mu1*P[1]+eps*mu2*P[2];          //C -> *
    A[2]=mu1*P[1];                                      //N1 -> 2 N1
```

```
    A[3]=P[1]*d + phi1*P[0];                          //N1 -> *
    A[4]=mu2*P[2];                                    //N2 -> 2 N2
    A[5]=P[2]*d + phi2*P[0];                    //N2 -> *
    A[6]=beta*phi1*P[0] + beta*phi2*P[0];   //P -> 2P
    A[7]=P[0]*d;                                //P -> *

    //choose timestep
    double a0=0;
    for (int i=2; i<noreac;i++){a0=a0+A[i];}
    double r1=r01();                                  //generate random number r1
    step=-log(r1)/a0;                   //solve eq1 -> timestep
    T=T+step/24;                                //new time (days)

    //choose reaction
    double r2=r01();                                  //generate random number r2
    m=2;
    double aux=A[m];
    while (aux<r2*a0) {
        m++;
        aux=aux+A[m];
    }

    // reaction m
    if(m==2){P[1]++;}
    if(m==3){P[1]--;}
    if(m==4){P[2]++;}
    if(m==5){P[2]--;}
    if(m==6){P[0]++;}
    if(m==7){P[0]--;}
    //evolve C
    dC=step*A[0]- step*A[1];
    C=max(C+dC,0.);

}

// main
int main (int argc, char * const argv[]) {

    gsl_rng_set(myRNG, time(0));
    cout<<"laeuft "<<endl;

    //different dilutionrates
    Rate[0]=0.030;
        start[0][0]=119;
        start[0][1]=1001092;
        start[0][2]=15041;
        start[0][3]=0;
    Rate[1]=0.035;
        start[1][0]=58;
```

```
    start[1][1]=1244249;
    start[1][2]=17675;
    start[1][3]=0;
Rate[2]=0.040;
    start[2][0]=56;
    start[2][1]=1214966;
    start[2][2]=54047;
    start[2][3]=0;
Rate[3]=0.042;
    start[3][0]=70;
    start[3][1]=1169799;
    start[3][2]=41116;
    start[3][3]=0;
Rate[4]=0.045;
    start[4][0]=78;
    start[4][1]=1124403;
    start[4][2]=55507;
    start[4][3]=0;
Rate[5]=0.050;
    start[5][0]=146;
    start[5][1]=0;
    start[5][2]=568852;
    start[5][3]=0;
Rate[6]=0.055;
    start[6][0]=246;
    start[6][1]=0;
    start[6][2]=488888;
    start[6][3]=0;

for (int j=6; j>=6; j--) {
            d=Rate[j];

        ofstream output;
        output.open(filename(d,0,"").c_str(), ios::app);
        output.precision(5);
        ofstream T1output;
        T1output.open(filename(d,0,"prey1").c_str(), ios::app);
        T1output.precision(5);
        ofstream T2output;
        T2output.open(filename(d,0,"prey2").c_str(), ios::app);
        T2output.precision(5);
        ofstream Tpoutput;
        Tpoutput.open(filename(d,0,"pred").c_str(), ios::app);
        Tpoutput.precision(5);

        for (int i=5; i<15; i++) {
            Vol=0.1 * i;                              // volume in ml
            time_t rawtime;
            struct tm * timeinfo;
```

```
            time (rawtime);timeinfo = localtime (rawtime);
            cout<<asctime(timeinfo)<<" "<<d<<" "<<Vol<<endl;

        avT1=0.0;
        avT2=0.0;
        avTp=0.0;
        data1=0;
        data2=0;
        datap=0;
        for (int k=0; k<runs; k++) {
            C=start[j][3]*Vol;                //initial values
            P[1]=round(start[j][1]*Vol);
            P[2]=round(start[j][2]*Vol);
            P[0]=round(start[j][0]*Vol);
            T=0.0;
            while ( ( (P[1]>0) || (j>=5) )  (P[2] > 0)  (P[0] > 0)  ( T<Tmax )
                  ) {
                                dynamics(d); }
            if ( (T<Tmax)  (P[1]==0)  (j<5) ){
                                avT1=avT1+T;
                                T1output<<d<<"\t"<<Vol<<"\t"<<T<<endl;
                                data1=data1+1; }
            if ( (T<Tmax)  (P[2]==0) ){
                                avT2=avT2+T;
                                T2output<<d<<"\t"<<Vol<<"\t"<<T<<endl;
                                data2=data2+1; }
            if ( (T<Tmax)  (P[0]==0) ){
                                avTp=avTp+T;
                                Tpoutput<<d<<"\t"<<Vol<<"\t"<<T<<endl;
                                datap=datap+1;}
        }
        if (data1>0){avT1=avT1/data1;}
        if (data2>0){avT2=avT2/data2;}
        if (datap>0){avTp=avTp/datap;}
                    output<<d<<"\t"<<Vol<<"\t"<<avT1<<"\t"<<avT2<<"\t"<<avTp<<"
                          \t..\t"<<data1<<"\t"<<data2<<"\t"<<datap<<endl;
    }
        output.close();
        T1output.close();
        T2output.close();
        Tpoutput.close();
    }
    gsl_rng_free(myRNG);
    return 0;
}
```

A.3 BIFURCATION DIAGRAM

```
Clear["Global`*"];

fx[d_] := (C0 - x)*d - \[Mu]max1*
    x*(C0 - x - y - z)/(Ks1 + x) - \[Mu]max2*x*y/(Ks2 + x);
fy[d_] := \[Mu]max2*x*y/(Ks2 + x) - \[Phi]max2*z*y/(KN2 + y) - d*y;
fz[d_] := \[Phi]max1*
    z*(C0 - x - y - z)/(KN1 + (C0 - x - y - z)) + \[Phi]max2*z*
    y/(KN2 + y) - d*z;

C0 = 3;
\[Epsilon] = 2*10^(-6);
\[Beta] = (1/4000);
\[Mu]max1 = 0.15;
Ks1 = 0.0274;
\[Mu]max2 = 0.172;
Ks2 = 0.002;
\[Phi]max1 = 150*\[Beta];
KN1 = 422000*\[Epsilon];
\[Phi]max2 = 400*\[Beta];
KN2 = 400000*\[Epsilon];

fixpt[d_] := NSolve[{fx[d] == 0, fy[d] == 0, fz[d] == 0}, {x, y, z}]

eqx[d_] := x'[t] == (fx[d] /. {x -> x[t], y -> y[t], z -> z[t]})
eqy[d_] := y'[t] == (fy[d] /. {x -> x[t], y -> y[t], z -> z[t]})
eqz[d_] := z'[t] == (fz[d] /. {x -> x[t], y -> y[t], z -> z[t]})

eqns[d_] := {eqx[d], eqy[d], eqz[d], x[0] == x0[[1]], y[0] == x0[[2]],
   z[0] == x0[[3]]}
vars := {x, y, z}

sol[d_] :=
 NDSolve[eqns[d], vars, {t, 0, 20000}, MaxSteps -> \[Infinity]]

list = {};
For [i = 1, i <= Length[fixpt[0.043]], i++,
 If[(x /. fixpt[0.043][[i]]) >=
    0 && (x + y + z <= 3 /.
     fixpt[0.043][[i]]) && (y /. fixpt[0.043][[i]]) >=
    0 && (z /. fixpt[0.043][[i]]) >= 0, {AppendTo[
    list, {x, y, z} /. fixpt[0.043][[i]]]}]]

x0 = list[[3]] + {0, 0.15, 0};

pts = Quiet[Flatten[Table[iterate[d], {d, 0.02, 0.06, 0.00001}], 1]];

sol[d_] :=
```

```
 NDSolve[eqns[d], vars, {t, 2000, 20000}, MaxSteps -> \[Infinity]]
iterate =
  Compile[{d}, {fsol = sol[d];
    Map[{d, #} &,
     FindMaxValue[x[t] /. fsol, {t, #, # + 500}] & /@
      Table[i, {i, 4000, 10000, 100}]]}];

pts = Quiet[Flatten[Table[iterate[d], {d, 0.01, 0.1, 0.00001}], 1]];

ListPlot[pts,
 PlotStyle ->
  Table[{PointSize[0.001], Darker[Green]}, {i, 1, Length[pts]}],
 Frame -> True, AxesOrigin -> {0, 0},
 FrameLabel -> {Style["d", Italic], Style["c", Italic]},
 ImageSize -> 800, PlotRange -> {All, {0, 2}}]
```

B SENSITIVITY OF COMPETITIVE CHAOS AND EQUILIBRIUM

B.1 MODEL SETUP ADAPTED FROM HUISMAN AND WEISSING

```
ClearAll["Global`*"];(*six bacterial strains feeding on glucose, \
phosphate, nitrate*)
S = {20, 7, 0.77};
(*resource concentration in nutrient medium [mgC per liter, mgN per \
liter, mgP per liter]*)
(*sweep in experiment 0.75 per day*)

m[i_, j_, R_] := (max[[i]]*R[[j]])/(k[[j, i]] + R[[j]])
μ[i_, R_] := Min[Table[m[i, j, R], {j, 1, 3}]]
n = Array[ToExpression[StringJoin["n", ToString[#], "[t]"]] &, 6];
R = Array[ToExpression[StringJoin["R", ToString[#], "[t]"]] &, 3];
dn := Array[n[[#]]*(μ[#, R] - sweep) &, 6]
dR := Array[ sweep*(S[[#]] - R[[#]]) - Sum[c[[#, i]]*μ[i, R]*n[[i]], {i, 1, 6}] &,
      3]
vars := {n, R};
k = {20, 7, 0.77}*
({{1, 0.75, 0.25, 0.7, 0.2, 0.65},{0.25, 1, 0.75, 0.2, 1.01, 0.55}, {0.75, 0.25, 1,
        1.1, 0.7, 0.95}}/10);
max = 3*{1, 1, 1, 1, 1, 1};
c = 10^(-9)*{20, 7, 0.77}*
({{.10, .20, .15, .05, .01, .40},{.15, .10, .20, .15, .30, .35},{.20, .15, .10,
      .25, .05, .20}})/10;
eqns := {D[n, t] == dn, D[R, t] == dR, n == 10^(9)*n0 /. {t -> 0},
   R == S /. {t -> 0}};
parsol :=
  ParametricNDSolve[eqns, vars, {t, 0, 4000}, {sweep},
   MaxSteps -> \[Infinity]];
```

B.2 PARAMETER VALUES FOR FIGURE 15

```
n0 := {0.11, 0.12, 0.13, 0.1, 0.1, 0.1, S[[1]], S[[2]], S[[3]]};
sweep = 0.25;
S = {10, 10, 10};
k = {{1, 0.75, 0.25, 0.7, 0.2, 0.65}, {0.25, 1, 0.75, 0.2, 1.01, 0.55}, {0.75,
      0.25, 1, 1.1, 0.7, 0.95}};
```

```
c = {{0.1, 0.2, 0.15, 0.05, 0.01, 0.4}, {0.15, 0.1, 0.2, 0.15, 0.3,  0.35},   {0.2,
      0.15, 0.1, 0.25, 0.05, 0.2}};
r = {1, 1, 1, 1, 1, 1};
```

B.3 TIME EVOLUTION

```
ticks1 = Table[{50*k, 50*k, {0, .01}}, {k, 5}];
ticks2 = Table[{10^(10)*k, NumberForm[10.^(10)*k, 10], {0, .01}}, {k,
    5}];
i = 0;
Do[n0 = start; i++;
 plot = Plot[Evaluate[n[0.75] /. parsol], {t, 0, 200},
   PlotRange -> All, PlotStyle -> Thick, Axes -> True,
   AspectRatio -> 1/3, TicksStyle -> Thin,
   Ticks -> {ticks1, ticks2},
   LabelStyle -> Directive[FontSize -> 15, FontFamily -> "Helvetica"],
    AxesStyle -> Directive[Medium, Plain, Arrowheads[{0, 0.03}]],
   AxesLabel -> {"days", "species abundances per liter"},
   ImageSize -> 500];
 Export[StringJoin["species-oscillations-dynamics", ToString[i],
   ".pdf"], plot],
 {start, {{15, 0, 0, 0, 0, 0}, {15, 30, 0, 0, 0, 0}, {15, 30, 10, 0,  0, 0}, {15,
      30, 10, 5, 0, 0}, {15, 30, 10, 5, 5, 0}, {15, 30, 10,  5, 5, 1}}}]
```

B.4 CONTOURPLOTS

```
n0 = {15, 30, 10, 5, 5, 1};
dmax = 3;
it = 300;
Tmin = 0; Tmax = 400;
Put["species-oscillations-survivor-400"];
"chop to 1" >>> "species-oscillations-survivor-400"
Do[{d, T, LengthWhile[Sort[Flatten[n[d] /. parsol /. t -> T], Greater], # > 1 &]}
      >>>  "species-oscillations-survivor-400",
  {d, 0, dmax, dmax/it}, {T, Tmin, Tmax, Tmax/it}]
Tmin = 400; Tmax = 4000;
Put["species-oscillations-survivor-4000"];
"chop to 1" >>> "species-oscillations-survivor-4000"
Do[{d, T,  LengthWhile[ Sort[Flatten[n[d] /. parsol /. t -> T], Greater], # > 1 &]}
       >>>  "species-oscillations-survivor-4000", {d, 0, dmax, dmax/it}, {T, Tmin,
      Tmax, Tmax/it}]
```

B.5 BIOMASS AND PRODUCTION

```
(* collect all 2-species-sets,3-species-sets,4-species-sets etc *)
(* \
time average *)

totalabundance = {{"number of species", "total abundance"}};
biomass = {{"number of species", "total biomass"}};
productivity = {{"number of species", "productivity"}};
xx = {15, 30, 10, 5, 5, 1};
Do[n0 = xx*start;
 parsol =  ParametricNDSolve[eqns, vars, {t, 0, 1000}, {sweep}, MaxSteps -> \[
      Infinity]];
 AppendTo[totalabundance, {Count[Evaluate[n[0.75] /. parsol /. t -> 1000], x_ /; x
      > 1],  Sum[((Evaluate[Integrate[n[0.75] /. parsol, {t, 900, 1000}]]/100)[[k
      ]]), {k, 1, 6}]}];
 AppendTo[biomass, {Count[Evaluate[n[0.75] /. parsol /. t -> 1000], x_ /; x > 1],
      Sum[c[[1, k]]*((Evaluate[Integrate[n[0.75] /. parsol, {t, 900, 1000}]]/100)[[
      k]]), {k, 1, 6}]}];
 AppendTo[productivity, {Count[Evaluate[n[0.75] /. parsol /. t -> 1000], x_ /; x >
      1],  0.75*Sum[ c[[1, k]]*((Evaluate[Integrate[n[0.75] /. parsol, {t, 900,
      1000}]]/100)[[k]]), {k, 1, 6}]}],
 {start, Tuples[{0, 1}, 6]}]
Do[Export[StringJoin[list, ".xls"], ToExpression[list]],
 {list, {"totalabundance", "biomass", "productivity"}}]
```

B.6 LARGEST LYAPUNOV EXPONENT

```
Put["species-oscillations-LLE"]
n0 = {15, 30, 10, 5, 5, 1};
acc = 12; steps = 30; tfin = 40; tstep = .1;

na = Array[ToExpression[StringJoin["na", ToString[#], "[t]"]] &, 6];
Ra = Array[ToExpression[StringJoin["Ra", ToString[#], "[t]"]] &, 3];
a = Join[na, Ra];

nb = Array[ToExpression[StringJoin["nb", ToString[#], "[t]"]] &, 6];
Rb = Array[ToExpression[StringJoin["Rb", ToString[#], "[t]"]] &, 3];
b = Join[nb, Rb];
For[j = 0, j <= steps, j++,
 sweep = 0.001 + j*(3.5 - 0.001)/steps;

 (*differential equations for one trajectory*)
 da = Join[Array[na[[#]]*(μ[#, Ra] - sweep) &, 6], Array[sweep*(S[[#]] - Ra[[#]]) -
       Sum[c[[#, i]]*μ[i, Ra]*na[[i]], {i, 1, 6}] &, 3]];

 (*same differential equations for a second trajectory*)
```

```
db = Join[Array[nb[[#]]*(μ[#, Rb] - sweep) &, 6], Array[sweep*(S[[#]] - Rb[[#]]) -
       Sum[c[[#, i]]*μ[i, Rb]*nb[[i]], {i, 1, 6}] &, 3]];

(*initial conditions*)
a0 = Join[n0, S];
a0 = Evaluate[(a /.  NDSolve[{D[a, t] == da, a == a0 /. {t -> 0}}, {a}, {t, 0,
     1000}][[1]]) /. t -> 1000];
dx0 = 10^-5;
b0 = a0 + Join[{dx0}, Array[0 &, 8]];

(*initial distance*)
d0 = Norm[a0 - b0];
sum = 0;
For[i = 1, i < tfin/tstep, i++,
  sdeq = {D[a, t] == da, D[b, t] == db, a == a0 /. {t -> 0},  b == b0 /. {t ->
       0}};
  sol = NDSolve[sdeq, {a, b}, {t, 0, tstep}, MaxSteps -> Infinity,  Method -> "
       Adams", PrecisionGoal -> acc, AccuracyGoal -> acc];
  aa[t_] = a /. sol[[1]];
  bb[t_] = b /. sol[[1]];

  d1 = Norm[aa[tstep] - bb[tstep]];
  sum += Log[d1/d0];
  dlle = sum/(tstep*i);
  δ = (aa[tstep] - bb[tstep])*(d0/d1);
  a0 = aa[tstep];
  b0 = a0 + δ;
  i = i++];
{sweep, dlle} >>> "species–oscillations–LLE"
]
```

B.7 STATISTICAL ANALYSIS

```
SeedRandom[1];
n0 = {1, 1, 1, 1, 1, 1};
Put["Huisman–coex–statistik–var–1"];            (* Distribution at day 400*)
Quiet[Do[aux = {}; Do[
        max = RandomReal[{2.7, 17}, 6];
         k = RandomReal[{10^(-4), 10}, {3, 6}];
        c = {RandomReal[{10^(-11), 10^(-9)}, 6],  RandomReal[{10^(-12), 10^(-10)},
             6], RandomReal[{10^(-13), 10^(-11)}, 6]};
        AppendTo[aux,   LengthWhile[Sort[Flatten[n[d] /. parsol /. t -> T], Greater
             ],  #1 > 1 & ]], {1000}];
        PutAppend[{d, T, aux}, "Huisman–coex–statistik–var–1"]; ,
        {d, {0.75}}, {T, {400}}]]
it = 300;

Put["Huisman–coex–statistik"];          (* Contourplot*)
Quiet[Do[aux = {}; Do[
```

```
max = RandomReal[{2.7, 17}, 6];
 k = RandomReal[{10^(-4), 10}, {3, 6}];
c = {RandomReal[{10^(-11), 10^(-9)}, 6], RandomReal[{10^(-12), 10^(-10)},
     6], RandomReal[{10^(-13), 10^(-11)}, 6]};
 AppendTo[aux,   LengthWhile[Sort[Flatten[n[d] /. parsol /. t -> T],
       Greater],  #1 > 1 & ]], {100}];
PutAppend[{d, T, Mean[aux]}, "Huisman-coex-statistik"]; ,
{d, 0, 3, 3/20}, {T, 0, 4000, 4000/it}]]
```

C INTERPLAY OF COMPETITION, COOPERATION AND SPECIALISATION

C.1 MODEL SETUP

```
ClearAll["Global'*"];
total = 10; tmax = 1000; imax = 100;
Vol = 1; c0 := 18.75*Vol
muhom[i_, j_, c_] := (max[[i, j]]*c)/k[[i, j]]
mumax[j_] := Max[max[[1, j]], max[[2, j]]] μpart1[j_, c1_, c2_] := (mumax[j]*muhom
     [1, j, c1])/(mumax[j] + muhom[1, j, c1] +
         muhom[2, j, c2]);  μpart2[j_, c1_, c2_] := (mumax[j]*muhom[2, j, c2])/(
              mumax[j] + muhom[1, j, c1] +  muhom[2, j, c2]);
(*parameter in mu g carbon*)
sweep = .75;
n = Array[ToExpression[StringJoin["n", ToString[#], "[t]"]] &,   total];
dnt = Array[ToExpression[StringJoin["n", ToString[#], "'[t]"]] &, total];
dn := Array[n[[#]]*(μpart1[#, c1, c2] + μpart2[#, c1, c2] - sweep) &, total]
dc1 := (c0 - c1)*sweep -  Sum[ μpart1[i, c1, c2]*ϵ[[1, i]]*n[[i]], {i, 1,  total}]
      ; (*primary carbon source*)

dc2 := Sum[ prod[[i]]*μpart1[i, c1, c2]*ϵ[[1, i]]*n[[i]], {i, 1,  total}]
- Sum[ μpart2[i, c1, c2]*ϵ[[2, i]]*n[[i]], {i, 1,  total}] - sweep*c2 ; (*
     secondary carbon source*)

rule = {c1 -> c1[t], c2 -> c2[t]};
eqn := Array[dnt[[#]] == (dn[[#]] /. rule) &, {total}];
eqc1 := c1'[t] == (dc1 /. rule);
eqc2 := c2'[t] == (dc2 /. rule);
vars := Join[ Array[ToExpression[StringJoin["n", ToString[#]]] &, total], {c1,  c2
     }];
eqns := {eqn, eqc1, eqc2, Join[Array[ ToExpression[StringJoin["n", ToString[#], "
     [o]==no[[", ToString[#], "]]"]] &,total], {c1[0] == c00, c2[0] == 0}]}

sol := NDSolve[eqns, vars, {t, 0, tmax}, MaxSteps -> \[Infinity]]

n0 := Array[1 &, total]*Vol; c00 = c0*Vol;
(*ϵ = reciprocal yield , ϵ[[i,j]] = (μg carbon \
uptake of Subscript[C, i] by bacteria  j)/(μg carbon utilized for \
reproduction bacteria of j) *)
```

C.2 TIME EVOLUTION

```
list2 = {};
list3 = {};
Do[
 Do[
  s = total - g;
  maxsetup = (Array[1 &, {2, total}] -
     Normal[SparseArray[Table[{2, i} -> 1, {i, g + 1, total}]]]);

  For[producers = 0, producers <= total, producers++,
   For[prodgen = Min[g, producers], prodgen >= Max[producers - s, 0], prodgen--,
    prodspecialists = producers - prodgen;
    prodsetup = Join[Array[1 &, prodgen], Array[0 &, g - prodgen], Array[1 &,
          prodspecialists], Array[0 &, s - prodspecialists]];
    list = {};
    For[i = 0, i < imax, i++,
     ϵ = 1/RandomReal[{0.1, 0.49}, {2, total}];
     prod = Table[RandomReal[{0.2, 0.5}], {i, 1, total}]*prodsetup;
     max = RandomReal[{1, 6}, {2, total}]*maxsetup;
     k = RandomReal[{0.002, 0.02}, {2, total}]*Vol;
     AppendTo[list, Count[Chop[Evaluate[n /. sol /. t -> T]], _?Positive, 2]];
     ];
    AppendTo[list2, BinCounts[list, {-0.5, total + 0.5, 1}]/imax];
    list = {};
    ]]
    ,{g, 0, total - 1, 2}];
 AppendTo[list3, Mean[list2]];
 list2 = {}
 ,{T, 0, tmax, 20}]
filename =
  NotebookDirectory[] <> FileBaseName[NotebookFileName[]] <> "—" <>
   ToString[tmax] <> "timeevolution of distribution" <> "days" <>
   "—" <> ToString[imax] <> "runs" <> ".xls";
Export[filename, list3]
```

C.3 MAPPING ALL CONFIGURATIONS WITH 20 INITIAL SPECIES

```
Do[
 s = total - g;

 export = {};
 maxsetup = (Array[1 &, {2, total}] - Normal[SparseArray[Table[{2, i} -> 1, {i, g +
       1, total}]]]);
 AppendTo[export, Join[{"producing generalists", "producing specialists", "
      producing species", "—"},
 Array["cases with " <> ToString[#] <> " survivors" &, {total + 1}, 0]]];
```

```
For[producers = 0, producers <= total, producers++,
 For[prodgen = Min[g, producers], prodgen >= Max[producers - s, 0],
  prodgen--,
  prodspecialists = producers - prodgen;
  prodsetup =
   Join[Array[1 &, prodgen], Array[0 &, g - prodgen],
    Array[1 &, prodspecialists], Array[0 &, s - prodspecialists]];
  list = {};
  For[i = 0, i < imax, i++,
   ϵ = 1/RandomReal[{0.1, 0.49}, {2, total}];
   prod = Table[RandomReal[{0.2, 0.5}], {i, 1, total}]*prodsetup;
   max = RandomReal[{1, 6}, {2, total}]*maxsetup;
   k = RandomReal[{0.002, 0.02}, {2, total}]*Vol;
   AppendTo[list, Count[Chop[Evaluate[n /. sol /. t -> tmax]], _?Positive, 2]];
   ];
  count = BinCounts[list, {-0.5, total + 0.5, 1}];
  AppendTo[export, Join[{prodgen, prodspecialists, prodgen + prodspecialists, "—"
        }, count/imax]]
  ]];

Export[filename, export],
{g, 6, total - 1}]
```

D IMPACT OF NETWORK STRUCTURE AND COMPLEXITY

```
ClearAll["Global`*"];
vert[mean_, var_] :=
 LogNormalDistribution[\[Mu], \[Sigma]] /. \[Mu] ->
    Log[mean] - \[Sigma]^2/2 /. \[Sigma] -> Sqrt[Log[1 + var/mean^2]]
(*carbon sources, phytoplankton, zooplankton, etc, auxilliary level*)

nooflevels := Length[speciesperlevel];
vars := Table[
   Table[ToExpression[StringJoin["s", ToString[i], ToString[j]]], {j,
     speciesperlevel[[i]]}], {i, nooflevels}];
n := Table[
   Table[ToExpression[
     StringJoin["s", ToString[i], ToString[j], "[t]"]], {j,
     speciesperlevel[[i]]}], {i, nooflevels}];

(*for species,ie. nooflevels >= levelno >= 2*)
growth[levelno_, speciesno_] :=
 Piecewise[{{r0[[speciesno]]*sweep, levelno == 1}},
     n[[levelno, speciesno]]*mumax[[levelno, speciesno]]*
       (Sum[b[[levelno, speciesno, i]]*n[[levelno - 1, i]],
           {i, 1, speciesperlevel[[levelno - 1]]}]/
          (1 + Sum[b[[levelno, speciesno, i]]*n[[levelno - 1, i]],
              {i, 1, speciesperlevel[[levelno - 1]]}]))]
loss[levelno_, speciesno_] :=
   Piecewise[{{n[[levelno, speciesno]]*(sweep +
       death[[levelno, speciesno]]),
         levelno == nooflevels}}, n[[levelno, speciesno]]*
       (sweep + death[[levelno, speciesno]] +
     Sum[growth[levelno + 1, i],
              {i, 1, speciesperlevel[[levelno + 1]]}]/
      Sum[n[[levelno, l]],
              {l, 1, speciesperlevel[[levelno]]}])]ds := Table[
  Table[growth[l, j] - loss[l, j], {j, speciesperlevel[[l]]}], {l, 1,
   nooflevels}]
diffs := Table[
   Table[ToExpression[
     StringJoin["s", ToString[i], ToString[j], "'[t]"]], {j,
     speciesperlevel[[i]]}], {i, nooflevels}];
eqns := Join[{diffs == ds}, {n == n0} /. t -> 0]
```

```
r0 := Table[i, {i, speciesperlevel[[1]]}];
n0 := Prepend[
   Table[Table[1/i, {j, speciesperlevel[[i]]}], {i, 2, nooflevels}],
   r0];
colors = (("DefaultPlotStyle" /. (Method /.
        Charting`ResolvePlotTheme["Scientific", SmoothHistogram])) /.
    Directive[x_, __] :> x);

    itmax = 500;
speciesperlevel = {3, 3, 6, 9, 12, 15};
seed = 1; SeedRandom[seed];
sweep = 1.;
Tmax = 230;
Tmin = 30;
Tstep = (Tmax - Tmin)/sweep/50;

SetDirectory[NotebookDirectory[]];
date = DateString["ISODate"];
Do[fname =
   "GeneralPlanktonSystem" <> " " <> date <> " " <>
    ToString[speciesperlevel] <> " " <> ToString[i];
 ToExpression["fname" <> ToString[i] <> "=fname"], {i, 1, 8}]
Do[ToExpression["data" <> ToString[i] <> "={}"], {i, 1, 8}]
Do[ToExpression[
   "PutAppend[{Seed, seed},fname" <> ToString[i] <> "]"], {i, 1, 8}]
PutAppend["death (rate)", fname1];
PutAppend["mumax (maximal growth rate)", fname2];
PutAppend["b", fname3];
PutAppend["N[Block[{t=Tmax},Chop[(n/.sol)]]], i.e. N[Tmax]", fname4];
PutAppend[
   "N[Chop[Integrate[n/.sol,{t,.9*Tmax,Tmax}]/0.1]], i.e. average <N>",
    fname5];
PutAppend[
   "N[LengthWhile[Block[{t=Tmax},Sort[Chop[Flatten[n/.sol]],Greater]],#\
>0&]], i.e. number of non-extinct species", fname6];
PutAppend["discrete N_i", fname7];
PutAppend["survivors per level", fname8];

style = Join[Table[Green, {speciesperlevel[[1]]}],
   Flatten[Table[
     colors[[i]], {i, 2, nooflevels}, {j, speciesperlevel[[i]]}]]];
style2 = Flatten[
   Table[colors[[i]], {i, 2, nooflevels}, {j, speciesperlevel[[i]]}]];

legend = SwatchLegend[Prepend[colors[[2 ;; nooflevels]], Green],
   Table[StringJoin["s", ToString[i], "i "], {i, 1, nooflevels}],
   LegendMarkers -> Graphics[{EdgeForm[Black], Rectangle[]}],
   LegendLabel -> "colors",
   LegendFunction -> (Framed[#, RoundingRadius -> 5] &),
```

```
   LegendMargins -> 5];

averagesurvive = {};
counterrors = 0;
Do[

 Print[DateString[DateString["DateTimeShort"]]];
 Monitor[
  Do[
   death =
    Prepend[Table[
      Table[RandomVariate[vert[sweep*.1/i, sweep^2*.1/i^2]], {j,
        speciesperlevel[[i]]}], {i, 2, nooflevels}],
      Table[0, {j, speciesperlevel[[1]]}]];
   mumax =
    Prepend[Table[
      Table[RandomVariate[vert[sweep*10/i, sweep^2*10/i^2]], {j,
        speciesperlevel[[i]]}], {i, 2, nooflevels}],
      Table[0, {j, speciesperlevel[[1]]}]];
   b = Prepend[
     Table[Table[
       Table[RandomVariate[vert[5/i, 10/i^2]], {k,
         speciesperlevel[[i - 1]]}], {j, speciesperlevel[[i]]}], {i,
       2, nooflevels}], Table[0, {speciesperlevel[[1]]}]];
   AppendTo[data1, death]; AppendTo[data2, mumax]; AppendTo[data3, b];
   sol =
    NDSolve[{eqns}, Flatten[vars], {t, 0, Tmax},
     MaxSteps -> \[Infinity], MaxStepSize -> 10^(-3)];
   av = Chop[Integrate[n /. sol, {t, .6*Tmax, Tmax}]/(.4*Tmax)];
   If[Block[{t = Tmax}, MemberQ[Chop[(n /. sol)], _?Negative, 3]] ||
     MatchQ[j, _?Positive],
    Do[ToExpression[
      "AppendTo[data" <> ToString[i] <> ",Integrationerror]"], {i, 4,
       8}]; counterrors = counterrors + 1
    ,

    Export["Plots/" <> "GeneralPlanktonSystem" <> " " <> date <>
      " " <> ToString[speciesperlevel] <> "-4-" <> ToString[it] <>
      ".pdf", Plot[Evaluate[n[[-1]] /. sol], {t, 0, Tmax},
      PlotRange -> Full,
      PlotStyle -> style[[-speciesperlevel[[-1]] ;; -1]],
      PlotLegends -> None, ImageSize -> Medium]];
    Export[
     "Plots/" <> "GeneralPlanktonSystem" <> " " <> date <> " " <>
      ToString[speciesperlevel] <> "-all-" <> ToString[it] <> ".pdf",
      Plot[Evaluate[n /. sol], {t, 0, Tmax}, PlotRange -> Full,
      PlotStyle -> style2, PlotLegends -> None, ImageSize -> Medium]];
    AppendTo[data4, N[Block[{t = Tmax}, Chop[(n /. sol)]]]];
    AppendTo[data5,
```

```
      N[Chop[Integrate[n /. sol, {t, .9*Tmax, Tmax}]/0.1]]];
     AppendTo[data6,
      N[LengthWhile[
        Block[{t = Tmax},
         Sort[Chop[Flatten[n /. sol]], Greater]], # > 0 &]]];
     AppendTo[data7,
      Table[Flatten[
        Table[Evaluate[{t, n[[l, k]]} /. {t -> T} /. sol], {T, Tmin,
          Tmax, Tstep}], 1], {l, 1, Length[speciesperlevel]}, {k, 1,
        speciesperlevel[[l]]}]];
     AppendTo[data8, Map[Count[#, n_ /; n > 0] &, av, {2}]];
     AppendTo[averagesurvive, Map[Count[#, n_ /; n > 0] &, av, {2}]]
     ];
    Do[ToExpression[
      "PutAppend[data" <> ToString[i] <> "[[j]],fname" <>
       ToString[i] <> "]"], {i, 1, 8}, {j, 1,
      Length[ToExpression["data" <> ToString[i]]]}];
    Do[ToExpression["data" <> ToString[i] <> "={}"], {i, 1, 8}];
    , {it, itmax}]
   , it]
  Print[DateString[DateString["DateTimeShort"]]];
 , {1}]
Mean[averagesurvive] // N
GraphicsRow[Table[Histogram[averagesurvive[[All, 1, i]]], {i, 2, 4}]]

Print[ToString[counterrors] <> " Fehler"]
NotebookSave[]
Print[averagesurvive]
averagesurvive = {};
counterrors = 0;
```

BIBLIOGRAPHY

[1] Anurag A Agrawal. Phenotypic plasticity in the interactions and evolution of species. *Science*, 294(5541):321–326, 2001.

[2] K. T. Allhoff, D. Ritterskamp, B. C. Rall, B. Drossel, and C. Guill. Evolutionary food web model based on body masses gives realistic networks with permanent species turnover. *Scientific Reports*, 5:10955 EP –, 06 2015.

[3] R.A. Armstrong and R. McGehee. Coexistence of two competitors on one resource. *Journal of Theoretical Biology*, 56(2):499 – 502, 1976.

[4] Robert A. Armstrong and Richard McGehee. Coexistence of species competing for shared resources. *Theoretical Population Biology*, 9(3):317 – 328, 1976.

[5] Robert A. Armstrong and Richard McGehee. Competitive exclusion. *American Naturalist*, pages 151–170, 1980.

[6] Hartmut Arndt, Andre Schieffer, Groll, Lutz Becks, Mar Monsonís Nomdedeu, Christine Willen, and Jennifer Arns. In Preparation, 2016.

[7] Jennifer Arns. Population dynamics of bacteria in one- and multi-species experimental system. Bachelor's thesis, Universität zu Köln, 2012.

[8] Lutz Becks and Hartmut Arndt. Transitions from stable equilibria to chaos, and back, in an experimental food web. *Ecology*, 89(11):pp. 3222–3226, 2008.

[9] Lutz Becks and Hartmut Arndt. Different types of synchrony in chaotic and cyclic communities. *Nat Commun*, 4:1359, 01 2013.

[10] Lutz Becks, Frank M. Hilker, Horst Malchow, Klaus Jurgens, and Hartmut Arndt. Experimental demonstration of chaos in a microbial food web. *Nature*, 435, 06 2005.

[11] Thomas Bell, Jonathan Newman, Bernard Silverman, Sarah Turner, and Andrew Lilley. The contribution of species richness and composition to bacterial services. *Nature*, 436(7054):1157–1160, 2005.

[12] Elisa Benincà, Elisa, Jef Huisman, Reinhard Heerkloss, Klaus D. Johnk, Pedro Branco, Egbert H. Van Nes, Marten Scheffer, and Stephen P. Ellner. Chaos in a long-term experiment with a plankton community. *Nature*, 451(7180):822–825, 02 2008.

[13] Peter Koefoed Bjørnsen. Automatic determination of bacterioplankton biomass by image analysis. *Applied and Environmental Microbiology*, 51 (6):1199–1204, 1986.

[14] Brendan J. M. Bohannan and Richard E. Lenski. Effect of prey heterogeneity on the response of a model food chain to resource enrichment. *The American Naturalist*, 153(1):73–82, 1999.

[15] Amy D Bradshaw. Evolutionary significance of phenotypic plasticity in plants. *Advances in genetics*, 13(1):115–155, 1965.

[16] William W.L. Cheung, Vicky W.Y. Lam, Jorge L. Sarmiento, Kelly Kearney, Reg Watson, and Daniel Pauly. Projecting global marine biodiversity impacts under climate change scenarios. *Fish and Fisheries*, 10(3):235–251, 2009.

[17] R. F. Costantino, R. A. Desharnais, J. M. Cushing, and Brian Dennis. Chaotic dynamics in an insect population. *Science*, 275(5298):389–391, 1997.

[18] Colomban De Vargas, Stéphane Audic, Nicolas Henry, Johan Decelle, Frédéric Mahé, Ramiro Logares, Enrique Lara, Cédric Berney, Noan Le Bescot, Ian Probert, et al. Eukaryotic plankton diversity in the sunlit ocean. *Science*, 348(6237):1261605, 2015.

[19] Brian Dennis, R.A. Desharnais, J.M. Cushing, and R.F. Costantino. Transitions in population dynamics: Equilibria to periodic cycles to aperiodic cycles. *Journal of Animal Ecology*, 66(5):pp. 704–729, 1997.

[20] U Dobramysl and U C Täuber. Environmental versus demographic variability in stochastic predator–prey models. *Journal of Statistical Mechanics: Theory and Experiment*, 2013(10):P10001, 2013.

[21] Alexander Dobrinevski and Erwin Frey. Extinction in neutrally stable stochastic lotka-volterra models. *Phys. Rev. E*, 85:051903, May 2012.

[22] Jennifer A Dunne, Richard J Williams, Neo D Martinez, Rachel A Wood, and Douglas H Erwin. Compilation and network analyses of cambrian food webs. *PLoS Biol*, 6(4):1–16, 04 2008.

[23] Stephen Ellner and Peter Turchin. Chaos in a noisy world: New methods and evidence from time-series analysis. *The American Naturalist*, 145(3):pp. 343–375, 1995.

[24] Charles Elton and Mary Nicholson. The ten-year cycle in numbers of the lynx in canada. *The Journal of Animal Ecology*, pages 215–244, 1942.

[25] Noah Fierer and Robert B. Jackson. The diversity and biogeography of soil bacterial communities. *Proceedings of the National Academy of Sciences of the United States of America*, 103(3):626–631, 2006.

[26] AG Fredrickson. Behavior of mixed cultures of microorganisms. *Annual Reviews in Microbiology*, 31(1):63–88, 1977.

[27] Gregor F. Fussmann, Stephen P. Ellner, Kyle W. Shertzer, and Nelson G. Hairston Jr. Crossing the hopf bifurcation in a live predator-prey system. *Science*, 290(5495):1358–1360, 2000.

[28] Sunita Gakkhar and Raid Kamel Naji. Order and chaos in a food web consisting of a predator and two independent preys. *Communications in Nonlinear Science and Numerical Simulation*, 10(2):105 – 120, 2005.

[29] Georgii F. Gause. *The struggle for existence*. Baltimore, The Williams & Wilkins company, 1934.

[30] William T Gibson and William G Wilson. Individual-based chaos: Extensions of the discrete logistic model. *Journal of theoretical biology*, 339:84–92, 2013.

[31] Daniel T. Gillespie. A general method for numerically simulating the stochastic time evolution of coupled chemical reactions. *Journal of Computational Physics*, 22(4):403 – 434, 1976.

[32] Daniel T. Gillespie. Exact stochastic simulation of coupled chemical reactions. *The Journal of Physical Chemistry*, 81(25):2340–2361, 1977.

[33] Michael E Gilpin. Limit cycles in competition communities. *American Naturalist*, pages 51–60, 1975.

[34] Michael E. Gilpin. Spiral chaos in a predator-prey model. *The American Naturalist*, 113(2):pp. 306–308, 1979.

[35] David W Graham, Charles W Knapp, Erik S Van Vleck, Katie Bloor, Teresa B Lane, and Christopher E Graham. Experimental demonstration of chaotic instability in biological nitrification. *The ISME journal*, 1(5):385–393, 2007.

[36] Joseph Grinnell. The origin and distribution of the chest-nut-backed chickadee. *The Auk*, 21(3):364–382, 1904.

[37] Fanny Groll, Alexander Altland, and Hartmut Arndt. Chaotic attractor in two-prey one-predator system originates from interplay of limit cycles. *Theoretical Ecology*, 2016. doi: 10.1007/s12080-016-0317-9.

[38] Thilo Gross, Wolfgang Ebenhöh, and Ulrike Feudel. Long food chains are in general chaotic. *Oikos*, 109(1):135–144, 2005.

[39] Thilo Gross, Lars Rudolf, Simon A. Levin, and Ulf Dieckmann. Generalized models reveal stabilizing factors in food webs. *Science*, 325(5941):747–750, 2009.

[40] J. P. Grover. *Resource Competition*. Chapman & Hall, London, UK, 1997.

[41] Garrett Hardin. The competitive exclusion principle. *Science*, 131:1292–1297, 1960.

[42] Alan Hastings and Thomas Powell. Chaos in a three-species food chain. *Ecology*, 72(3):896–903, 1991.

[43] A. Hector, B. Schmid, C. Beierkuhnlein, M. C. Caldeira, M. Diemer, P. G. Dimitrakopoulos, J. A. Finn, H. Freitas, P. S. Giller, J. Good, R. Harris, P. Högberg, K. Huss-Danell, J. Joshi, A. Jumpponen, C. Körner, P. W. Leadley, M. Loreau, A. Minns, C. P. H. Mulder, G. O'Donovan, S. J. Otway, J. S. Pereira, A. Prinz, D. J. Read, M. Scherer-Lorenzen, E.-D. Schulze, A.-S. D. Siamantziouras, E. M. Spehn, A. C. Terry, A. Y. Troumbis, F. I. Woodward, S. Yachi, and J. H. Lawton. Plant diversity and productivity experiments in european grasslands. *Science*, 286(5442):1123–1127, 1999.

[44] Shandelle M. Henson, R. F. Costantino, J. M. Cushing, Robert A. Desharnais, Brian Dennis, and Aaron A. King. Lattice effects observed in chaotic dynamics of experimental populations. *Science*, 294(5542): 602–605, 2001.

[45] Julia Heßeler, Julia K. Schmidt, Udo Reichl, and Dietrich Flockerzi. Coexistence in the chemostat as a result of metabolic by-products. *Journal of Mathematical Biology*, 53(4):556–584, 2006.

[46] Crawford S Holling. The components of predation as revealed by a study of small-mammal predation of the european pine sawfly. *The Canadian Entomologist*, 91(05):293–320, 1959.

[47] Jef Huisman and Franz J. Weissing. Biodiversity of plankton by species oscillations and chaos. *Nature*, 402(6760):407–410, 11 1999.

[48] Jef Huisman and Franz J Weissing. Fundamental unpredictability in multispecies competition. *The American Naturalist*, 157(5):488–494, 2001.

[49] Jef Huisman and Franz J Weissing. Biological conditions for oscillations and chaos generated by multispecies competition. *Ecology*, 82 (10):2682–2695, 2001.

[50] G. E. Hutchinson. The paradox of the plankton. *The American Naturalist*, 95(882):pp. 137–145, 1961.

[51] Julian Huxley. *Problems of relative growth*. Dial Press, 1932.

[52] Laura E. Jones, Lutz Becks, Stephen P. Ellner, Nelson G. Hairston, Takehito Yoshida, and Gregor F. Fussmann. Rapid contemporary evolution and clonal food web dynamics. *Philosophical Transactions of the Royal Society of London B: Biological Sciences*, 364(1523):1579–1591, 2009.

[53] J. L. Jost, J. F. Drake, A. G. Fredrickson, and H. M. Tsuchiya. Interactions of tetrahymena pyriformis, escherichia coli, azotobacter vinelandii, and glucose in a minimal medium. *J. Bacteriol.*, 113(2):834–840, 1973.

[54] James L Kaplan and James A Yorke. Competitive exclusion and nonequilibrium coexistence. *The American Naturalist*, 111(981):1030–1036, 1977.

[55] Barry C. Kelly, Michael G. Ikonomou, Joel D. Blair, Anne E. Morin, and Frank A. P. C. Gobas. Food web-specific biomagnification of persistent organic pollutants. *Science*, 317(5835):236–239, 2007.

[56] Aaron A. King, R. F. Costantino, J. M. Cushing, Shandelle M. Henson, Robert A. Desharnais, and Brian Dennis. Anatomy of a chaotic attractor: Subtle model-predicted patterns revealed in population data. *Proceedings of the National Academy of Sciences of the United States of America*, 101(1):408–413, 2004.

[57] Aaron Klebanoff and Alan Hastings. Chaos in one-predator, two-prey models: General results from bifurcation theory. *Mathematical Biosciences*, 122(2):221–233, 1994.

[58] Arthur L. Koch. Competitive coexistence of two predators utilizing the same prey under constant environmental conditions. *Journal of Theoretical Biology*, 44(2):387 – 395, 1974.

[59] B.W. Kooi and M. P. Boer. Chaotic behaviour of a predator–prey system in the chemostat. *Dynamics of Continuous, Discrete and Impulsive Systems, Series B: Applications and Algorithms*, 10(2):259–272, 2003.

[60] Vlastimil Křivan and Jan Eisner. The effect of the holling type {II} functional response on apparent competition. *Theoretical Population Biology*, 70(4):421–430, 2006.

[61] Mathew A Leibold. A graphical model of keystone predators in food webs: trophic regulation of abundance, incidence, and diversity patterns in communities. *American Naturalist*, pages 784–812, 1996.

[62] Urs Lendenmann, Thomas Egli, et al. Kinetic models for the growth of escherichia coli with mixtures of sugars under carbon-limited conditions. *Biotechnology and bioengineering*, 59(1):99–107, 1998.

[63] Bruce R Levin, Frank M Stewart, and Lin Chao. Resource-limited growth, competition, and predation: a model and experimental studies with bacteria and bacteriophage. *American Naturalist*, 111(977): 3–24, 1977.

[64] Simon A. Levin. Community equilibria and stability, and an extension of the competitive exclusion principle. *The American Naturalist*, 104 (939):pp. 413–423, 1970.

[65] Jonathan M Levine and Janneke HilleRisLambers. The importance of niches for the maintenance of species diversity. *Nature*, 461(7261):254–257, 09 2009.

[66] Richard Levins. *Evolution in changing environments: some theoretical explorations*. Number 2 in Monographs in population biology. Princeton University Press, 1968.

[67] Eckhard Limpert and Werner A Stahel. Problems with using the normal distribution –and ways to improve quality and efficiency of data analysis. *PLoS ONE*, 6(7):e21403, 2011.

[68] M. Loreau, S. Naeem, P. Inchausti, J. Bengtsson, J.P. Grime, A. Hector, D.U. Hooper, M.A. Huston, D. Raffaelli, B. Schmid, D. Tilman, and D.A. Wardle. Biodiversity and ecosystem functioning: Current knowledge and future challenges. *Science*, 294(5543):804–808, 2001.

[69] Alfred James Lotka. *Elements of Physical Biology*. Williams and Wilkins, Baltimore, 1925.

[70] Leo S Luckinbill. Coexistence in laboratory populations of paramecium aurelia and its predator didinium nasutum. *Ecology*, pages 1320–1327, 1973.

[71] Robert MacArthur and Richard Levins. Competition, habitat selection, and character displacement in a patchy environment. *Proceedings of the National Academy of Sciences*, 51(6):1207–1210, 1964.

[72] Thomas Robert Malthus. *An Essay on the Principle of Population*. 1798.

[73] Adam C Martiny, Jasper A Vrugt, and Michael W Lomas. Concentrations and ratios of particulate organic carbon, nitrogen, and phosphorus in the global ocean. *Scientific Data*, 1:140048 EP –, 12 2014.

[74] Robert M. May. Biological populations with nonoverlapping generations: Stable points, stable cycles, and chaos. *Science*, 186(4164):645–647, 1974.

[75] Robert M. May. Simple mathematical models with very complicated dynamics. *Nature*, 261(5560):459–467, June 1976.

[76] Robert M May and Warren J Leonard. Nonlinear aspects of competition between three species. *SIAM Journal on Applied Mathematics*, 29(2): 243–253, 1975.

[77] Richard McGehee and Robert A Armstrong. Some mathematical problems concerning the ecological principle of competitive exclusion. *Journal of Differential Equations*, 23:30–52, 1977.

[78] A. J. McKane and T. J. Newman. Predator-prey cycles from resonant amplification of demographic stochasticity. *Phys. Rev. Lett.*, 94(21): 218102, Jun 2005.

[79] R. Milo, S. Shen-Orr, S. Itzkovitz, N. Kashtan, D. Chklovskii, and U. Alon. Network motifs: Simple building blocks of complex networks. *Science*, 298(5594):824–827, 2002.

[80] Jacques Monod. The growth of bacterial cultures. *Annual Review of Microbiology*, 3(1):371, 1949.

[81] Shahid Naeem, Emmett Duffy, and Erika Zavaleta. The functions of biological diversity in an age of extinction. *Science*, 336(6087):1401–1406, 2012.

[82] Mar Monsonis Nomdedeu, Christine Willen, Andre Schieffer, and Hartmut Arndt. Temperature-dependent ranges of coexistence in a model of a two-prey-one-predator microbial food web. *Marine Biology*, 159(11):2423–2430, 2012.

[83] Robert T. Paine. Food web complexity and species diversity. *The American Naturalist*, 100(910):65–75, 1966.

[84] Matt Parker and Alex Kamenev. Mean extinction time in predator-prey model. *Journal of Statistical Physics*, 141(2):201–216, 2010.

[85] Matthew Parker and Alex Kamenev. Extinction in the lotka-volterra model. *Physical Review E*, 80(2):021129, 2009.

[86] AC Redfield. On the proportions of organic derivations in seawater and their relation to the composition of plankton (reprint). *Benchmark Papers in Ecology*, 1, 1934.

[87] Gregory T. Reeves, Atul Narang, and Sergei S. Pilyugin. Growth of mixed cultures on mixtures of substitutable substrates: the operating diagram for a structured model. *Journal of Theoretical Biology*, 226(2): 143 – 157, 2004.

[88] Thomas Reinthaler and Gerhard J Herndl. Seasonal dynamics of bacterial growth efficiencies in relation to phytoplankton in the southern north sea. *Aquatic Microbial Ecology*, 39(1):7–16, 2005.

[89] Aldo Rescigno and Irvin Richardson. On the competitive exclusion principle. *Bulletin of Mathematical Biology*, 27:85–89, 1965. 10.1007/BF02477264.

[90] Michael L. Rosenzweig. Paradox of enrichment: Destabilization of exploitation ecosystems in ecological time. *Science*, 171(3969):385–387, 1971.

[91] Michael L. Rosenzweig and Robert H MacArthur. Graphical representation and stability conditions of predator-prey interactions. *The American Naturalist*, 97(895):209–223, 1963.

[92] Otto E. Rössler. An equation for continuous chaos. *Physics Letters A*, 57(5):397–398, 7 1976.

[93] Ram Sarkar and J. Chattopadhayay. A technique for estimating maximum harvesting effort in a stochastic fishery model. *Journal of Biosciences*, 28:497–506, 2003. 10.1007/BF02705124.

[94] Andre Schieffer. *Studies on diversity and coexistence in an experimental microbial community*. PhD thesis, Universität zu Köln, 2012.

[95] Noam Shoresh, Matthew Hegreness, and Roy Kishony. Evolution exacerbates the paradox of the plankton. *Proceedings of the National Academy of Sciences*, 105(34):12365–12369, 2008.

[96] Steve Smale. On the differential equations of species in competition. *Journal of Mathematical Biology*, 3(1):5–7, 1976.

[97] Carl Sprengel. *Chemie für Landwirthe, Forstmänner und Cameralisten*. Number Bd. 1 in Chemie für Landwirthe, Forstmänner und Cameralisten. Vandenhoek U. Ruprecht, 1831.

[98] J. C. Sprott. Some simple chaotic flows. *Phys. Rev. E*, 50(2):R647–R650, Aug 1994.

[99] Robert W Sterner, Tom Andersen, James J Elser, Dag O Hessen, James M Hood, Edward McCauley, and Jotaro Urabe. Scale-dependent carbon: nitrogen: phosphorus seston stoichiometry in marine and freshwaters. *Limnology and Oceanography*, 53(3):1169, 2008.

[100] Steven H Strogatz. *Nonlinear dynamics and chaos: with applications to physics, biology and chemistry*. Perseus publishing, 2001.

[101] Shinichi Sunagawa, Luis Coelho, Samuel Chaffron, Jens Kultima, Karine Labadie, Guillem Salazar, Bardya Djahanschiri, Georg Zeller, Daniel Mende, Adriana Alberti, Francisco Cornejo-Castillo, Paul Costea, Corinne Cruaud, Francesco d'Ovidio, Stefan Engelen, Isabel Ferrera, Josep Gasol, Lionel Guidi, Falk Hildebrand, Florian Kokoszka, Cyrille Lepoivre, Gipsi Lima-Mendez, Julie Poulain, Bonnie Poulos, Marta Royo-Llonch, Hugo Sarmento, Sara Vieira-Silva, Céline Dimier, Marc Picheral, Sarah Searson, Stefanie Kandels-Lewis, Tara Coordinators, Chris Bowler, Colomban de Vargas, Gabriel Gorsky, Nigel Grimsley, Pascal Hingamp, Daniele Iudicone, Olivier Jaillon, Fabrice Not, Hiroyuki Ogata, Stephane Pesant, Sabrina Speich, Lars Stemmann, Matthew Sullivan, Jean Weissenbach, Patrick Wincker, Eric Karsenti, Jeroen Raes, Silvia Acinas, Peer Bork, Emmanuel Boss, Chris Bowler, Michael Follows, Lee Karp-Boss, Uros Krzic, Emmanuel Reynaud, Christian Sardet, Mike Sieracki, and Didier Velayoudon. Structure and

function of the global ocean microbiome. *Science*, 348(6237):1261359, 2015.

[102] Yasuhiro Takeuchi and Norihiko Adachi. The existence of globally stable equilibria of ecosystems of the generalized volterra type. *Journal of Mathematical Biology*, 10:401–415, 1980. 10.1007/BF00276098.

[103] Yasuhiro Takeuchi and Norihiko Adachi. Existence and bifurcation of stable equilibrium in two-prey, one-predator communities. *Bulletin of Mathematical Biology*, 45(6):877 – 900, 1983.

[104] John N Thompson. Rapid evolution as an ecological process. *Trends in Ecology & Evolution*, 13(8):329 – 332, 1998.

[105] David Tilman. *Resource competition and community structure*. Princeton University Press, 1982.

[106] David Tilman. Causes, consequences and ethics of biodiversity. *Nature*, 405(6783):208–211, 05 2000.

[107] David Tilman, Clarence L Lehman, and Kendall T Thomson. Plant diversity and ecosystem productivity: theoretical considerations. *Proceedings of the national academy of sciences*, 94(5):1857–1861, 1997.

[108] David Tilman, Forest Isbell, and Jane M. Cowles. Biodiversity and ecosystem functioning. *Annual Review of Ecology, Evolution, and Systematics*, 45(1):471–493, 2014.

[109] Arne Traulsen, Jens Christian Claussen, and Christoph Hauert. Stochastic differential equations for evolutionary dynamics with demographic noise and mutations. *Physical Review E*, 85(4):041901, 2012.

[110] H. M. Tsuchiya, J. F. Drake, J. L. Jost, and A. G. Fredrickson. Predator-prey interactions of dictyostelium discoideum and escherichia coli in continuous culture. *J. Bacteriol.*, 110(3):1147–1153, 1972.

[111] Peter Turchin. *Complex population dynamics: a theoretical/empirical synthesis*, volume 35. Princeton University Press, 2003.

[112] Jasper van Ruijven and Frank Berendse. Diversity–productivity relationships: Initial effects, long-term patterns, and underlying mechanisms. *Proceedings of the National Academy of Sciences of the United States of America*, 102(3):695–700, 2005.

[113] Richard R. Vance. Predation and resource partitioning in one predator – two prey model communities. *The American Naturalist*, 112(987):797–813, 1978.

[114] D. V. Vayenas and Stavros Pavlou. Chaotic dynamics of a food web in a chemostat. *Mathematical Biosciences*, 162(1-2):69 – 84, 1999.

[115] Pierre-François Verhulst. Notice sur la loi que la population suit dans son accroissement. correspondance mathématique et physique publiée par a. *Quetelet*, 10:113–121, 1838.

[116] Sara Via, Richard Gomulkiewicz, Gerdien De Jong, Samuel M Scheiner, Carl D Schlichting, and Peter H Van Tienderen. Adaptive phenotypic plasticity: consensus and controversy. *Trends in Ecology & Evolution*, 10 (5):212–217, 1995.

[117] Vito Volterra. Fluctuations in the abundance of a species considered mathematically. *Nature*, 118:558–560, 1926.

[118] Vito Volterra. Variations and fluctuations of the number of individuals in animal species living together. *Journal du Conseil*, 3(1):3–51, 1928.

[119] Justus Freiherr von Liebig. *Die organische Chemie in ihrer Anwendung auf Agricultur und Physiologie*. Vieweg, 1840.

[120] B. A. Ward, S. Dutkiewicz, O. Jahn, and M. J. Follows. A size-structured food-web model for the global ocean. *Limnology and Oceanography*, 57(6):1877–1891, 2012.

[121] Mary Jane West-Eberhard. *Developmental plasticity and evolution*. Oxford University Press, 2003.

[122] Richard J. Williams and Neo D. Martinez. Simple rules yield complex food webs. *Nature*, 404(6774):180–183, 03 2000.

[123] Sabine Wollrab, Sebastian Diehl, and André M. De Roos. Simple rules describe bottom-up and top-down control in food webs with alternative energy pathways. *Ecology Letters*, 15(9):935–946, 2012.

[124] Justin P. Wright, Gregory M. Ames, and Rachel M. Mitchell. The more things change, the more they stay the same? when is trait variability important for stability of ecosystem function in a changing environment. *Philosophical Transactions of the Royal Society B: Biological Sciences*, 371(1694), 2016.

[125] John David Zicarelli. *Mathematical analysis of a population model with several predators on a single prey*. PhD thesis, Univ. of Minnesota, 1975.

[126] Manfred Zinn, Bernard Witholt, and Thomas Egli. Dual nutrient limited growth: models, experimental observations, and applications. *Journal of Biotechnology*, 113:263 – 279, 2004. Highlights from the ECB11: Building Bridges between Biosciences and Bioengineering.

DANK

für die Möglichkeit dieser Promotion, interessierte Diskussionen, Begeisterung, Austausch von Ideen und Begutachtung der Arbeit
Prof. Dr. Alexander Altland, Prof. Dr. Hartmut Arndt, Prof. Dr. Joachim Krug

für Erläuterungen der experimentellen Seite, Gespräche, Anregungen und geduldigen Ausbau meines Wörterbuchs Biologie-Physik/Physik-Biologie
Dr. Lutz Becks, Prof. Dr. Frank Hilker, Dr. Alexandra Jeuck, Dr. Mar Monsonís Nomdedeu, Dr. Andre Schieffer

für die allmähliche Verfertigung der Gedanken beim Reden, für moralische und kulinarische Unterstützung, für unzählige Kaffeepausen (auch ohne Kaffee), für mehr oder weniger Grummeligkeit im Büro, für last-minute proof-reading, für Anregungen mich von der Arbeit abzuhalten und dafür mich aus dem Büro zu zwingen und mich an die wichtigen Dinge im Leben zu erinnern
meiner Familie, meinen Mädels, der Kaffeepausenrunde, Freund(inn)en und Kolleg(inn)en aus dem Institut für Theoretische Physik

ERKLÄRUNG

Ich versichere, dass ich die von mir vorgelegte Dissertation selbstständig angefertigt, die benutzten Quellen und Hilfsmittel vollständig angegeben und die Stellen der Arbeit - einschließlich Tabellen, Karten und Abbildungen -, die anderen Werken im Wortlaut oder dem Sinn nach entnommen sind, in jedem Einzelfall als Entlehnung kenntlich gemacht habe; dass diese Dissertation noch keiner anderen Fakultät oder Universität zur Prüfung vorgelegen hat; dass sie - abgesehen von unten angegebenen Teilpublikationen - noch nicht veröffentlicht worden ist sowie, dass ich eine solche Veröffentlichung vor Abschluss des Promotionsverfahrens nicht vornehmen werde. Die Bestimmungen der Promotionsordnung sind mir bekannt. Die von mir vorgelegte Dissertation ist von Prof. Dr. Alexander Altland betreut worden.

Köln, 27. Oktober 2016

Fanny Groll

Teilpublikationen:

1. Hartmut Arndt, Andre Schieffer, Groll, Lutz Becks, Mar Monsonís Nomdedeu, Christine Willen, and Jennifer Arns. In Preparation, 2016 [6]

2. Fanny Groll, Alexander Altland, and Hartmut Arndt. Chaotic attractor in two-prey one-predator system originates from interplay of limit cycles. *Theoretical Ecology*, 2016. doi:10.1007/s12080-016-0317-9. [37]